

7-12-2011

# Exergoeconomic Analysis of Solar Organic Rankine Cycle for Geothermal Air Conditioned Net Zero Energy Buildings

Rambod Rayegan

*Florida International University, rrayegan@gmail.com*

**DOI:** 10.25148/etd.FI11080805

Follow this and additional works at: <https://digitalcommons.fiu.edu/etd>

---

## Recommended Citation

Rayegan, Rambod, "Exergoeconomic Analysis of Solar Organic Rankine Cycle for Geothermal Air Conditioned Net Zero Energy Buildings" (2011). *FIU Electronic Theses and Dissertations*. 470.

<https://digitalcommons.fiu.edu/etd/470>

This work is brought to you for free and open access by the University Graduate School at FIU Digital Commons. It has been accepted for inclusion in FIU Electronic Theses and Dissertations by an authorized administrator of FIU Digital Commons. For more information, please contact [dcc@fiu.edu](mailto:dcc@fiu.edu).

FLORIDA INTERNATIONAL UNIVERSITY

Miami, Florida

EXERGOCHEMICAL ANALYSIS OF SOLAR ORGANIC RANKINE CYCLE FOR  
GEOHERMAL AIR CONDITIONED NET ZERO ENERGY BUILDINGS

A dissertation submitted in partial fulfillment of the

requirements for the degree of

DOCTOR OF PHILOSOPHY

in

MECHANICAL ENGINEERING

by

Rambod Rayegan

2011

To: Dean Amir Mirmiran  
College of Engineering and Computing

This dissertation, written by Rambod Rayegan, and entitled Exergoeconomic Analysis of Solar Organic Rankine Cycle for Geothermal Air Conditioned Net Zero Energy Buildings, having been approved in respect to style and intellectual content, is referred to you for judgment.

We have read this dissertation and recommend that it be approved.

---

Ali Ebadian

---

Yiding Cao

---

Yimin Zhu

---

Yong X. Tao, Major Professor

Date of Defense: July 12, 2011

The dissertation of Rambod Rayegan is approved.

---

Dean Amir Mirmiran  
College of Engineering and Computing

---

Interim Dean Kevin O'Shea  
University Graduate School

Florida International University, 2011

## DEDICATION

I dedicate this dissertation to my parents and my wife for their never-ending love.

## ACKNOWLEDGMENTS

I am grateful to my major advisor Dr. Yong Tao for his support and guidance throughout my studies. The discussions I had with Dr. Tao were a great source of learning and encouragement for me. I am truly thankful for his patience, support and valuable advices. I would also like to recognize and thank Dr. Ali Ebadian, Dr. Yiding Cao and Dr. Yimin Zhu for serving on my advisory committee.

The work and its findings in this paper are made possible by the financial support from US Department of Energy Geothermal Program under the Award No. DE-EE0002802, which is greatly appreciated. Finally, I would like to acknowledge the financial support of Florida International University Doctoral Evidence Acquisition Fellowship.

ABSTRACT OF THE DISSERTATION  
EXERGOC ECONOMIC ANALYSIS OF SOLAR ORGANIC RANKINE CYCLE FOR  
GEOTHERMAL AIR CONDITIONED NET ZERO ENERGY BUILDINGS

by

Rambod Rayegan

Florida International University, 2011

Miami, Florida

Professor Yong X. Tao, Major Professor

This study is an attempt at achieving Net Zero Energy Building (NZEB) using a solar Organic Rankine Cycle (ORC) based on exergetic and economic measures. The working fluid, working conditions of the cycle, cycle configuration, and solar collector type are considered the optimization parameters for the solar ORC system.

In the first section, a procedure is developed to compare ORC working fluids based on their molecular components, temperature-entropy diagram and fluid effects on the thermal efficiency, net power generated, vapor expansion ratio, and exergy efficiency of the Rankine cycle. Fluids with the best cycle performance are recognized in two different temperature levels within two different categories of fluids: refrigerants and non-refrigerants. Important factors that could lead to irreversibility reduction of the solar ORC are also investigated in this study.

In the next section, the system requirements needed to maintain the electricity demand of a geothermal air-conditioned commercial building located in Pensacola of Florida is considered as the criteria to select the optimal components and optimal working condition of the system. The solar collector loop, building, and geothermal air

conditioning system are modeled using TRNSYS. Available electricity bills of the building and the 3-week monitoring data on the performance of the geothermal system are employed to calibrate the simulation. The simulation is repeated for Miami and Houston in order to evaluate the effect of the different solar radiations on the system requirements.

The final section discusses the exergoeconomic analysis of the ORC system with the optimum performance. Exergoeconomics rests on the philosophy that exergy is the only rational basis for assigning monetary costs to a system's interactions with its surroundings and to the sources of thermodynamic inefficiencies within it. Exergoeconomic analysis of the optimal ORC system shows that the ratio  $R_{ex}$  of the annual exergy loss to the capital cost can be considered a key parameter in optimizing a solar ORC system from the thermodynamic and economic point of view. It also shows that there is a systematic correlation between the exergy loss and capital cost for the investigated solar ORC system.

## TABLE OF CONTENTS

CHAPTER	PAGE
1. INTRODUCTION .....	1
1.1 Research Background.....	1
1.2 Exergoeconomic Point of View .....	4
1.3 Objectives and Significance of Study .....	5
1.4 Framework of the Research.....	6
2. A CRITICAL REVIEW ON SINGLE COMPONENT WORKING FLUIDS FOR ORGANIC RANKINE CYCLES (ORCs).....	9
2.1 Introduction .....	9
2.2 General criteria for Selecting Working Fluids in ORC.....	10
2.3 Studies Based on Critical Temperature .....	14
2.4 Studies Based on Molecular Complexity .....	18
2.5 Comparison in Efficiency among Selected Fluids .....	22
2.6 ORCs at Supercritical Region .....	27
2.7 Major Findings .....	28
3. A PROCEDURE TO SELECT WORKING FLUIDS FOR SOLAR ORGANIC RANKINE CYCLES .....	35
3.1. Introduction .....	35
3.2. Preliminary Selection .....	36
3.3. Thermodynamic cycle .....	37
3.4. Analysis.....	42
3.4.1 Basic cycle.....	42
3.4.2 Regenerative cycle.....	49
3.5. Results and discussion.....	51
3.5.1. Dominant factors influencing the performance of an ORC.....	51
3.5.2. Maximum thermal efficiency of the ORC for different working fluids .....	52
3.5.3. Comparing procedure of preselected working fluids .....	54
3.5.4. Exergy efficiency enhancement in a solar ORC.....	60
3.6. Conclusions .....	68
4. EXERGOECONOMIC ANALYSIS OF SOLAR ORGANIC RANKINE CYCLE FOR A BUILDING IN HOT AND HUMID CLIMATE .....	72
4.1 Introduction .....	72
4.2 TRNSYS Software .....	73
4.3 Building and GSHP System Description .....	74
4.4 Building and GSHP System Modeling Details .....	75
4.5 Calibration Procedure.....	80
4.6 ORC System Modeling Details .....	84
4.7 The Optimal Solar ORC Components and Working Condition.....	89
4.8 Solar Radiation Intensity Effect on the Solar ORC Performance .....	95



4.9 Economic Comparison between the Solar ORC and PV Panel System.....	98
4.10 Exergoeconomic Analysis of the Optimal Solar ORC System.....	104
4.11 Conclusions .....	108
5. CONCLUSIONS AND FUTURE WORK.....	110
5.1 Conclusions .....	110
5.1 Future work .....	115
LIST OF REFERENCES.....	116
VITA.....	119

## LIST OF TABLES

TABLE	PAGE
Table 2.1 Optimization results for a regenerative biomass ORC (Drescher and Bruggemann, 2007).....	16
Table 2.2 Optimization results for a regenerative waste heat ORC for fluids with different molecular complexity (Invernizzi et al., 2007).....	21
Table 2.3 Summary of the most important characteristics of the fluids and cycle for selected fluids.....	31
Table 2.3 Summary of the most important characteristics of the fluids and cycle for selected fluids (Continued).....	32
Table 3.1 Preselected working fluids.....	38
Table 3.2 Practical limits of the ORC for preselected working fluids.....	41
Table 3.3 Values of the coefficients for the thermal loss coefficient of the LS-3 PTC absorber tube [Delgado-Torres and Garcia-Rodriguez (2007a)].....	48
Table 3.4 Maximum delivery of an ORC employing different working fluids.....	53
Table 3.5 Regeneration Effects on thermal efficiency, exergy efficiency, and irreversibility of a solar ORC employing IND300 and LS-3 solar collectors for different working fluids.....	64
Table 3.6 Molecular complexity of working fluids.....	65
Table 4.1 Key properties of constituent layers of the building envelope’s main components.....	76
Table 4.2 Made assumptions in modeling building and GSHP.....	81
Table 4.3 Temperature difference between the inside and outside of the building for February and March in Pensacola based on measured data and simulation results.....	85
Table 4.4 Power consumption of the building in Pensacola based on simulation results and available billing information.....	86
Table 4.5 Selected solar collector specifications.....	88

Table 4.6 Low temperature flat plate collector ORC system performance and collector requirements for different working fluids in Pensacola.....	91
Table 4.7 Low temperature evacuated tube collector ORC system performance and collector requirements for different working fluids in Pensacola.....	92
Table 4.8 Medium temperature evacuated tube collector ORC system performance and collector requirements for different working fluids in Pensacola.....	93
Table 4.9 Annual power demand of the building and the annual power generation per collector unit for the solar ORC which employs evacuated tube collector and Isopentane as the working fluid for Pensacola, Miami and Houston.....	98
Table 4.10 Derate factors for AC power rating at Standard Testing Condition .....	101
Table 4.11 Selected PV panel and inverter specifications .....	103
Table 4.12 Required area and total cost for the suggested solar ORC system (employing low-temperature evacuated tube and Isopentane as working fluid) and PV panel system to maintain the power demand of the building .....	104
Table 4.13 The exergy loss, capital cost, payback period and $R_{ex}$ of the ORC system which employs low temperature evacuated tube collector for different working fluids in Pensacola.....	106

## LIST OF FIGURES

FIGURE	PAGE
Fig. 2.1 Framework of the research. ....	8
Fig. 2.1 Organic fluids with lower specific vaporization heat produce less irreversibility (Larjola, 1995).....	12
Fig. 2.2 (a) Plant layout (b) Typical T-S diagram for a regenerative ORC (Drescher and Bruggemann, 2007).....	17
Fig. 2.3 The effect of molecular complexity on the T <sub>r</sub> -S diagram (Mago et al., 2008)....	19
Fig. 2.4 Parabolic Trough Collector (PTC) .....	26
Fig. 2.5 Pressure ratios and vapor expansion ratio across the turbine for selected fluids	33
Fig. 2.6 Variation of the fluid and cycle characteristics for linear hydrocarbons.....	33
Fig. 2.7 Variation of the critical temperature, boiling temperature and efficiency for refrigerants .....	34
Fig. 3.1 Higher pressure limit of the ORC.....	40
Fig. 3.2 Actual saturated basic ORC.....	43
Fig. 3.3 Enthalpy calculation procedure in a saturated basic ORC .....	44
Fig. 3.4 Heat transfer components to/from a solar ORC .....	45
Fig. 3.5 Actual saturated regenerative ORC .....	49
Fig. 3.6 Supplementary enthalpy calculation procedure in a saturated regenerative ORC .....	50
Fig. 3.7 Variation of performance factors with respect to T <sub>eva</sub> of an ORC employing R-236ea as working fluid (a) VER and w <sub>net</sub> (b) η <sub>th</sub> and η <sub>ex</sub> .....	52
Fig. 3.8 Thermal and exergy efficiency of the ORC for different working fluids at T <sub>eva</sub> =130°C .....	56
Fig. 3.9 Net output power of the ORC for different working fluids at T <sub>eva</sub> =130°C .....	57
Fig. 3.10 Vapor expansion ratio in the ORC for different working fluids at T <sub>eva</sub> =130°C	58

Fig. 3.11 Thermal and exergy efficiency of the ORC for different working fluids at $T_{eva}=85^{\circ}\text{C}$ .....	60
Fig. 3.12 Net output power of the ORC for different working fluids at $T_{eva}=85^{\circ}\text{C}$ .....	61
Fig. 3.13 Vapor expansion ratio in the ORC for different working fluids at $T_{eva}=85^{\circ}\text{C}$ ..	62
Fig. 3.14 (a) Irreversibility reduction, (b) Exergy efficiency enhancement by increasing collector efficiency from 70% to 100% for Isopentane. ....	63
Fig. 3.15 (a) Thermal and exergy efficiency enhancement, (b) Irreversibility reduction by using regenerative ORC based on molecular complexity of working fluids ( $T_{eva}=130^{\circ}\text{C}$ ) .....	66
Fig. 3.16 (a) Thermal and exergy efficiency enhancement, (b) Irreversibility reduction by using regenerative ORC based on molecular complexity of working fluids ( $T_{eva}=85^{\circ}\text{C}$ ) .....	67
Fig. 3.17 Proposed selection procedure of the working fluid in a solar ORC .....	68
Fig 4.1 Building and GSHP system TRNSYS model SketchUp .....	77
Fig 4.2 The building geometry created in Google SketchUp .....	79
Fig 4.3 The electrical power consumption of the north zone heat pump unit based on measured data and simulation results .....	82
Fig 4.4 Monthly average of indoor and outdoor temperatures for each hour of every day in February in Pensacola .....	83
Fig 4.5 Monthly average of indoor and outdoor temperature for each hour of every day in March in Pensacola .....	84
Fig 4.6 Solar collector loop TRNSYS model .....	89
Fig 4.7 Required collector area for running the solar ORC which employs low temperature evacuated tube collector and Isopentane as the working fluid for Pensacola, Miami and Houston.....	95
Fig 4.8 Monthly power generation per collector unit for the solar ORC which employs low temperature evacuated tube collector and Isopentane as the working fluid for Pensacola, Miami and Houston.....	97
Fig 4.9 Monthly average of solar radiation incident upon the collector surface for Miami, Pensacola and Houston .....	97

Fig 4.10 A snapshot of the input page of the PVWatts 2..... 100

Fig 4.11  $R_{ex}$  variation versus ambient temperature for an ORC system which employs  
low temperature evacuated tube collector in Pensacola ..... 107

Fig. 5.1 Proposed selection procedure of the working fluid in a solar ORC ..... 111

## LIST OF SYMBOLS

$C_g$	geometric concentration ratio of solar collector [-]
$Ex$	exergy [W]
$F_e$	dirt degree of the collector mirrors [-]
$G_b$	direct solar irradiance [ $W/m^2$ ]
$h$	specific enthalpy [J/kg]
$K$	incidence angle modifier [-]
$K_g$	capital cost [USD]
$L_{ex}$	exergy loss [W]
$L_{ex}^a$	annual exergy loss [kWh]
$\dot{m}$	mass flow rate [kg/s]
$P$	pressure [Pa]
$P_d^a$	annual power demand of the building [kWh]
$Ph$	higher pressure limit of Rankine cycle [Pa]
$Q$	heat transfer rate [W]
$Q^*$	irradiation rate [W]
$Q_0$	ambient heat loss rate of solar collector [W]
$q$	heat transfer per unit mass [J/kg]
$R$	gas constant [J/kg K]
$R_{ex}$	ratio of the annual exergy loss to the capital cost [kWh/USD]
$s$	specific entropy [J/kg K]
$S_{gen}$	entropy generation rate [W/K]
$\Delta T$	temperature difference [K]

$T$	temperature [K]
$T_{bp}$	boiling point [°C]
$T^*$	apparent sun temperature [K]
$U_{LS}^{abs}$	thermal loss coefficient per unit area of the absorber tube [W/m <sup>2</sup> K]
$W$	power [W]
$w$	power per unit mass [J/kg]

### Greek Symbols

$\varepsilon_{reg}$	regeneration efficiency [-]
$\eta$	efficiency [%]
$\eta_{opt,0}$	collector optical efficiency at a zero incidence angle [%]
$\sigma$	molecular complexity [-]
$\varphi$	angle of incidence of the direct solar radiation [rad]

### Subscripts

a	actual
abs	absorber
c	collector
CHP	combined heat and power
con	condenser
cr	critical
eva	evaporator
ex	exergy



f	saturated liquid
g	saturated vapor
in	inlet flow
inside	inside of the building
j	cycle component index
L	low
ME	measured data
TR	TRNSYS simulation results
net	net output
out	outlet flow
outside	outside of the building
p	pump
r	reduced property
s	isentropic
SV	saturation vapor
t	turbine
th	thermal
WH	water heating
wf	working fluid
0	ambient

## Superscripts

–	average
Sat	saturation state

## Acronyms

DIPPR	Design Institute for Physical Properties
GSHP	Ground Source Heat Pump
HVAC	Heating, Ventilating and Air Conditioning
NZEB	Net Zero Energy Building
ODP	Ozone Depletion Potential
ORC	Organic Rankine Cycle
PTC	Parabolic Trough Collector.
PV	Photovoltaic
SHGC	Solar Heat Gain Coefficient
SRCC	Solar Rating and Certification Corporation
STC	Standard Test Conditions

# CHAPTER 1

## INTRODUCTION

### 1.1 Research Background

Buildings have a significant impact on energy consumption. The Net Zero Energy Building (NZEB) concept is a promising approach to overcoming the energy crisis of our time. The NZEB is a residential or commercial building with greatly reduced energy needs achieved through efficiency gains such that the balance of energy needs can be supplied with renewable technologies on an annual basis. This study is an attempt at achieving NZEB using a solar-assisted geothermal heat pump.

Air conditioning systems are usually the most energy consuming devices in regular residential and commercial buildings especially in hot and humid climates. Among different air conditioning systems, the heat pump is the most common system in which the amount of heat absorption from its condenser in cooling mode, has a great effect on the efficiency of the system. Ground Source Heat Pumps (GSHPs) use the relatively constant temperature of ground. Heat is extracted from the ground and delivered to the space during the winter, and removed from the space and rejected into the ground during the summer. The cooling Energy Efficiency Ratio (EER) of a GSHP is higher than its heating EER which makes the GSHP a better choice for cooling dominated regions. For this reason GSHPs have recently become more popular for residential and commercial space cooling applications.

Electricity generation for a GSHP is another challenge. It is clear that in a net zero energy building, the input energy of the electricity generation system should be a form of

sustainable energy. Solar radiation has the highest capacity and the lowest replenishment time among sustainable energies. There are different technologies available to convert solar radiation to electricity. Because of the low efficiency and high capital costs of PV panels and also the high energy consumption and CO<sub>2</sub> production rate of the manufacturing process of PV panels, this technology has not been widely commercialized for residential and commercial building application. Enhancement of the PV panel manufacturing process may alter this conclusion in the future. Therefore the use of solar irradiation as a heat source to run heat engines is of great interest.

Because of the limitation of solar irradiation and efficiency of collectors, the conventional Rankine cycle is economically feasible only for large scale power plants. The Organic Rankine cycle (ORC) is a substitutive technology which is applicable for small scale power generation for use in residential and commercial buildings. ORC employs low grade heat from different sources such as biomass, geothermal, solar and waste heat of industrial processes. The main difference between ORC and the conventional Rankine cycle is in the working fluid. The boiling point of the working fluid in ORC is much lower than steam, hence there is no need to achieve high temperatures to generate vapor for running a micro-turbine or expander. As a result ORC can be driven at lower temperatures than the Rankine cycles that use water.

Hot and humid climate has been selected for the study due to its high solar intensity and long solar radiation time through the year. In addition in such a cooling dominant region, the GSHP system has a better annual performance and electricity demand profile of the building better follows the electricity generation profile by the solar ORC system.

A solar ORC can be optimized with respect to different parameters. Parameters that will be considered for solar ORC optimization in this study are as follows: the working fluid, the working conditions of the cycle, the cycle configuration and the solar collector type.

In most of the papers that have been reviewed so far ORC optimization has been done for a limited number of fluids or the optimization procedure has been applied on an ORC system using one specific working fluid.

Mago et al. (2008) determined the influence of the boiling point temperature on the system thermal efficiency for both basic and regenerative ORCs by comparing simulation results for R113, R123, R245ca and Isobutane. Angelino et al. (1984) suited the performance of the ORC system employing seven linear hydrocarbons from C<sub>4</sub>H<sub>10</sub> (n-butane) to C<sub>10</sub>H<sub>22</sub> (n-decane). Hung (1995) compared ORC efficiency and irreversibility for selected refrigerants and hydrocarbons. He selected R-113 and R-123 from refrigerants and p-Xylene (C<sub>8</sub>H<sub>10</sub>), Toluene (C<sub>7</sub>H<sub>8</sub>) and Benzene (C<sub>6</sub>H<sub>6</sub>) from aromatic hydrocarbons. Hettiarachchi et al. (2007) compared a geothermal ORC optimum performance for ammonia, R123, n-Pentane and PF5050 as the working fluid. Thermal stability over the range of operating temperatures and a minimal degradation rate over time is the only criteria in the preliminary selection of the working fluids for a given ORC in Prabha's analysis (2006). A regenerative cascade cycle with toluene as the topping fluid and butane as the bottoming fluid is the optimized solar ORC plant relative to this study.

A comparison between Toluene and some selected siloxanes for different superheating temperatures, condensation temperatures and recuperator's efficiencies in a

100 KW power ORC in the medium range temperature has been carried out by Delgado-Torres and Garcia-Rodriguez (2007a).

Karellas and Schuster (2008) studied the effects of using working fluids at their supercritical region on the ORC performance. The R-245fa was chosen as the working fluid for calculations.

As can be seen, because of the wide variety of fluid parameters and the cycle conditions that have been considered in the literature, there have been very limited attempts at systematically categorizing the selection of working fluids, working condition and cycle configuration for an ORC. In addition previous investigations on the ORC using solar heat are very limited and often emphasize the optimized cycle that results in different working conditions for different working fluids. The best performance of each fluid in a Rankine cycle has not been compared under the relatively same benchmark conditions for solar heat applications. The employment of a specific solar collector in a specific geographic region often limits its temperature range. Therefore the highest allowed temperature for a working fluid in the ORC is not necessarily achievable through solar heat source. Therefore it is necessary to develop a meaningful procedure to compare capabilities of working fluids when they are employed in solar Rankine cycles with similar working conditions.

## **1.2 Exergoeconomic Point of View**

Among the methods that have been used to evaluate the performance of a thermal energy system, there are techniques that combine thermodynamic and economic principles. Thermoeconomics is a general term that describes any combination of a

thermodynamic analysis with an economic one. Compared with energy, exergy is a more consistent measure of economic value. Exergoeconomics rests on the philosophy that exergy is the only rational basis for assigning monetary costs to a system's interactions with its surroundings and to the sources of thermodynamic inefficiencies within it. The ratio  $R_{ex}$  of the exergy loss to the capital cost is the key parameter of exergoeconomic analysis of energy systems.

Ozgener et al. (2007) believe that for any technology there is an appropriate value for  $R_{ex}$  where the design of the device is more successful if the  $R_{ex}$  for that device approaches that appropriate value. Rosen et al. (2003a) speculate that mature technologies have achieved a balance of exergy loss and capital cost over the time that is appropriate to the circumstances.

The main perspective in the exergoeconomic analysis of the Solar ORC system in this study is to examine the relation between the exergy loss and the capital cost for the optimal solar ORC system using the exergoeconomic key parameter  $R_{ex}$ .

### **1.3 Objectives and Significance of Study**

Fossil fuel depletion, atmospheric pollution, global warming and ozone layer destruction are serious problems experts face in finding more sustainable ways to satisfy the requirements of human life. Buildings account for 40% of the energy used annually worldwide. In the U.S. about as much construction and demolition waste is produced as municipal garbage. As a result, both the constructions and Heating, Ventilating and Air Conditioning (HVAC) industries are under increasing pressure from government and environmental groups to replace conventional methods with more sustainable processes.

This research can give us applied guidelines for using sustainable resources of energy for space air conditioning. By considering how the solar collector type, solar collector size, working fluid selection, temperature and pressure of each section of cycle influence the exergy loss, as well as their effects on the capital cost of the solar ORC system, for a building with a specific power demand a unique combination of all these parameters - the optimized condition - will be determined. This will inevitably be an important step toward creating a sustainable society.

#### **1.4 Framework of the Research**

This research mainly focuses on employing exergoeconomic principles in order to select optimal working fluids, cycle configuration, solar collector type and operation conditions for solar ORCs to maintain power demand of a building in hot and humid climate. Among above mentioned parameters, the selection of working fluids is the base to determine the optimal performance of ORCs. In other words, other parameters including cycle configuration, solar collector type, and operation conditions are addressed in the selection process of working fluids for solar ORCs.

Chapter 2 presents a comprehensive review on the ORC literature. Second law efficiency and exergetic studies on ORCs have thus far drawn less attention by researchers. In addition, in most of papers that have been reviewed so far ORC optimization has been done for a limited number of fluids or the optimization procedure has been applied on an ORC system using one specific working fluid. In general, there is no systematic procedure in the literature to compare capabilities of working fluids when they are employed in ORCs with similar working conditions.



Chapter 3 is an attempt at filling above mentioned gaps in selecting working fluids for the solar ORCs with a consideration of exergetic measures. In this chapter, a procedure is developed to compare ORC working fluids in two different operation conditions (i.e., two different temperature levels). The comparison is based on fluids molecular components, temperature-entropy diagram of the fluid, and fluid effects on the thermal efficiency, net power generated, vapor expansion ratio, and exergy efficiency of the Rankine cycle. Fluids with the best cycle performance are recognized in two different temperature levels within two different categories of fluids: refrigerants and non-refrigerants. The optimal cycle configuration for the selected working fluids is identified through an exergetic analysis.

In Chapter 4, the optimization process is finalized by identifying the best collector type and its corresponding temperature level, and exergoeconomic principles are applied on the optimal solar ORC. In the first section of chapter 4, the best collector-temperature combination for the solar ORC which maintains the electricity demand of a geothermal air-conditioned commercial building located in Pensacola of Florida is determined with exergetic and economic considerations. Selected fluids in chapter 3 are employed in this analysis. The solar collector loop, building, and geothermal air conditioning system are modeled using TRNSYS. Available electricity bills of the building and the 3-week monitoring data on the performance of the geothermal system are employed to validate the simulation. By the end of this section, the optimal working fluids, cycle configuration, solar collector type, and operation conditions of the solar ORC are determined.

Second section of chapter 4 discusses the exergoeconomic analysis of the optimal

solar ORC system. The analysis shows that the ratio  $R_{ex}$  of the annual exergy loss to the capital cost can be considered a key parameter in optimizing a solar ORC system from the thermodynamic and economic point of view. It also shows that there is a systematic correlation between the exergy loss and capital cost for the investigated solar ORC system. The framework of the research can be summarized and illustrated in Fig. (2.1).

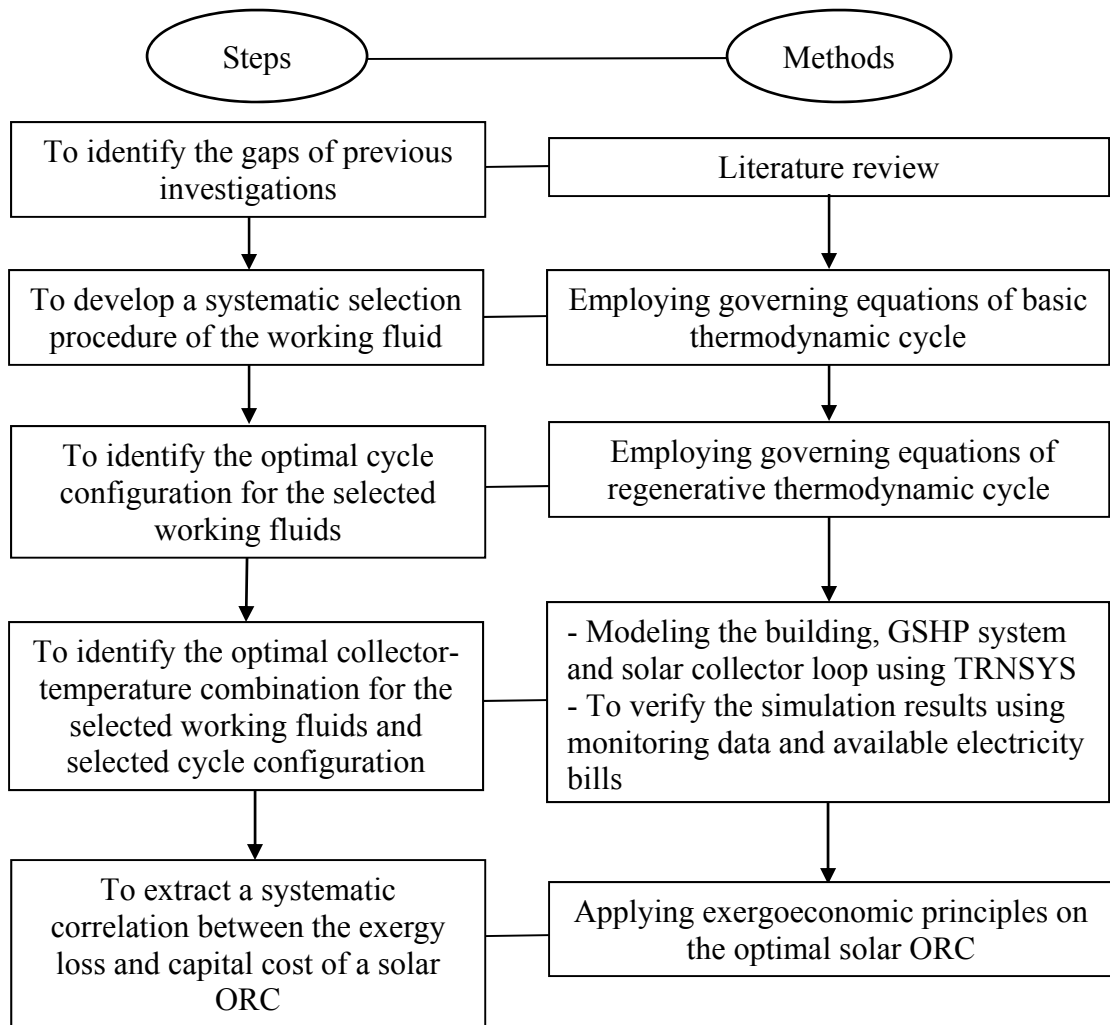


**Fig. 2.1** Framework of the research.

*Note: All steps are taken with exergetic considerations.*

## CHAPTER 2

# A CRITICAL REVIEW ON SINGLE COMPONENT WORKING FLUIDS FOR ORGANIC RANKINE CYCLES (ORCs)

### 2.1 Introduction

The main difference between the ORC and the conventional Rankine cycle is the working fluid. The boiling point of working fluid in the ORC is much lower than steam, hence there is no need to achieve high temperatures to generate vapor for running a micro-turbine or expander. As a result ORCs can be driven at lower temperatures than the Rankine cycles that use water.

The selection of working fluid and operation conditions has a great effect on the system operation, and its energy efficiency and impact on the environment. The selection of working fluid is the base to determine the optimal performance of ORCs. In other words, other optimization parameters including cycle configuration, solar collector type, and operation conditions are addressed in the selection process of working fluids for solar ORCs.

The main advantage of using multicomponent organic fluids in the Rankine cycle is non-isothermal phase change processes in the evaporator and condenser. Siloxanes have the same advantage among single component working fluids. In addition, multicomponent organic fluids cover an unlimited number of fluids and studies on them are more fundamental than practical. For those reasons this literature review has been narrowed to single component working fluids to reach to more practical conclusions.

Single component organic fluids have different categories which have desirable and undesirable properties for use in ORC. This chapter presents a critical review on single component working fluids in Organic Rankine Cycles (ORCs). The study focuses on practical considerations for providing guidelines for the categorization of working fluids based on their capabilities and shortcomings for power generation in a Rankine cycle.

## **2.2 General criteria for Selecting Working Fluids in ORC**

There are some general desirable properties of the working fluids in a thermodynamic cycle regardless of its application that help reduce equipment size and decrease different types of fluid loss (i.e. heat and pressure loss) while passing through a component or fluid interaction with its environment. Some of these desirable properties of working fluids in ORCs can be listed as follows:

- Small specific volume
- Low viscosity and surface tension
- High thermal conductivity
- Suitable thermal stability
- Non-corrosive, non-toxic and compatible with engine materials and lubricating oils
- Moderate vapor pressure in the range (0.1-2.5 Mpa) in the heat exchange units
- High availability and low costs
- Low safety, health and environmental hazards

Low Ozone Depletion Potential (ODP) is one of the most important environmental characteristic of the fluid used as the working fluid in the ORC system. Chlorine containing fluids are not Ozone-safe and have been banned by Montreal protocol and thus should be avoided in new systems.

We can also recognize properties of working fluids that are generally beneficial for ORCs and help us for preliminary selection of fluids before computing calculations.

Depending on the slope of the temperature-entropy curve to be infinity, positive, or negative, working fluids can be classified into isentropic, dry, or wet respectively. Dry or isentropic working fluids are more appropriate for ORC systems. This is because dry or isentropic fluids are superheated after isentropic expansion. Therefore there is no concern for existing liquid droplets at the turbine outlet.

When the heat source is waste heat, organic fluids with lower specific vaporization heat are preferred. Lower vaporization heat of the working fluid causes the heat transfer process in the evaporator to occur mostly at variable temperature. Therefore the temperature profile of the working fluid in the evaporator better follows the temperature profile of heating fluid in the heat source. This means that the temperature difference between fluids in the heat exchanger is reduced as illustrated in Fig. 2.1. Hence the irreversibility in the heat transfer process is decreased.

A few parameters which have the main effects on the cycle's thermodynamic performance are introduced as follows:

- Critical Temperature: At the fixed evaporating temperature ( $T_{eva}$ ) and condensing temperature ( $T_{con}$ ) the higher critical temperature ( $T_{cr}$ ) results in higher pressure ratio but lower condensing pressure which could conflict with

cycle components design.

- Molecular complexity: More complex fluids usually are dry fluids. Majority of organic fluids are fluids with high complexity molecules. This means most organic fluids can satisfy the dry condition to be employed in a Rankine cycle.

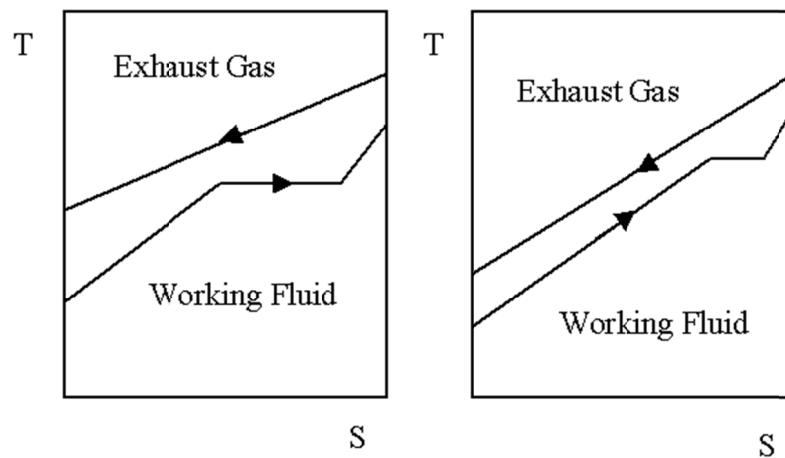


**Fig. 2.1** Organic fluids with lower specific vaporization heat produce less irreversibility (Larjola, 1995)

- Molecular mass: In general for heavy fluids a lower vapor expansion ratio occurs across the turbine. Then the turbine tends to have a low peripheral speed and a small number of stages.

From the structural point of view and type of atoms in the fluid molecule, the ORC working fluids can be categorized under four main classes:

1. Hydrocarbons including linear (n-Butane, n-Pentane), branched (Isobutane, Isopentane), and aromatic hydrocarbons (Toluene, Benzene) have:

- Desirable thermodynamic properties
  - Flammability issues
2. Perfluorocarbons (Fully fluorinated hydrocarbons) (Hexafluorobenzene) are/have:
    - Extremely inert and stable
    - Extreme molecular complexity
    - Thermodynamically undesirable
  3. Partially fluoro-substituted straight chain hydrocarbons
    - There are several zero ODP fluids among them which are of considerable potential interest
  4. Siloxanes (MM, MM/MDM/MD2M)
    - Attractive for a mix of physical and thermal properties (low toxicity and flammability level; high molecular mass; prolonged use as a high temperature heat carrier)
    - They are often available as mixtures rather than as pure fluids
    - Isobaric condensation and evaporation are not isothermal and exhibit a certain glide

As we can see there is no single category of fluids that satisfies all desirable properties for use in an ORC system. Hence after preliminary selection of fluids by discarding chlorine containing and wet fluids, we seek an optimization process that may lead to the final choice for better cycle performance.

In most of papers that have been reviewed so far ORC optimization has been done for a limited number of fluids or the optimization procedure has been applied on an ORC system using one specific working fluid.

Because of the wide variety of fluid parameters and the cycle conditions that have been considered in the literature there have been very limited attempts at systematically categorizing the selection of working fluids for an ORC. In the following sections we will fill this gap by categorizing the results in the literature based on our selection criteria.

### **2.3 Studies Based on Critical Temperature**

Bruno et al. (2008) have accomplished a wide-ranging study on the working fluids in an ORC system that produces energy for running a reverse osmosis desalination system. The authors considered the Aspen plus software library as their reference. At the first step they discarded chlorine included, wet and isentropic fluids.

During the second step for the preliminary selected working fluids the optimum high and low pressure of the saturated cycle maintaining the maximum first law efficiency of the cycle were found.

In general, employing a fluid with higher critical temperature results in higher efficiency but lower condensing pressure. Three groups of fluids can be recognized in the results: (A) fluids with a high efficiency close to 30% with low condensing pressures under atmospheric pressure, such as the siloxane fluids, (B) fluids with atmospheric pressure at the condensing section and with medium efficiency of around 20%, such as n-Pentane and Isopentane. Isopentane has the best performance according to the efficiency (27.2 %) and the minimum pressure in the cycle (1 bar). Therefore Isopentane is the best



choice for the ORC cycle if the heat source can provide the proper evaporating temperature (about 180 °C) (C) there is another group of fluids such as Isobutane working at high condensing pressures showing an efficiency lower than 15%.

For a practical comparison between fluids at this stage, a complementary study is necessary to increase the group A condensing pressure to atmospheric pressure and repeat the simulation process to find the cycle efficiency at new working conditions.

In the last step for four different types of solar collectors the optimization to find the best high temperature in a superheated ORC cycle has been done by Bruno and his coworkers (2008). Generally, superheating in an ORC increases the first law efficiency of the cycle with a very low slope but decreases the second law efficiency of the cycle. Then superheated cycles are never recommended unless in cases which high power output is desired even by running a low efficiency cycle. In addition, in solar cycles increasing the maximum temperature of the collector increases the heat loss from the collector.

Except for the general trend of increasing the efficiency of the cycle with the critical temperature of the working fluid no discussion about the relation between fluid properties and the ORC efficiency can be found in the Bruno and his coworkers' study (2008).

Drescher and Bruggemann (2007) fulfilled an inclusive research to identify the most suitable fluids for ORC in biomass power and heat plants. In this study the Design Institute for Physical Properties (DIPPR) database has been considered as the reference. For preliminary selection, the authors extracted cycle pressure and temperature requirements for an ORC with a biomass heat source from literature.

About 700 substances of the DIPPR database pass the pre-selection criteria and are included in the subsequent comparison.

The efficiency of the 100 best-suited fluids ranges from 24.3% to 25.4% for the regenerative ORC. According to the results, the efficiency rises to approximately 25% at 1 MPa with a slight decrease for higher pressures. The slight decrease can be explained by the needed work of the feed pump. This means that there is an optimal maximum process pressure.

In Drescher and Bruggemann's study (2007), a detailed analysis for typical fluids was carried out to demonstrate critical temperature effect on the cycle efficiency. Results and typical fluid properties are shown in Table 2.1.

**Table 2.1** Optimization results for a regenerative biomass ORC (Drescher and Bruggemann, 2007)

Working fluid	T <sub>cr</sub> (°C)	P <sub>cr</sub> (MPa)	P <sub>max</sub> (MPa)	T <sub>max</sub> (°C)	P <sub>min</sub> (kPa)	T <sub>min</sub> (°C)	[(h <sub>5</sub> -h <sub>4</sub> )/(h <sub>6</sub> -h <sub>3</sub> )] (%)	η (%)
OMTS	291	1.44	1.34	287	13.8	90	15	22.5
Toluene	319	4.11	2.00	263	54.1	90	42	23.2
Ethylbenzene	344	3.61	2.00	297	24.3	90	36	24.3
Propylbenzene	365	3.20	1.41	300	11.4	90	40	24.9
Butylbenzene	388	2.89	0.92	300	5.0	91	43	25.3

To illustrate the influence of vaporization enthalpy (h<sub>5</sub> - h<sub>4</sub>), its ratio to input enthalpy (h<sub>6</sub> - h<sub>3</sub>) has been considered as an index that we call the vaporization enthalpy ratio. Fig. 2.2 shows the different states of the fluid in the plan layout and typical T-S diagram for a regenerative ORC.

Toluene has the highest vaporization enthalpy ratio, but at a low temperature level. Thus, toluene shows the worst efficiency of the alkylbenzenes. On the other hand

OMTS has a high vaporization temperature but the lowest vaporization enthalpy ratio. It has the lowest efficiency of the selected fluids. Therefore both high vaporization temperature and enthalpy result in high ORC efficiency. This means that fluids with a higher critical temperature and wider saturation dome are most efficient fluids for an ORC.

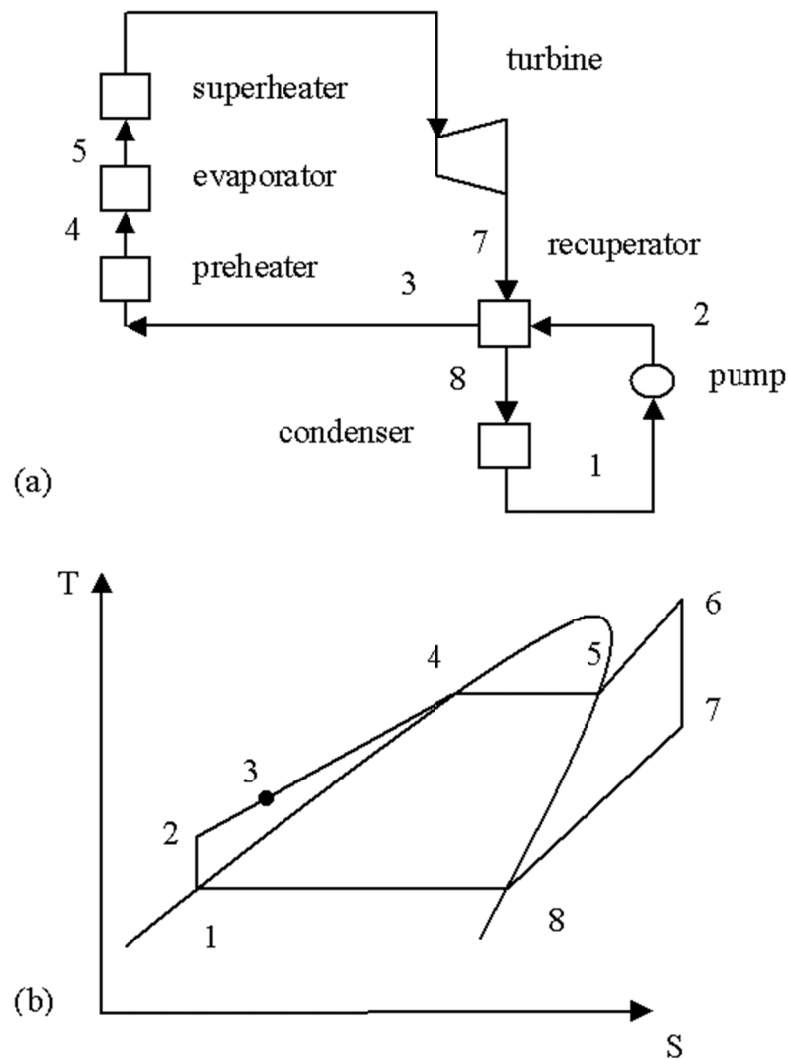


**Fig. 2.2** (a) Plant layout (b) Typical T-S diagram for a regenerative ORC (Drescher and Bruggemann, 2007)

Mago et al. (2008) determined the influence of the boiling point temperature ( $T_{bp}$ ) on the system thermal efficiency for both basic and regenerative ORCs by comparing simulation results for R113, R123, R245ca and Isobutane. Since fluids with higher boiling temperature have higher critical temperature, this study can be considered as a critical temperature based study.

The results demonstrate that the fluid which shows the best thermal efficiency is the one that has the highest boiling point among the selected fluids (R113,  $T_{bp} = 47.59$  °C), while the fluid with the worst thermal efficiency has the lowest boiling point temperature (Isobutane,  $T_{bp} = -11.61$ °C). Therefore, it can be concluded that the higher the boiling point temperature of the organic fluid the better the thermal efficiency that will be achieved by the ORC.

## 2.4 Studies Based on Molecular Complexity

Invernizzi et al. (2007) presented a relation between molecular complexity ( $\sigma$ ) and thermodynamic properties of the fluid. They also introduced the acentric factor ( $\omega$ ) as a new effective factor on the cycle performance. Molecular complexity and acentric factor are defined by equations (2.1) and (2.2) respectively.

$$\sigma = \left(\frac{T_{cr}}{R}\right) \left(\frac{\partial S}{\partial T}\right)_{SV, T_r=0.7} \quad (2.1)$$

$$\omega = -1 - \log(P_r^{Sat})_{T_r=0.7} \quad (2.2)$$

where  $P_r$  and  $T_r$  are reduced pressure and temperature respectively.

The  $\sigma$  is primarily a function of the heat capacity of the vapor and consequently is directly related to the molecular structure of the fluid. As can be seen the molecular complexity is a function of the slope of the temperature-entropy curve. Hence there is a relation between the molecular complexity and wetness of the fluid. For simple molecules the slope of the saturated vapor line in the T-S plan is negative. The slope of the saturated line increases by increasing the molecular complexity of the fluid as illustrated in Fig. 2.3. Thus simple molecule fluids are wet and complex molecule fluids are dry. The acentric factor represented the acentricity or nonsphericity of a molecule; for spherical molecules  $\omega = 0$ . At present, it is used as measure for the complexity of a molecule with respect to both the geometry and polarity.

Invernizzi et al. (2007) believe that as a rule, the critical temperature of a fluid increases with the molecular complexity, but as we will see later this rule is only correct for fluids in the same category (i.e. hydrocarbons or siloxanes). For homologous fluids,  $\sigma$  increases with the number of atoms in the molecule.

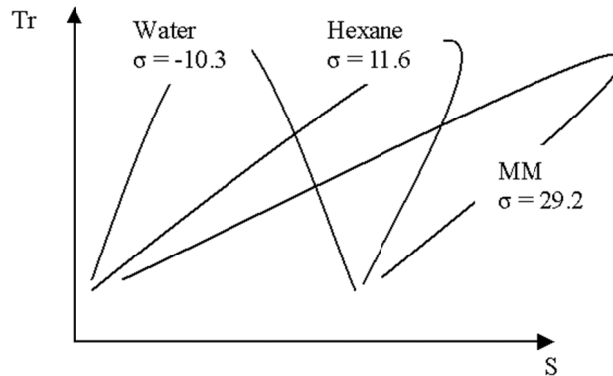


**Fig. 2.3** The effect of molecular complexity on the  $T_r$ -S diagram (Mago et al., 2008)

Invernizzi and his coworkers' analysis has been done for an ORC that employs exhaust gas of a micro –gas turbine as a heat source. The working fluids have been selected from fluids with critical temperatures between 180 °C and 320 °C with positive molecular complexity. Categories of selected fluids are linear and branched hydrocarbons, linear CFCs, aromatic fluoro-carbons, and linear and cyclic siloxanes.

In a comparison made among different working fluids with the same heat source (1 kg/s of 300 °C hot gas), condensing temperature (30 °C) and evaporating temperature (170 °C) it can be seen:

- The ORC thermodynamic efficiency mostly increases with the molecular complexity because of its effect on critical temperature and subsequently on regeneration efficiency.
- At the fixed molecular complexity, fluids with higher  $T_{cr}$  have higher thermodynamic efficiency.
- The overall efficiency is influenced by both thermodynamic and heat recovery efficiencies. The thermodynamic efficiency increases and heat recovery efficiency decreases with increasing molecular complexity  $\sigma$  as implied in Table 2.2. The predominant effect is related to the heat recovery efficiency so that an increase of the molecular complexity  $\sigma$  results in a decrease of the power output of the recovery cycle.
- From this analysis it can be concluded that from a thermodynamic point of view it would be better to employ fluids with a rather low molecular complexity; thanks to the less specific heat duty requested by the regenerator and to their higher capacity of cooling the micro-turbine exhausts.

- Preliminary design of turbine shows us that the lower molecular complexity in single stage turbines lead to lower isentropic efficiency at the same turbine size.

**Table 2.2** Optimization results for a regenerative waste heat ORC for fluids with different molecular complexity (Invernizzi et al., 2007)

Working fluid	n-Pentane	C <sub>6</sub> F <sub>6</sub>	MM	MD2M
Molecular complexity	7	13	29	72
Exit gas temperature	74	90	106	120
Power out put	46	46	43	43

As different types of molecules show different thermal and physical behaviors, it makes more sense if we look for the relationship between cycle operation and fluid properties at least among fluids with some common characteristics.

Study of seven linear hydrocarbons from C<sub>4</sub>H<sub>10</sub> (n-butane) to C<sub>10</sub>H<sub>22</sub> (n-decane) shows the increase in molecular complexity has the effect of rising the fluid critical temperature while reducing its critical pressure. This means the fluid with more molecular complexity has the higher normal boiling point.

For a cycle with the high and low temperatures equal to 100°C and 40°C respectively the following results have been obtained:

- Condensation pressure variation : From 377 to 0.49 kPa
- Evaporation pressure variation: From 1508 to 9.56 kPa
- Pressure ratio variation: From 4 to 20
- Optimized stage rotating speed variation in turbine: From 57000 rpm to 1800 rpm
- Turbine mean diameter variation: From 0.074 to 2.11 m

- Efficiency variation: increasing with molecular complexity, mainly if the cycle includes regeneration.
- Pump work variation: decreasing with molecular complexity

## 2.5 Comparison in Efficiency among Selected Fluids

Hung (1995) compared ORC efficiency and irreversibility for selected refrigerants and hydrocarbons. He selected R-113 and R-123 from refrigerants and p-Xylene ( $C_8H_{10}$ ), Toluene ( $C_7H_8$ ) and Benzene ( $C_6H_6$ ) from aromatic hydrocarbons. A constant 10 MW waste heat source is employed. The cycle is saturated. Irreversibility and efficiency of the cycle have been compared between selected working fluids. Irreversibility changes are completely dependent on the heat source conditions.

At a fixed heat source temperature ( $T_H=600$  K) when turbine inlet pressure varied from 500 to 1800 kPa, the following observations have been made:

- For all fluids, irreversibility of the cycle (**Irr.**) is decreasing with increasing inlet turbine pressure.
- **Irr.** p-Xylene < **Irr.** Toluene < **Irr.** Benzene < **Irr.** R113 < **Irr.** R123
- Among aromatic hydrocarbons : The higher molecular weight, the lower irreversibility

For a fixed temperature difference between the turbine inlet and the heat source ( $15^\circ C$ ) when turbine inlet pressure varied from 800 to 2200 kPa, the following observations have been made:

- **Irr.** R123 < **Irr.** R113 < **Irr.** Benzene < **Irr.** Toluene < **Irr.** p-Xylene
- For all fluids, irreversibility is increasing with increasing inlet turbine



pressure.

ORC efficiency calculations for the selected fluids at different turbine inlet pressures show that:

- $\eta_{R123} < \eta_{R113} < \eta_{Benzene} < \eta_{Toluene} < \eta_{p\text{-Xylene}}$
- For all fluids, efficiency is increasing with increasing inlet turbine pressure.
- The working fluids with higher boiling temperature will have greater efficiency.
- The lower condenser exit temperature (lower ambient temp), the higher efficiency.
- System efficiency and total irreversibility have opposite trends. Using the operation conditions at the intersection point of the efficiency curve and the availability ratio (ratio of the available energy to the total energy obtained from the heat source) curve would lead to the optimal balance between the two conflicting factors.

Hettiarachchi et al. (2007) compared a geothermal ORC optimum performance for ammonia, R123, n-Pentane and PF5050 as the working fluid. The ratio of the total heat exchanger area to net power output is considered as the objective function.

Ammonia has minimum objective function and maximum geothermal water utilization (Net work / Geothermal water mass flow rate), but not necessarily maximum cycle efficiency. PF5050 and Ammonia have the worst performance from the exergy efficiency point of view. This means not considering the objective function, Ammonia cannot be a choice because of its low ORC cycle and exergy efficiency.

The fluids, n-Pentane and R123, have better cycle efficiency than PF5050, although the latter has better physical and chemical characteristics compared to other fluids considered.

Liu et al. (2004) examined the influence of various working fluids on the thermal efficiency and on the total heat-recovery efficiency of ORC for a waste heat recovery system. Finding a relation between the molecular structure of the fluid and its T-S vapor saturation line slope is one of the achievements of Liu and his coworkers' study. The results show that the presence of a hydrogen bond in certain molecules, such as water, ammonia, and ethanol results in wet fluids and is considered as inappropriate for ORC systems. The authors claim that although the thermal efficiency for working fluids with lower critical temperature is lower; the critical temperature of the fluid has not significant effect on the thermal efficiency of the cycle. An explanation for the contradiction between this conclusion and previous studies may lie on the use of a correlation (Watson relation) to calculate the vaporization enthalpy of the fluid by Liu and his coworkers (2004). The heat recovery efficiency is higher for higher inlet temperatures of the waste heat and higher critical temperature fluids. The effect of the heat source temperature profile on the system performance has been approved by the results of Liu and his coworkers' study (2004).

Thermal stability over the range of operating temperatures and a minimal degradation rate over time is the only criteria in preliminary selection of the working fluids for a given ORC in Prabha's analysis (2006).

Benzene is the most thermally stable of the candidate working fluids. Next after Benzene is Toluene. Isobutane is a thermally stable fluid in Low temperature range. In this study the author concentrates on cascade solar ORCs.

A regenerative cascade cycle with toluene as the topping fluid and butane as the bottoming fluid is the optimized solar ORC plant relative to Prabha's study.

A comparison between Toluene and some selected siloxanes for different superheating temperatures, condensation temperatures and recuperator's efficiencies in a 100 KW power ORC in the medium range temperature has been carried out by Delgado-Torres and Garcia-Rodriguez (2007b).

Direct solar vapor generation configuration of solar ORC has been analyzed and characterized with LS3 and IND300 Parabolic Trough Collector (PTC) models. The Parabolic Trough Collector has been depicted in Fig. 2.4.

In the working fluid selection part D4, D5, MM and MD4M were considered from siloxanes. Then D5 and MD4M were discarded because of their low condensation pressure in the temperature range of 35-115 °C. The ORC system with a vaporization temperature 10 to 15°C lower than the critical temperature for each fluid has been simulated.

In a 100 kW gross mechanical output solar ORC with identical condensation temperatures toluene presents the overall efficiency followed by D4 and MM. The difference between toluene and D4 and MM is particularly important if the regeneration process is not considered.

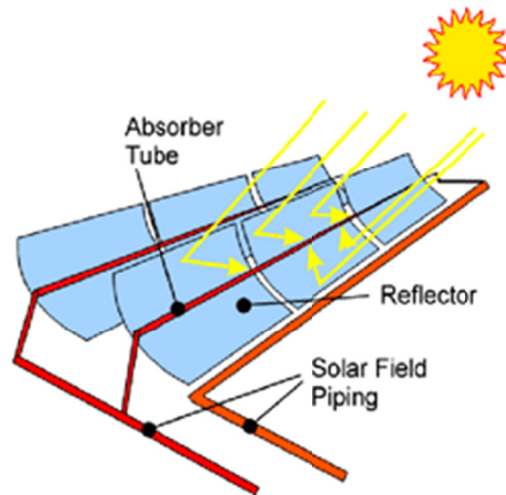


**Fig. 2.4** Parabolic Trough Collector (PTC)

Delgado-Torres and Garcia-Rodriguez (2007b) continued their work with a second ORC that is powered by the thermal power rejected by the top ORC, forming a double cascade ORC. This configuration has been one of the proposed by Prabhu for the system called Solar Trough Organic Rankine Electricity System (STORES).

The top temperature cycle generates 100 kW of raw power with regenerator effectiveness,  $\epsilon_{\text{reg}} = 0.8$  and a condensation temperature of 115°C. The analysis has been done for the top cycle with Toluene and MM as the working fluid. The heat rejected from the top cycle is absorbed by the bottom cycle with a condensation temperature at 35°C. The vaporization temperature of the bottom cycle is equal to 105°C.

Butane, isobutene, pentane, isopentane and neopentane are evaluated among working fluids proposed in the literature for Organic Rankine Cycles within the temperature ranges of the bottom cycles.

From the results obtained, isopentane is selected as the most suitable working fluid for the low temperature cycle since pentane and isopentane shows superior behavior but the normal boiling point of pentane is above 35°C.

It should be pointed out that the above discussion does not consider the difference or similarity of the thermal properties among the fluids.

## **2.6 ORCs at Supercritical Region**

Karellas and Schuster (2008) studied the effects of using working fluids at their supercritical region on the ORC performance. The R-245fa was chosen as the working fluid for calculations. The authors found that in a high temperature ORC that employed exhaust gas at a temperature around 490 °C, supercritical cycle achieved more than 9% relative efficiency gain with respect to the subcritical one.

In the low temperature ORC with a geothermal heat source at temperatures between 80 °C and 160 °C supercritical cycle showed a different behavior. Two working fluids have been taken into consideration because of their critical points: the working fluids R134a and R227ea. In most cases the supercritical cycle has lower thermal efficiency than the subcritical one. The expansion in the turbine ends in the two-phase area, so no recuperator can be used. That is the reason why the thermal efficiency in these cases of supercritical parameters is much lower than the subcritical ones, in which a recuperator is used.

Angelino et al. (2000) showed for a waste heat ORC that using toluene at its supercritical region increased recovered thermal power with respect to the subcritical cycle with no significant change in the cycle thermal efficiency. The Maximum

temperatures for subcritical and supercritical cycles were 308.6 °C and 342.1 °C respectively.

Zhang et al. (2006) analyzed a novel solar energy-powered Rankine cycle for combined power and heat generation using supercritical carbon dioxide. Results show higher efficiency than conventional Rankine cycle with water at maximum temperatures between 32 °C and 177.4 °C but the efficiency is still low (less than 12%) to be proper for practical power plants.

## **2.7 Major Findings**

The above literatures on working fluids for Organic Rankine Cycles (ORCs) can be analyzed as below:

In general, using supercritical cycles are only recommended for relatively high temperature cycles and for lower temperatures the first law efficiency of supercritical cycles are even lower than subcritical ones. In addition, saturation cycles have an advantage of being less expensive and involving simpler heat exchangers.

It can be noticed from the survey that there is no specific category of fluids that satisfies all desirable characteristics for an ORC system. In the majority of papers no specific relation between thermodynamic properties and cycle performance can be recognized.

For the better observation of the results in the literature, a number of fluids have been chosen and the most important characteristics of the fluids and the cycle have been summarized in Table 2.3. In this selection there are four linear hydrocarbons (Pentane, Hexane, Heptane, and Octane), two branched hydrocarbons (Isobutane and Isopentane),

two aromatic hydrocarbons (Benzene and Toluene) and four refrigerants (R218, 113, R123, and R236ea).

The following findings can be illustrated:

- The higher critical temperature allows setting the evaporation temperature at a higher level that leads to the higher efficiency of the cycle.
- In the fluids of one category, at the fixed  $T_{\text{eva}}$  and  $T_{\text{con}}$ , the higher critical temperature results in higher pressure ratio but lower condensing pressure.
- Fluids with higher pressure ratio in the cycle have higher vapor expansion ratio across the turbine as illustrated in Fig. 2.5. Thus the higher vapor expansion ratio is an undesirable subsequence of using high critical temperature fluid in a Rankine cycle. If for a small amount of work, a high vapor expansion ratio occurs across the turbine, supersonic flow problems, higher turbine size or greater number of stages are inevitable.
- Generally, high efficiency ORCs are achievable by using hydrocarbons rather than refrigerants. It means hydrocarbons have a higher potential to produce power in a Rankine cycle than refrigerants because of their relatively high critical temperature. But Hydrocarbons are more flammable in comparison with refrigerants.
- The molecular complexity increases with the number of atoms in the molecule for homologous fluids.
- In linear hydrocarbons fluids with higher number of atoms have higher critical and boiling temperatures, higher molecular complexity, and higher molecular

mass and higher efficiency. As shown in Fig. 2.6, the variation of above mentioned parameters, excluding efficiency, is very close to linear with respect to the number of atoms in the molecule.

- Except in linear hydrocarbons no relation between molecular mass and cycle efficiency can be recognized.
- In hydrocarbons, acentric factor increases with their molecular complexity. Thus acentric factor can be used as an index to compare hydrocarbons' wetness.
- Molecular mass mostly is in inverse relation with vapor expansion ratio across the turbine. Therefore turbines in cycles using heavier fluids are smaller or have less number of stages.
- Among refrigerants, fluids with higher critical temperature have higher normal boiling point and higher efficiency as demonstrated in Fig. 2.7.

As different fluids show different pros and cons, fluid selection is completely dependent on the priorities in the project design. Hence, after preliminary selection of fluids by discarding chlorine containing and wet fluids, the optimization process gives us the final choice for better cycle performance. Second law efficiency and exergetic studies on ORCs have thus far drawn less attention by researchers. In general, there is no systematic procedure in the literature to compare capabilities of working fluids when they are employed in ORCs with similar working conditions. In chapter 3 a study to fill these gaps for the solar ORCs will be done.



**Table 2.3** Summary of the most important characteristics of the fluids and cycle for selected fluids

Fluid	Isobutane	Isopentane	n-Pentane	n-Hexane	n-Heptane	n-Octane
Relative Vapor Density (air=1)	2	2.2	1.8	1.3	3.46	3.94
NFPA, NPCA-HMIS Hazard Codes	Health	1	1	1	1	0
	Flammability	4	4	4	3	3
	Instability /Reactivity	0	0	0	0	0
Flash Point (°C)	Flammable Gas	< -51	- 49	-23.3	- 4	13
Autoignition Temperature (°C)	460	420	309	225	285	220
Critical Temperature (°C)	134.7	187.2	196.6	234.7	267.0	296.2
Boiling Temperature (°C)	-12	28	36	69	98	126
Reduced $T_{eva}$	0.981	0.981	0.983	0.989	0.988	0.989
Specific Vaporization Heat at $T_h$ (kJ/kg)	116.41	111.45	109.75	85.65	80.95	75.01
Vaporization Heat Ratio at $T_h$ (%)	30.2	25.2	23.9	17.8	15.9	15.4
Vapor Expansion Ratio	13	49	52	180	650	627
Molecular Complexity	1.14	7.20	6.5	11.6	17.6	23.5
Molecular Mass (kg/kmol)	58.1	72.2	72.2	86.2	100.2	114.2
Acentric Factor	0.185	0.2296	0.251	0.299	0.349	0.393
Reported Condition	Saturated regenerative cycle $T_h=126.9^\circ\text{C}$ $P_h=32$ bar $T_l=29.9^\circ\text{C}$ $P_l=4$ bar	Saturated regenerative cycle $T_h=178.5^\circ\text{C}$ $P_h=30$ bar $T_l=26.8^\circ\text{C}$ $P_l=1$ bar	Saturated regenerative cycle $T_h=188.7^\circ\text{C}$ $P_h=30$ bar $T_l=35.9^\circ\text{C}$ $P_l=1$ bar	Saturated regenerativ e cycle $T_h=229^\circ\text{C}$ $P_h=28$ bar $T_l=34.4^\circ\text{C}$ $P_l=0.3$ bar	Saturated regenerative cycle $T_h=260.3^\circ\text{C}$ $P_h=25$ bar $T_l=28.7^\circ\text{C}$ $P_l=0.075$ bar	Saturated regenerative cycle $T_h=289.7^\circ\text{C}$ $P_h=23$ bar $T_l=52.2^\circ\text{C}$ $P_l=0.075$ bar
Efficiency at Reported Condition	13.94	27.2	16.74	29.28	29.67	33.75

**Table 2.3** Summary of the most important characteristics of the fluids and cycle for selected fluids (Continued)

Fluid	Benzene	Toluene	R218	R113	R123	R236ea	
Relative Vapor Density (air=1)	1.2	3.1	6.65	2.9	5.3	N/A	
NFPA, NPCA-HMIS Hazard Codes	Health	2	2	1	1	2	N/A
	Flammability	3	3	0	0	1	N/A
	Instability /Reactivity	0	0	0	1	0	N/A
Flash Point (°C)	-11	4	N/A	N/A	N/A	N/A	
Autoignition Temperature (°C)	498	480	N/A	680	770	N/A	
Critical Temperature (°C)	288.9	318.6	71.9	214.1	183.7	139.3	
Boiling Temperature (°C)	80	111	-36.8	48	27.8	6.2	
Reduced $T_{eva}$	0.960	0.983	0.990	0.958	0.926	0.983	
Specific Vaporization Heat at $T_h$ (kJ/kg)	166.06	104.34	25.55	64.53	93.91	59.20	
Vaporization Heat Ratio at $T_h$ (%)	24.8	18.3	31.1	28.5	42.9	32.12	
Vapor Expansion Ratio	195.5	841.9	4.0	43.9	16.3	14.8	
Molecular Complexity	4.22	8.91	4.68	6.59	1.68	3.02	
Molecular Mass (kg/kmol)	78.1	92.1	188	187.4	152.9	152.0	
Acentric Factor	0.2092	0.266	0.317	0.25253	0.28192	0.3794	
Reported Condition	Saturated basic cycle $T_h=266.5^\circ\text{C}$ $P_h=37$ bar $T_l=40.0^\circ\text{C}$ $P_l=0.25$ bar	Saturated regenerative cycle $T_h=308.4^\circ\text{C}$ $P_h=35$ bar $T_l=39.5^\circ\text{C}$ $P_l=0.075$ bar	Saturated regenerative cycle $T_h=68.6^\circ\text{C}$ $P_h=25$ bar $T_l=29.9^\circ\text{C}$ $P_l=10$ bar	Saturated basic cycle $T_h=193.5^\circ\text{C}$ C $P_h=25$ bar $T_l=40.0^\circ\text{C}$ $P_l=0.78$ bar	Saturated basic cycle $T_h=150.0^\circ\text{C}$ $P_h=21$ bar $T_l=40^\circ\text{C}$ $P_l=1.54$ bar	Saturated regenerative cycle $T_h=132.2^\circ\text{C}$ $P_h=30$ bar $T_l=36.4^\circ\text{C}$ $P_l=3.00$ bar	
Efficiency at Reported Condition	24.5	29.43	4.6	18.2	15.9	13.67	

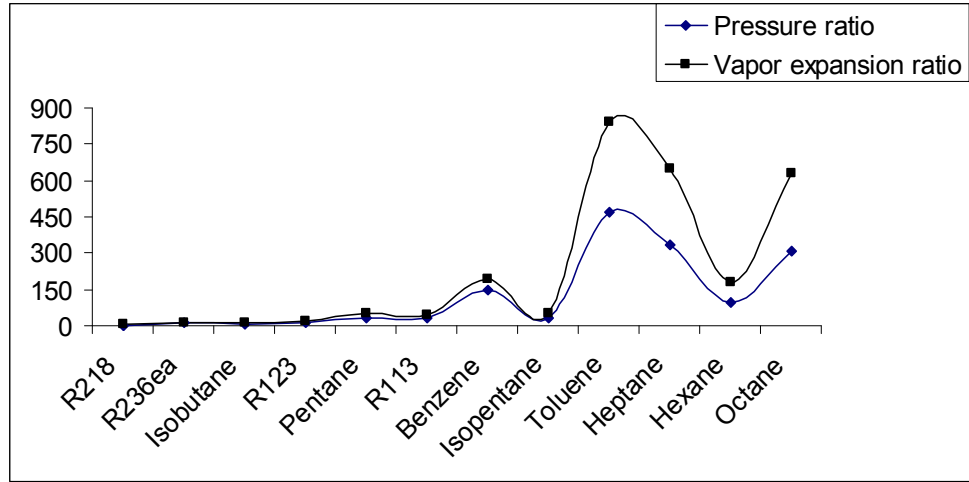


**Fig. 2.5** Pressure ratios and vapor expansion ratio across the turbine for selected fluids

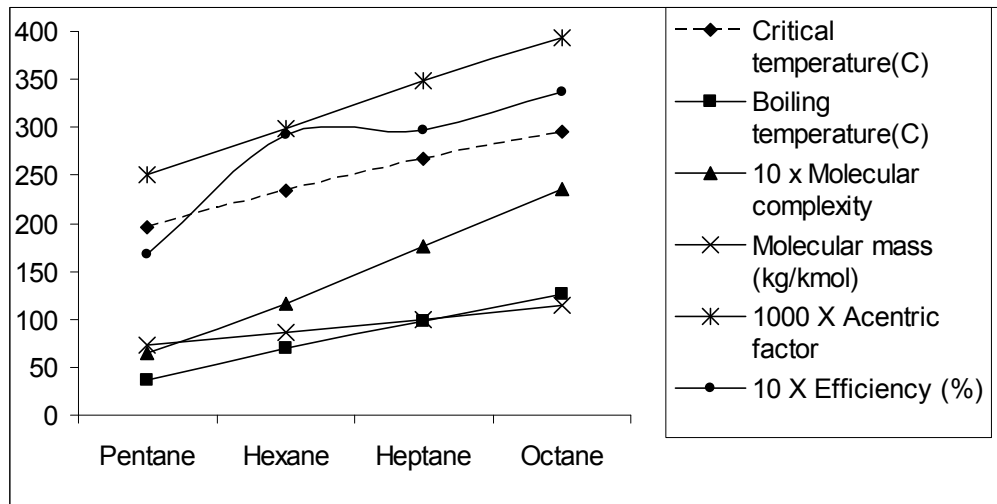


**Fig. 2.6** Variation of the fluid and cycle characteristics for linear hydrocarbons

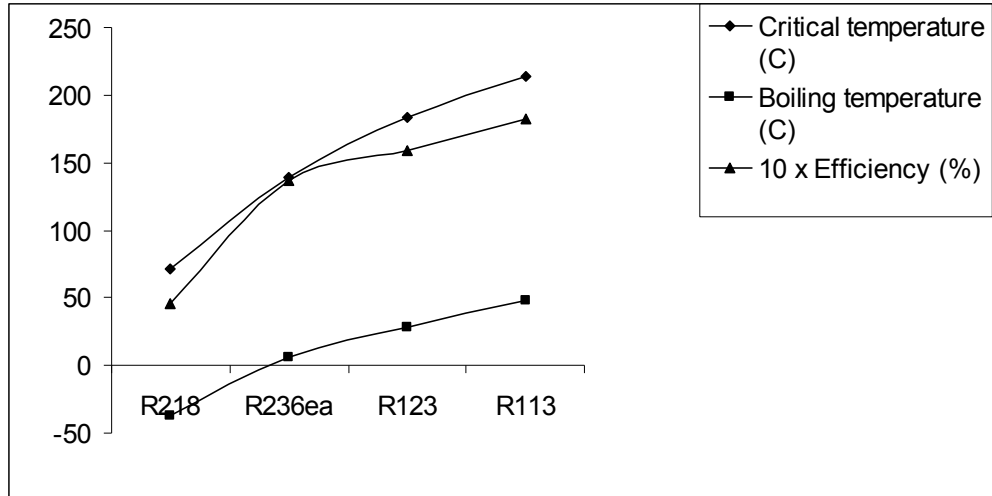


**Fig. 2.7** Variation of the critical temperature, boiling temperature and efficiency for refrigerants

## CHAPTER 3

### A PROCEDURE TO SELECT WORKING FLUIDS FOR SOLAR ORGANIC RANKINE CYCLES

#### 3.1. Introduction

Previous investigations on the ORC using solar heat are very limited and often emphasize the optimized cycle that results in different working conditions for different working fluids. The best performance of each fluid in a Rankine cycle has not been compared under the relatively same benchmark conditions for solar heat applications in previous studies. The employment of a specific solar collector in a specific geographic region often limits its temperature range. Therefore the highest allowed temperature for a working fluid in the ORC is not necessarily achievable through a solar heat source. The main purpose of this study is to develop a meaningful procedure to compare capabilities of working fluids when they are employed in solar Rankine cycles with similar working conditions.

The procedure is presented based on working fluids molecular components, temperature-entropy diagram and fluid effects on thermal efficiency, net power generated, vapor expansion ratio, and exergy efficiency of the Rankine cycle. Refprop 8.0 database has been considered as the reference in this study. This program, developed by the National Institute of Standards and Technology, provides tables and plots of the thermodynamic and transport properties of industrially important fluids and their mixtures with an emphasis on refrigerants and hydrocarbons. Refprop 8.0 consists of 85 pure fluids and 55 predefined mixtures. Among them 63 pure fluids and 54 predefined

mixtures are organic. R508A and R508B have very low critical temperatures. Therefore they are not proper to be employed in a Rankine cycle. A total of 115 pure fluids and predefined mixtures from the Refprop 8.0 database are investigated.

Irreversibility in solar thermal systems is relatively high because of the high temperature difference between the solar collector and the apparent sun temperature. Important factors that could lead to irreversibility reduction of the solar ORC by collector efficiency improvement and using regenerative cycles are investigated at the last section of this chapter.

### **3.2. Preliminary Selection**

In the preliminary selection Chlorine included fluids and wet fluids should be discarded. Chlorine containing fluids are not Ozone-safe and have been banned by Montreal protocol and thus should be avoided in new systems. Among pure fluids of the Refprop 8.0 database, 12 fluids are chlorine included. Six of them are CFCs and six fluids are HCFCs. Among predefined mixtures, there are 28 chlorine included fluids. 23 mixtures are CFC included; three mixtures are HCFC included and two of them include both CFC and HCFC.

Depending on the slope of the temperature-entropy curve to be infinity, positive, or negative, working fluids can be classified into isentropic, dry, or wet respectively. Dry or isentropic working fluids are more appropriate for ORC systems. This is because dry or isentropic fluids are superheated after isentropic expansion. Therefore there is no concern for existing liquid droplets at the turbine outlet. The slope of the temperature-entropy curve for some wet fluids is very close to infinity. Furthermore the isentropic

efficiency of turbine is less than 100% in the practical cycle. Subsequently the turbine outlet will be in the dry region that means employing such a fluid causes no problem for the turbine. There are four wet fluids among the final preselected fluids. Table 3.1 shows the critical properties of preselected organic fluids with their critical properties.

### **3.3. Thermodynamic cycle**

The heat absorption process in an ORC may end in a saturated vapor state or superheated vapor state. Generally, superheating in an ORC increases the thermal efficiency of the cycle with a very low slope but decreases the exergy efficiency of the cycle. Then superheated cycles are never recommended unless in order to gain more power at the expense of losing efficiency. In addition, increasing the maximum temperature of the collector in solar cycles increases the heat loss of it. Because of these reasons the saturated Rankine cycle has been investigated in this study instead of a superheated cycle.

Assumptions of the analysis are as follows: steady state condition; no pressure drop in heat exchangers and connecting pipes, and isentropic efficiencies of the pump and the turbine are equal to 0.8.

During the next step we should determine the practical pressure and temperature limits of the cycle. As the higher pressure ratio leads to a higher efficiency, we prefer to expand higher and lower pressure limits of the cycle, but there are always some practical restrictions.

**Table 3.1** Preselected working fluids

Working fluid	Alternative name(s)	P <sub>cr</sub> (MPa)	T <sub>cr</sub> (°C)
Acetone*	-	4.700	234.9
Benzene	-	4.894	288.9
Butane	-	3.796	152.0
Butene	-	4.005	146.1
Perfluorobutane	C <sub>4</sub> F <sub>10</sub>	2.323	113.2
Perfluoropentane	C <sub>5</sub> F <sub>12</sub>	2.045	147.4
Cis-butene	-	4.225	162.6
Cyclohexane	-	4.075	280.5
Decane	-	2.103	344.5
Dodecane	-	1.817	384.9
Difluoromethane	R32, E134	4.228	147.1
Heptane	-	2.736	267.0
Hexane	-	3.034	234.7
Isobutane	-	3.64	134.7
Isobutene	-	4.010	144.9
Isohexane	-	3.040	224.5
Isopentane	-	3.396	187.2
Neopentane	-	3.196	160.6
Nonane	-	2.281	321.4
Octane	-	2.497	296.2
Pentane	-	3.370	196.5
Octafluoropropane	R218	2.640	71.9
1,1,1,2,3,3,3-Heptafluoropropane	R-227ea	2.999	102.8
1,1,1,2,3,3-Hexafluoropropane	R-236ea	3.502	139.3
1,1,1,3,3,3-Hexafluoropropane	R-236fa	3.200	124.9
1,1,2,2,3-Pentafluoropropane	R-245ca	3.925	174.42
1,1,1,3,3-Pentafluoropropane	R-245fa	3.640	154.0
1,1,1,3,3-Pentafluorobutane	R-365mfc	3.240	186.75
Octafluorocyclobutane	R-C318	2.777	115.2
Toluene	-	4.126	318.6
Trans-butene	-	4.027	155.5
R413A <sup>a</sup>	-	4.022	96.6
R423A <sup>a</sup>	-	3.563	99.1
R426A <sup>a</sup>	-	4.088	99.8

\* Wet fluids



Near critical pressure, small changes in temperature are equivalent to large changes in pressure that make the system unstable. Therefore a reasonable distance between the higher limit of the cycle and the critical point of the fluid should be considered. But there is no unique interpretation of the reasonable distance from critical point in the literature. Drescher and Bruggemann (2007) suggested setting the higher pressure limit of the cycle 0.1 MPa lower than critical pressure. Delgado-Torres and Garcia-Rodriguez (2007b) considered the higher temperature of the cycle to be 10-15 °C lower than critical temperature. Because of the difference between the critical properties of working fluids, a fixed pressure or temperature interval near the critical point of the fluid may not be a consistent way to determine the distance between the higher limit of the cycle and the critical point of the fluid. For example a 15 °C temperature difference next to the critical point of Dodecane is equivalent to a 0.332 MPa pressure difference, while for R-227ea it is equivalent to 0.800 MPa.

The slope of the temperature –entropy diagram has been used to determine the higher limit of the Rankine cycle in this study. To avoid the presence of liquid in every single section of the turbine, the highest input pressure of the turbine is the pressure that the slope of temperature-entropy diagram is equal to infinity at that point (point “A” in Fig. 3.1). Calculating the higher pressure and temperature limit of the cycle based on this criterion shows that for most of fluids a large capacity of producing power is neglected. For example for R32 and Cis-butene, point “A” is 45.1°C and 44.6°C lower than their own critical temperature respectively.

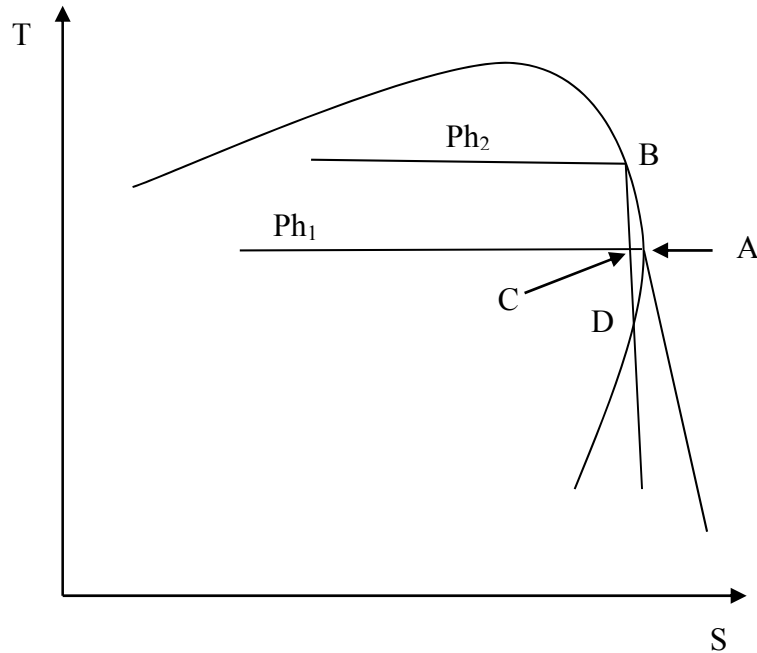


**Fig. 3.1** Higher pressure limit of the ORC

To modify this criterion, increasing the higher limit of the cycle in expense of liquid droplet presence across a small portion of the turbine process is proposed. As has been shown in Fig. 3.1, by increasing the higher pressure limit of the cycle from  $Ph_1$  to  $Ph_2$  liquid droplets present in the turbine across BD. The maximum mass fraction of liquid in this process belongs to point C. In the modified method the highest allowed mass fraction of the liquid across the turbine is restricted to one percent. In this method for both R32 and Cis-butene, higher pressure limit of the cycles are  $25^\circ\text{C}$  lower than their own critical temperature.

Condensing temperature has been set to  $25^\circ\text{C}$  in this study. If necessary, the condenser temperature is raised to make the condenser pressure equal to 5 kPa, the lowest pressure accepted for the condenser. Table 3.2 shows the practical higher and lower limit

of the cycle for each working fluid. Decane, Dodecane, Octane, and Nonane are removed from the list because of their high condensing temperatures.

**Table 3.2** Practical limits of the ORC for preselected working fluids

Working fluid	Maximum $P_{eva}$ (MPa)	Maximum $T_{eva}$ (°C)	Minimum $P_{con}$ (kPa)	Minimum $T_{con}$ (°C)
Acetone	3.379	213	30.7	25
Benzene	4.067	274	12.7	25
Butane	3.013	138	234.7	25
Butene	2.808	125	297.2	25
C <sub>4</sub> F <sub>10</sub>	2.057	107	268.3	25
C <sub>5</sub> F <sub>12</sub>	1.803	141	84.7	25
Cis-butene	3.035	142	213.7	25
Cyclohexane	3.665	272	13.0	25
Decane	1.896	337	5.1	85
Dodecane	1.723	381	5.1	121
E134	2.747	125	212.8	25
Heptane	2.410	258	6.1	25
Hexane	2.680	226	20.2	25
Isobutane	2.890	121	350.5	25
Isobutene	2.877	125	305.0	25
Isohexane	2.682	216	28.2	25
Isopentane	2.887	177	91.8	25
Neopentane	2.788	152	171.4	25
Nonane	2.059	314	5.0	65
Octane	2.200	287	5.0	44
Pentane	2.865	186	68.3	25
R218	1.899	57	867.5	25
R-227ea	2.352	91	455.2	25
R-236ea	2.955	132	205.9	25
R-236fa	2.288	108	272.4	25
R-245ca	2.951	158	100.8	25
R-245fa	2.817	140	149.4	25
R-365mfc	2.712	177	53.4	25
R-C318	2.314	106	312.5	25
Toluene	3.576	307	5.1	31
Trans-butene	2.906	136	234.1	25
R413A	1.839	59	720.2	25
R423A	2.966	90	598.0	25
R426A	1.562	55	687.8	25

### 3.4. Analysis

The equations used to calculate the different parameters to evaluate the performance of the cycle are presented in this section. The first law of thermodynamics is applied to the individual components of the cycle and the second law of thermodynamics is applied to the whole cycle to determine heat transfer, work input and output, and irreversibility of the cycle. The first law of thermodynamics for steady state steady flow processes when potential and kinetic energy changes are negligible can be expressed as:

$$Q - W = \dot{m}(h_{out} - h_{in}) \quad (3.1)$$

where  $Q$ ,  $W$ ,  $\dot{m}$ ,  $h_{out}$  and  $h_{in}$  are the heat transfer rate, the power exchange, the mass flow rate and outgoing and incoming flow enthalpies respectively.

The irreversibility rate for a cycle in steady state steady flow condition can be expressed as:

$$L_{ex} = T_0 S_{gen} = T_0 \dot{m} \sum (q_j / T_j) = Ex_{in} - Ex_{out} \quad (3.2)$$

where  $L_{ex}$ ,  $T_0$ ,  $S_{gen}$ ,  $Ex_{in}$  and  $Ex_{out}$  are the irreversibility (exergy loss), the entropy generation rate and incoming and outgoing exergy flows respectively.  $q_j$  is the heat transfer per unit mass and  $T_j$  is the temperature of the  $j^{\text{th}}$  component of the cycle.

#### 3.4.1 Basic cycle

Fig. 3.2 shows a general representation of the actual saturated basic Rankine cycle in the T-s diagram considering assumptions that were mentioned in the previous section.

States  $1a$  and  $3a$  are the actual exit states of the pump and the turbine, respectively, and  $1s$  and  $3s$  are the corresponding states for the isentropic case. Heat transfer and power in each component of the cycle are calculated by applying the first law of thermodynamics on them.

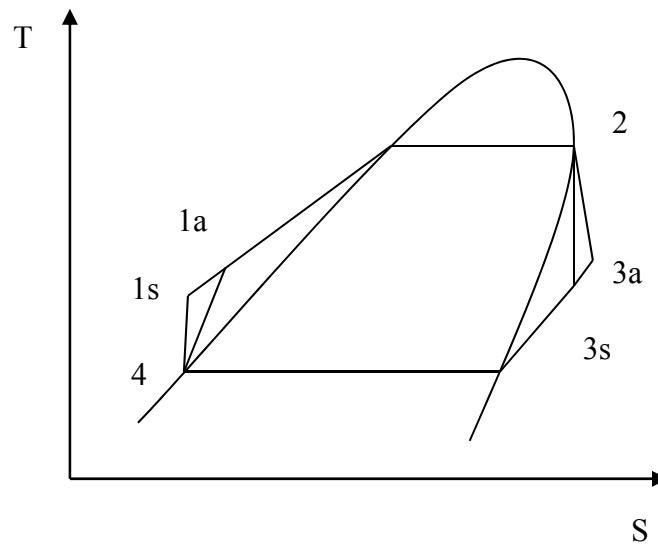


**Fig. 3.2** Actual saturated basic ORC

Evaporator:

$$q_{eva} = h_2 - h_{1a} \quad (3.3)$$

Turbine/ Expander:

$$w_t = h_2 - h_{3a} \quad (3.4)$$

Condenser:

$$q_{con} = h_{3a} - h_4 \quad (3.5)$$

Pump:

$$w_p = h_{1a} - h_4 \quad (3.6)$$

where  $q_{eva}$ ,  $w_t$ ,  $q_{con}$ , and  $w_p$  are absolute values of heat transfer in evaporator, turbine power, heat transfer in condenser and pump power respectively.

The thermal efficiency of the cycle is:

$$\eta_{th} = \frac{(h_2 - h_{3a}) - (h_{1a} - h_4)}{h_2 - h_{1a}} \quad (3.7)$$

The procedure to calculate required enthalpies has been depicted in Fig. 3.3.

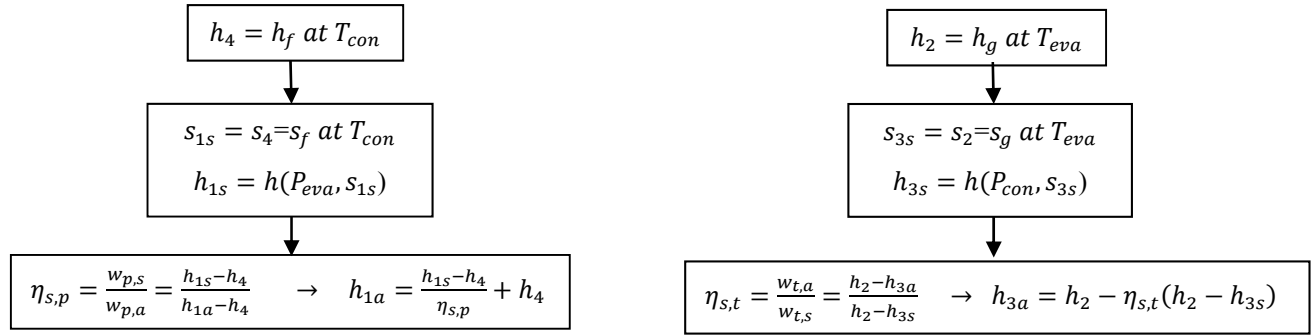


**Fig. 3.3** Enthalpy calculation procedure in a saturated basic ORC

Heat transfer components to/from a solar ORC have been shown in Fig. 3.4. The solar collector receives solar radiation at the rate  $Q^*$ .  $Q_0$  and  $Q_{con}$  represent the solar collector ambient heat loss and heat rejection through the condenser respectively. Eq. (3.2) can be rewritten as:

$$S_{gen} = \frac{Q_0}{T_0} + \frac{Q_{con}}{T_L} - \frac{Q^*}{T^*} \quad (3.8)$$

where  $T^*$  is the apparent sun temperature as an exergy source,  $T_0$  is the ambient temperature, and  $T_L$  is the temperature of the heat carrying fluid in condenser. In this study the value suggested by Petela for  $T^*$  is adopted that is approximately equal to  $\frac{3}{4} T_s$ , where  $T_s$  is the apparent black body temperature of the sun, which is about 6000K. Therefore, the  $T^*$  considered here is 4500 K.

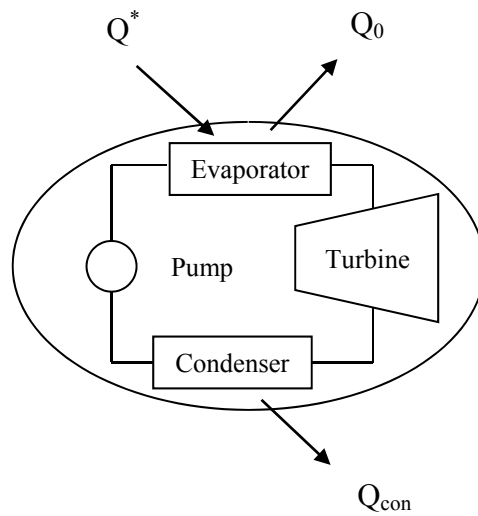


**Fig. 3.4** Heat transfer components to/from a solar ORC

Assuming that the temperature difference between the heat carrying fluid and the condenser is  $\Delta T$  yields

$$T_L = T_{con} - \Delta T \quad (3.9)$$

$\Delta T$  has been considered 15°C in this analysis. The net heat absorption by the evaporator ( $Q_{eva}$ ) will be the difference between the solar radiation received by the collector ( $Q^*$ ) and the solar collector ambient heat loss ( $Q_0$ ).

$$Q_{eva} = Q^* - Q_0 \quad (3.10)$$

The solar collector's efficiency  $\eta_c$  is defined as that fraction of the solar radiation which reaches the receiver and is absorbed there:

$$\eta_c = \frac{Q_{eva}}{Q^*} \quad (3.11)$$

By using Eqs. (3.9), (3.10), and (3.11), Eq. (3.8) can be written as:

$$S_{gen} = \frac{Q_{eva}}{\eta_c} \left[ \frac{1 - \eta_c}{T_0} - \frac{1}{T^*} \right] + \frac{Q_{con}}{T_L} \quad (3.12)$$

The only parameter that we should determine to fulfill calculations is the solar collector efficiency. Every single type of a solar collector has its own formula to calculate its efficiency that is a function of the geometry of the collector and the thermo physical properties of the materials that have been used to build it. In this analysis the Parabolic Trough Collectors (PTCs) suggested by Delgado-Torres and Garcia-Rodriguez (2007a) are adopted: LS-3 and IND300.



The LS-3 model is one of the biggest collectors within the family of commercial PTCs that has been used in some of the largest solar energy plants built in Mojave Desert in California. It was also the PTC chosen to demonstrate the technical feasibility of the direct steam generation process within the scope of Direct Solar Steam (DISS) project.

The efficiency of the LS-3 PTC is given by the following expression:

$$\eta_{LS3}(\bar{T}_{abs}, G_b, \varphi) = \eta_{opt,0} \cdot K(\varphi) \cdot F_e - \frac{U_{LS}^{abs}}{C_g} \cdot \frac{(\bar{T}_{abs} - T_0)}{G_b} \quad (3.13)$$

where  $\eta_{opt,0}$  is the collector efficiency at a zero incidence angle,  $\varphi$  is the angle of incidence of the direct solar radiation,  $K(\varphi)$  is the incidence angle modifier,  $F_e$  is the dirt degree of the collector mirrors,  $U_L^{abs}$  is the thermal loss coefficient per unit area of the absorber tube,  $C_g$  is the geometric concentration ratio,  $\bar{T}_{abs}$  is the absorber's tube average temperature,  $T_0$  is the ambient temperature and  $G_b$  is the direct solar irradiance.

The thermal loss coefficient per unit area of the tube is given by Eq. (3.14).

$$U_{LS}^{abs} = a + b(\bar{T}_{abs} - T_0) + c(\bar{T}_{abs} - T_0)^2 \left[ \frac{W}{m^2 \cdot K} \right] \quad (3.14)$$

The values for the coefficients a, b, and c are shown in Table 3.3. The rest of the parameters in Eq. (3.13) are set as follows:  $\eta_{opt,0} = 0.77$ ,  $K(\varphi) = 1$ ,  $F_e = 0.967$ ,  $C_g = 26.2$ ,  $T_0 = 300K$ , and  $G_b = 850 \text{ W/m}^2$ . In this analysis it has been assumed that the average

temperature of the working fluid in the collector and the average temperature of the absorber's tube are the same.

**Table 3.3** Values of the coefficients for the thermal loss coefficient of the LS-3 PTC absorber tube [Delgado-Torres and Garcia-Rodriguez (2007a)]

	a	b	c
$\bar{T}_{abs} < 200^{\circ}\text{C}$	0.68726	0.002	$2.6 \times 10^{-5}$
$200^{\circ}\text{C} < \bar{T}_{abs} < 300^{\circ}\text{C}$	1.43324	-0.01	$4.6 \times 10^{-5}$
$\bar{T}_{abs} > 300^{\circ}\text{C}$	2.89547	-0.016	$6.5 \times 10^{-5}$

The IND300 model is a smaller PTC in comparison to the LS-3 made by the Israeli company Solel Solar Systems. The IND300 PTC's efficiency is given by Eq. (3.15).

$$\eta_{IND300} = 0.733 - 0.238 \left( \frac{\bar{T}_{wf} - T_0}{G_b} \right) - 0.0013 G_b \left( \frac{\bar{T}_{wf} - T_0}{G_b} \right)^2 \quad (3.15)$$

where  $\bar{T}_{wf}$  is the average temperature of the working fluid in the collector.  $T_0$  and  $G_b$  for IND300 PTC have the same value for the LS-3 model.

The exergy efficiency of the cycle is defined by:

$$\eta_{ex} = \frac{\text{Exergy recovered}}{\text{Exergy supplied}} = \frac{W_{net}}{W_{rev}} = \frac{W_{net}}{W_{net} + L_{ex}} = \frac{W_{net}}{W_{net} + T_0 S_{gen}} \quad (3.16)$$

where  $W_{net}$  is the net power output of the cycle.

### 3.4.2 Regenerative cycle

To reduce the high irreversibility of the solar ORC, regenerative ORC with regeneration efficiency  $\varepsilon_{reg} = 0.8$  has been investigated in this study. Fig. 3.5 shows a general representation of the actual saturated regenerative Rankine cycle in the T-s diagram. Regeneration efficiency is expressed by:

$$\varepsilon_{reg} = \frac{h_5 - h_{1a}}{h_{5'} - h_{1a}} \quad (3.17)$$

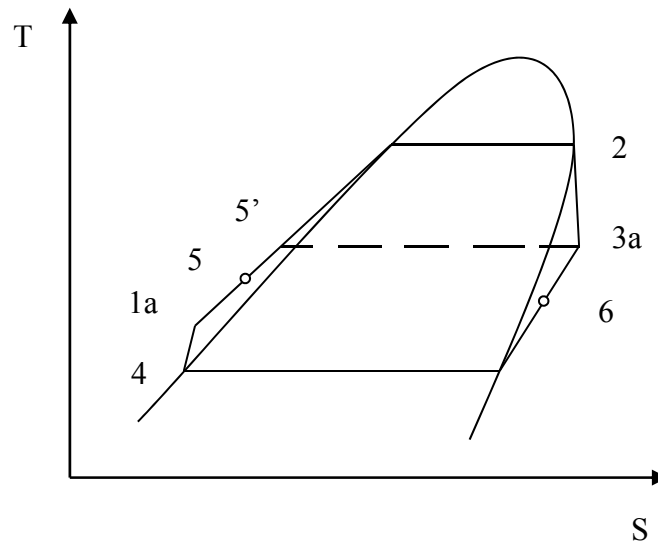


**Fig. 3.5** Actual saturated regenerative ORC

Regeneration has no effect on the turbine and pump power but heat transfer through the evaporator and condenser change in the regenerative cycle in comparison to

the basic cycle. Applying the first law of thermodynamics on the evaporator and condenser processes yields:

Evaporator:

$$q_{eva} = h_2 - h_5 \quad (3.18)$$

Condenser:

$$q_{con} = h_6 - h_4 \quad (3.19)$$

The procedure to calculate enthalpies of common states with basic cycle (4, 1a, 2, and 3a) are exactly the same. The enthalpy calculation procedure of states 5 and 6 has been shown in Fig. 3.6. It should be noticed that in this procedure it is assumed that the regenerator is well insulated and changes in kinetic and potential energies are negligible. For exergy efficiency calculations in the regenerative ORC, the same equations of the basic ORC are applicable.

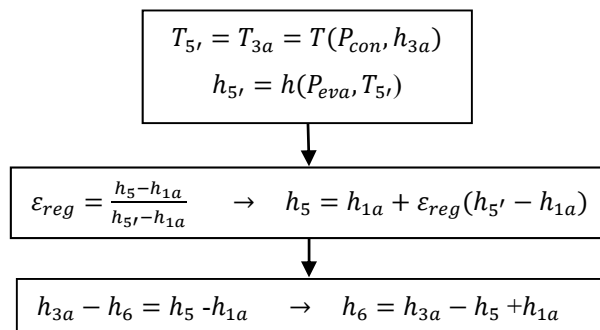


**Fig. 3.6** Supplementary enthalpy calculation procedure in a saturated regenerative ORC

### **3.5. Results and discussion**

In this section four main subjects will be discussed. The first subject is to choose dominant factors influencing the performance of an ORC. The second is the calculation of maximum practical thermal efficiency of an ORC through employing each working fluid. The third subject is to complete the comparing procedure of working fluids, started at section 2, based on their effects on the performance of the ORC. The fourth subject focuses on investigation of different methods to reduce irreversibility of the ORC.

#### **3.5.1. Dominant factors influencing the performance of an ORC**

The first factor which is always the center of attention among different factors in a Rankine cycle is the thermal efficiency or the first law efficiency of the cycle. For a specific working fluid and particular amount of input heat rate the higher thermal efficiency leads to the higher net power output. As we want to compare different working fluids in the Rankine cycle, the net power output should be considered along with the thermal efficiency.

If for a small amount of work, a high vapor expansion ratio occurs across the turbine (VER), supersonic flow problems, higher turbine size or greater number of stages are inevitable. Thus the high vapor expansion ratio across the turbine is an undesirable factor in an ORC. Exergy efficiency or second law efficiency is the factor which helps us to choose working fluids that recover a greater portion of input exergy of the cycle.

Consequently; thermal efficiency, net power output, vapor expansion ratio across the turbine, and exergy efficiency of the cycle are the most important factors to be considered as the performance improvement of an ORC.

### 3.5.2. Maximum thermal efficiency of the ORC for different working fluids

Maximum practical thermal efficiency and corresponding performance factors for preselected working fluids are calculated in this section. Because of the increasing trend of  $\eta_{th}$ ,  $w_{net}$ , VER, and  $\eta_{ex}$  with  $T_{eva}$  in all fluids, their maximum happen at maximum  $T_{eva}$ . Figure 3.7 shows this increasing trend for R-236ea as an example. Calculation results for best possible performance of each working fluid in an ORC can be seen in Table 3.4. Results have been sorted from smallest to largest maximum  $T_{eva}$ .

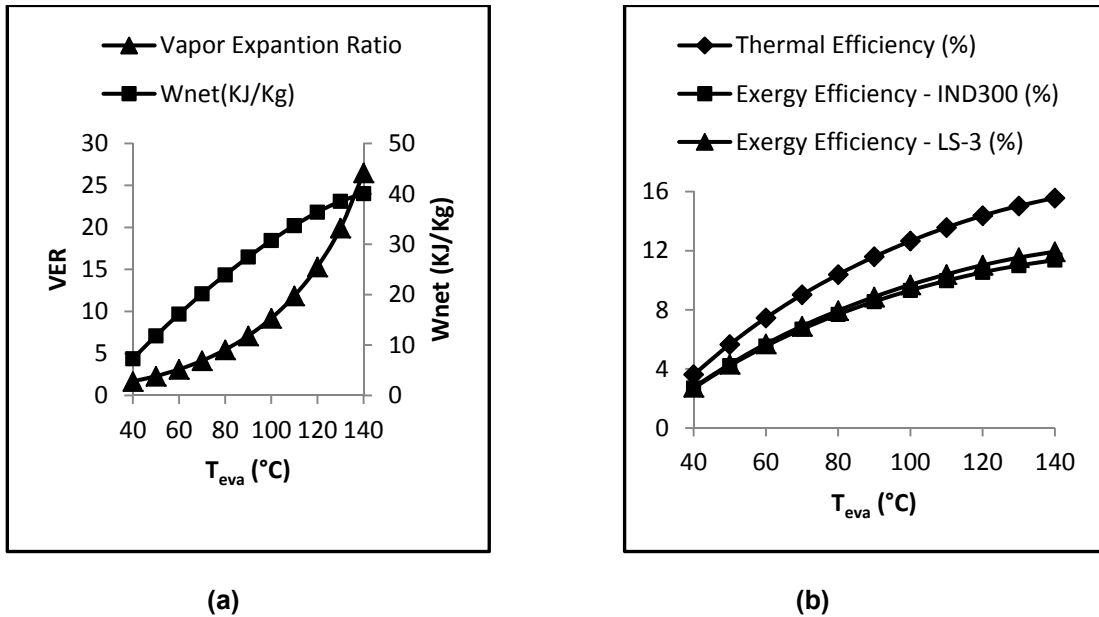


**Fig. 3.7** Variation of performance factors with respect to  $T_{eva}$  of an ORC employing R-236ea as working fluid (a) VER and  $w_{net}$  (b)  $\eta_{th}$  and  $\eta_{ex}$

Results shown in Table 3.4 confirm conclusions of chapter 2. The higher critical temperature allows setting the evaporation temperature at a higher level that leads to the higher thermal efficiency of the cycle. Generally, high thermal efficiency ORCs are achievable by using hydrocarbons rather than refrigerants. This means hydrocarbons have

**Table 3.4** Maximum delivery of an ORC employing different working fluids

Working fluid	Maximum $T_{eva}$ (°C)	Minimum $T_{con}$ (°C)	Maximum $\eta_{th}$ (%)	Maximum $w_{net}$ (KJ/Kg)	Maximum VER	Maximum $\eta_{ex}$ for IND300 (%)	Maximum $\eta_{ex}$ for LS-3 (%)
R426A	55	25	6.37	11.92	2.35	4.74	4.86
R218	57	25	5.73	5.03	2.86	4.28	4.38
R413A	59	25	7.05	12.60	2.66	5.25	5.38
R423A	90	25	10.28	16.50	6.93	7.59	7.85
R-227ea	91	25	10.11	14.06	7.65	7.49	7.74
R-C318	106	25	11.22	16.20	11.74	8.31	8.62
C <sub>4</sub> F <sub>10</sub>	107	25	10.53	13.87	13.47	7.85	8.13
R-236fa	108	25	12.31	22.93	12.02	9.07	9.43
Isobutane	121	25	13.78	58.08	11.73	10.10	10.55
Butene	125	25	14.78	66.53	12.08	8.62	8.94
Isobutene	125	25	14.65	66.27	12.35	10.70	11.20
E134	125	25	14.79	37.08	16.29	10.80	11.31
R-236ea	132	25	14.29	30.40	21.60	10.48	10.97
Trans-butene	136	25	15.84	77.05	16.17	11.53	12.11
Butane	138	25	15.48	74.78	17.61	11.30	11.86
R-245fa	140	25	15.57	40.04	26.50	11.37	11.94
C <sub>5</sub> F <sub>12</sub>	141	25	12.37	21.31	38.19	9.28	9.71
Cis-butene	142	25	16.50	82.09	25.91	11.98	12.62
Neopentane	152	25	15.52	71.78	26.90	11.40	11.99
R-245ca	158	25	16.96	48.20	43.12	12.34	13.03
Isopentane	177	25	17.75	97.10	50.62	12.94	13.75
R-365mfc	177	25	17.55	56.28	84.27	12.82	13.61
Pentane	186	25	18.51	108.12	67.40	13.45	14.34
Acetone	213	25	22.54	155.44	128.27	15.87	17.24
Isohexane	216	25	19.27	123.32	169.34	14.07	15.17
Hexane	226	25	20.08	135.54	232.50	14.59	15.81
Heptane	258	25	20.81	158.24	720.95	15.14	16.64
Cyclohexane	272	25	23.49	170.22	508.92	16.71	18.48
Benzene	274	25	25.79	179.00	428.71	17.88	19.92
Toluene	307	31	25.60	190.82	1106.28	17.87	20.09

a higher potential to produce power in a Rankine cycle than refrigerants because of their relatively high critical temperature. On the other hand hydrocarbons are more flammable in comparison to refrigerants. These results add to previous conclusions that the exergy efficiency has almost the same trend of thermal efficiency with respect to the critical

temperature of the fluid. In general, the same as thermal efficiency, the exergy efficiency of refrigerants are lower than hydrocarbons.

### **3.5.3. Comparing procedure of preselected working fluids**

A specific solar collector in a region with a definite direct solar irradiance can maintain temperatures within restricted limits. Therefore the highest allowed temperature for a working fluid in the ORC is not necessarily achievable through solar heat source. Thus the capabilities of different working fluids should be compared in ORCs with similar collector temperatures. Solar collectors can be categorized based on the temperature level that they can maintain. Generally there are three temperature level solar collectors:

- (1) Low temperature solar collectors: with the output temperature less than 85 °C. Flat plate solar collectors are in this category.
- (2) Medium temperature solar collectors: with the output temperature below 130-150 °C. Most evacuated tube collectors are in this category.
- (3) High temperature solar collectors: with the output temperature higher than 150 °C. Parabolic trough collectors are mainly in this category.

High temperature solar collectors are suitable for large scale power generation applications. In this section a comparison between performance factors of ORCs employing different working fluids at  $T_{eva}=85$  °C and 130°C will be made. Figures (3.8) to (3.13) show variation of performance factors of the ORC for different working fluids at two evaporating temperatures.



As it can be observed for almost all fluids in both evaporating temperatures, the thermal efficiency and exergy efficiency of the ORC have the same trend with respect to changing working fluids. Therefore the thermal efficiency and exergy efficiency of the cycle play the same role in selecting the proper working fluid.

The main criterion to select working fluid is considered the cycle thermal/exergy efficiency in this study. Among fluids with the same order of the cycle thermal/exergy efficiency, the net power output of the ORC is a determinant factor to select the working fluid. The third step will be eliminating fluids with a high VER at the close level of efficiencies and  $w_{net}$ .

As maximum thermal efficiency calculations show and Figures (3.8) to (3.13) confirm, refrigerants have a lower capacity to produce power through the ORC. On the other hand refrigerants are less flammable and in some cases less hazardous than non-refrigerant fluids. Therefore fluids can be analyzed in two different categories: refrigerants and non-refrigerants.

Figures (3.8) and (3.9) show that among refrigerants, R245fa, R265mfc, and R245ca provide higher cycle efficiency and  $w_{net}$ . R365mfc have a higher VER in the cycle but almost the same cycle efficiency and  $w_{net}$  as shown in Fig. (3.10). Thus the final refrigerants selected at medium temperature level ( $T_{eva}=130^{\circ}\text{C}$ ) will be R245fa and R245ca.

For non-refrigerants, at the medium temperature level, Toluene, Cyclohexane, Acetone, and Benzene provide a higher cycle efficiency as illustrated in Fig. (3.8). Among them, Acetone and Benzene produce more  $w_{net}$  as can be recognized in Fig. (3.9). Fig. (3.10) shows that Benzene has higher VER in the cycle, but because of higher cycle

efficiency with respect to Acetone, we will keep it in our final fluids' list. According to Fig (3.8) and (3.9), there are eight non-refrigerant fluids, cycle efficiency and  $w_{net}$  of which are about the same level. However their cycle efficiency and power level is lower than cycle efficiency and power level of the other four non-refrigerant fluids mentioned above, it is good to find the most suitable fluids out of this group to add to the final fluids' list. Fig. (3.10) shows that from this group of eight, Butane , Isopentane, Trans-butene, and Cis-butene have a lower VER in the cycle, so they can be in the final list as medium performance non-refrigerants.

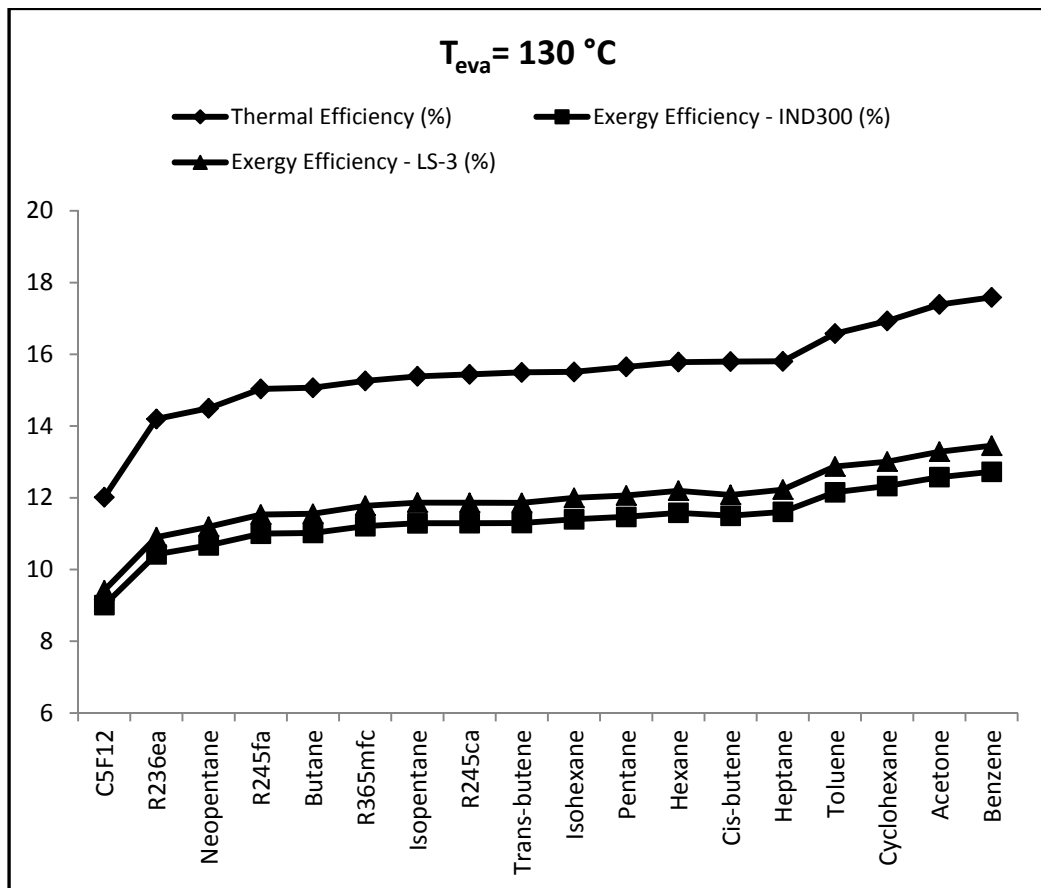


**Fig. 3.8** Thermal and exergy efficiency of the ORC for different working fluids at  $T_{eva} = 130\text{ °C}$

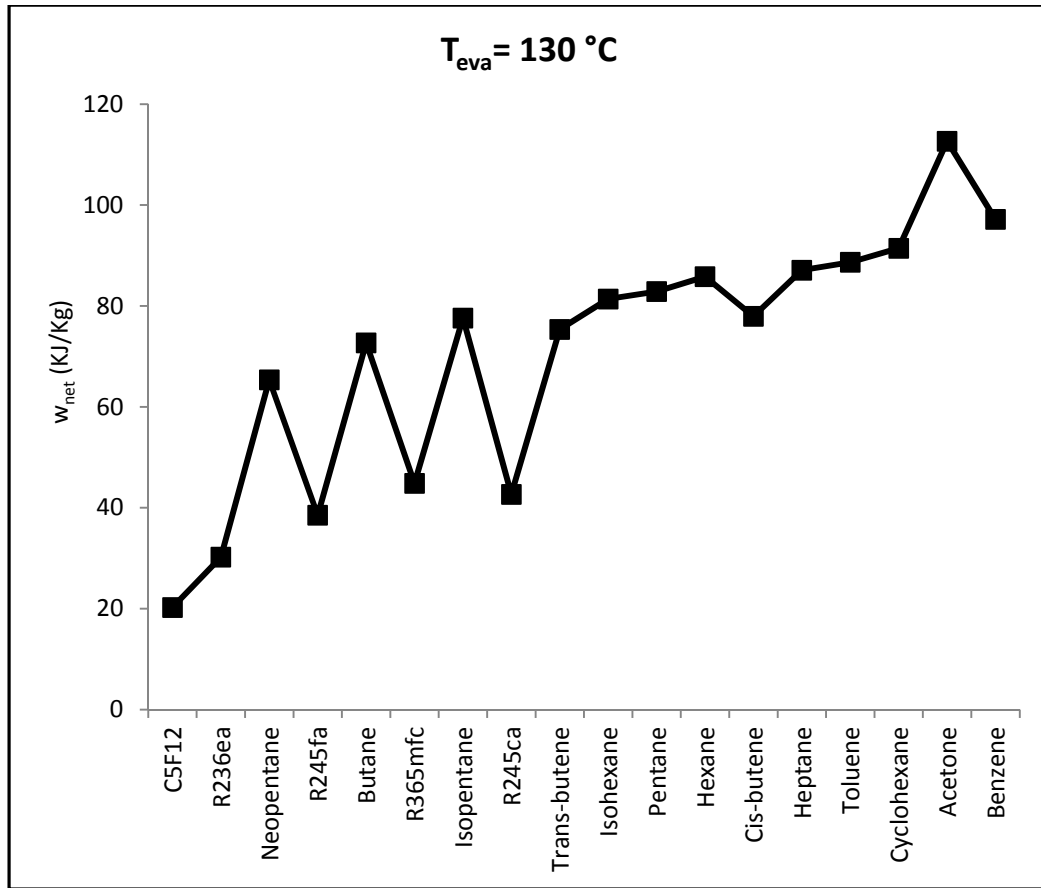


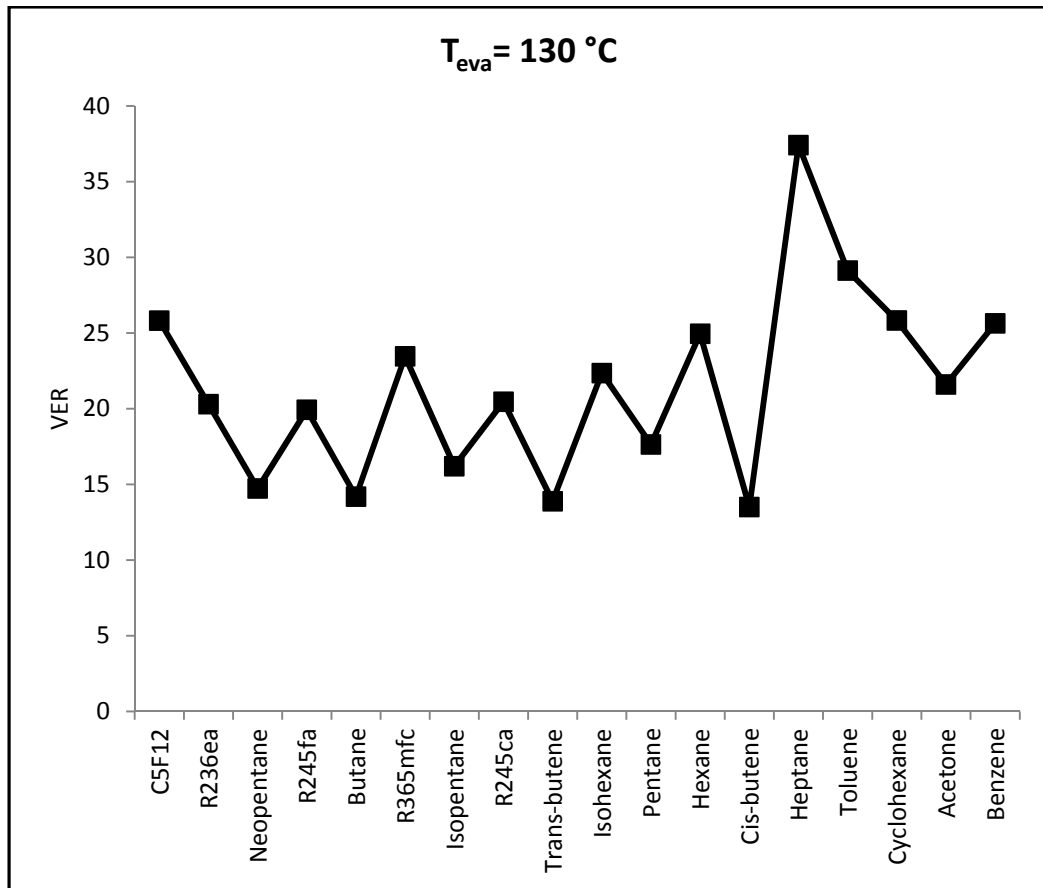
**Fig. 3.9** Net output power of the ORC for different working fluids at  $T_{eva}=130^{\circ}\text{C}$

All together, the final selected fluids for a solar ORC at medium temperature level are as follows:

- (a) R245fa and R245ca in the refrigerant group
- (b) Acetone and Benzene in the high performance non-refrigerant group
- (c) Butane, Isopentane, Trans-butene, and Cis-butene in the medium performance non-refrigerant group

At the low temperature level the procedure is exactly the same as at the medium temperature level. As some fluids have low critical temperatures (i.e. R227ea) they are included in the low temperature level analysis but are not included in the medium

temperature level analysis. The only liquid that is included in the medium temperature analysis but it is not included in the low temperature analysis is Acetone. Acetone is a wet fluid whose slope of temperature-entropy curve is very close to infinity. The isentropic efficiency of the turbine is assumed 80% in this study. With this amount of isentropic efficiency the fluid across the turbine falls into the wet region for  $T_{eva}$  less than  $124^{\circ}\text{C}$ . This means that for Acetone in addition to the higher limit, there is lower limit for  $T_{eva}$ .



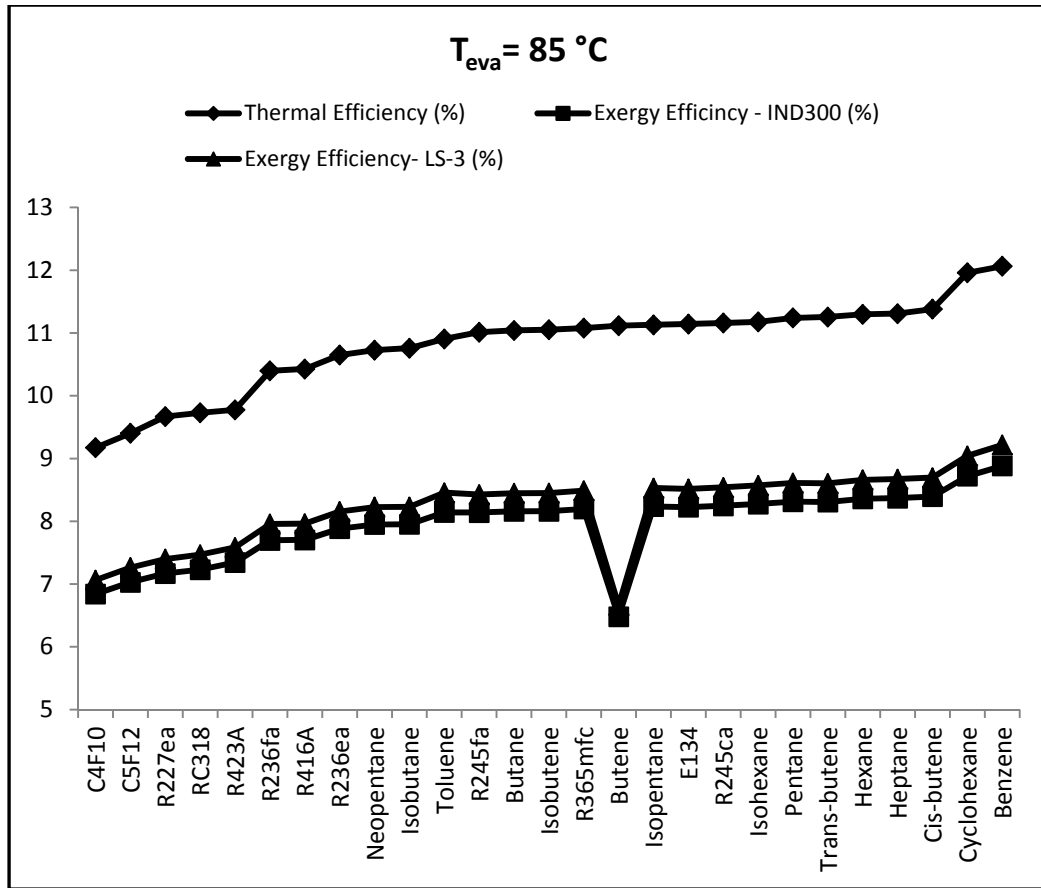
**Fig. 3.10** Vapor expansion ratio in the ORC for different working fluids at  $T_{eva}=130^{\circ}\text{C}$

Fig. (3.11) and (3.12) show that among refrigerants R245fa, R365mfc, E134, and R245ca provide a higher cycle efficiency and  $w_{net}$ . R365mfc has a higher VER but almost the same cycle efficiency and  $w_{net}$  as shown in Fig. (3.13). Thus the final refrigerants selected at the low temperature level ( $T_{eva}=85^{\circ}\text{C}$ ) will be R245fa, E134, and R245ca.

For non-refrigerants at the low temperature level Toluene, Cyclohexane and Benzene provide higher cycle efficiency as illustrated in Fig. (3.11). As can be seen in Fig. (3.12) and (3.13), their  $w_{net}$  and VER are at the same level. As depicted in Fig (3.11) and (3.12), eleven non-refrigerant fluids have very close cycle efficiencies and power outputs. Although their cycle efficiencies and power outputs are lower than cycle efficiencies and power outputs of non-refrigerants mentioned above, it is good to pick the most suitable fluids out of this group as it has been done for the medium temperature level. Fig. (3.11) shows that from this group of eleven, Butene has a lower exergy efficiency; Toluene, Isohexane, Pentane, Hexane, and Heptane have a higher VER as illustrated in Fig. (3.13). Since Butane, Isobutene, Isopentane, Trans-butene, and Cis-butene have a lower VER in the cycle, they can be in the final list as medium performance non-refrigerants.

All together, the final selected fluids for a solar ORC at the low temperature level are as follows:

- (a) R245fa, E134 and R245ca in the refrigerant group
- (b) Benzene and Cyclohexane in the high performance non-refrigerant group
- (c) Butane, Isobutene, Isopentane, Trans-butene, and Cis-butene in the medium performance non-refrigerant group



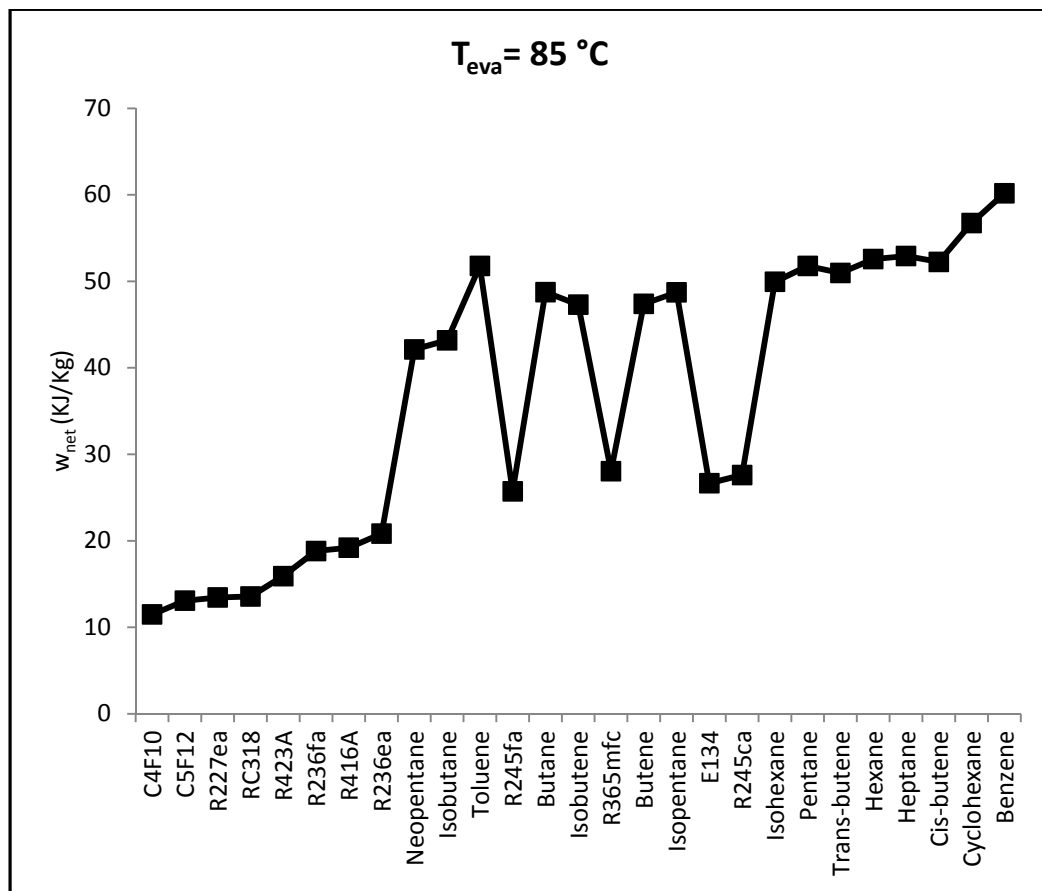
**Fig. 3.11** Thermal and exergy efficiency of the ORC for different working fluids at  $T_{eva}=85^{\circ}\text{C}$

### 3.5.4. Exergy efficiency enhancement in a solar ORC

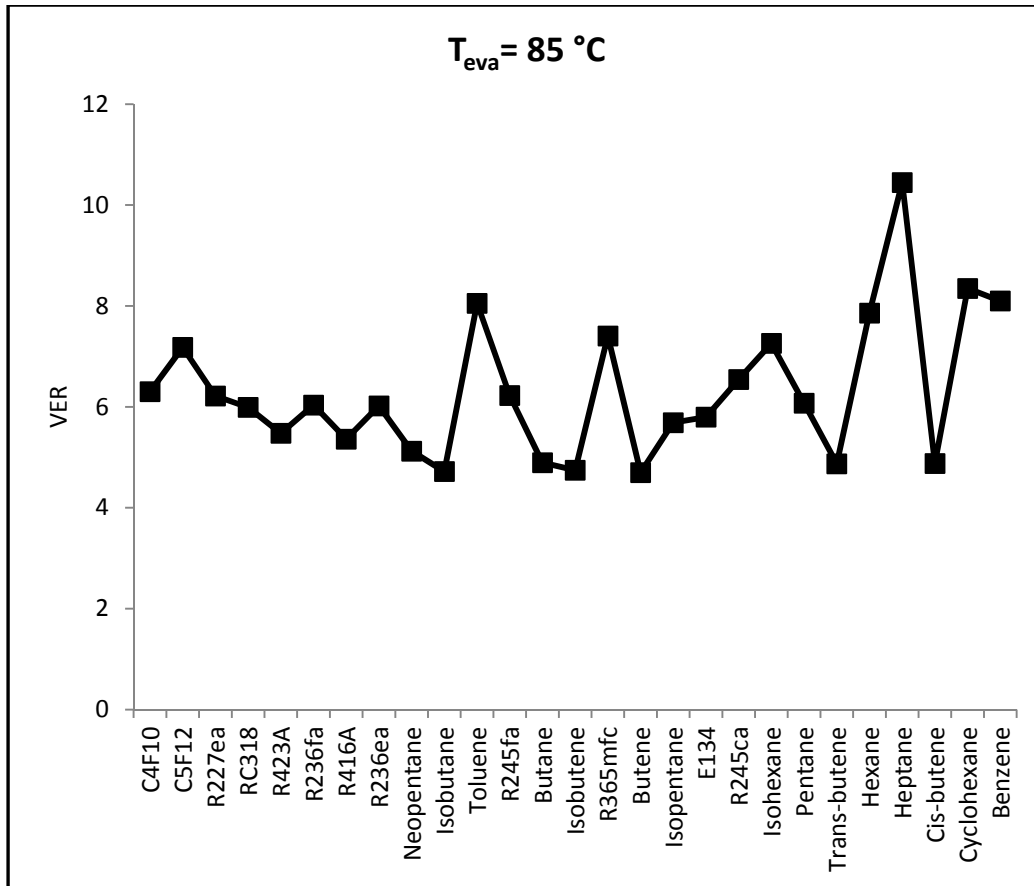
Irreversibility in solar thermal systems is relatively high because of the high temperature difference between the solar collector and the apparent sun temperature. Collector efficiency improvement and use of the regenerative ORC instead of the basic cycle are investigated in this section to reduce irreversibility of a solar ORC.

Exergy efficiency enhancement and irreversibility reduction are calculated for all 11 selected fluids when the collector efficiency increases from 70% to 100% at low and medium temperature levels. Seventy percent has been selected as a benchmark because

the collector efficiency for two selected models, IND300 and LS-3, for most analyzed fluids in this study is close to 70% for a large interval of  $T_{eva}$ . Calculations show that the exergy efficiency variation with respect to collector efficiency at each temperature level not only has the same trend but also the exergy efficiency enhancement percentage is almost the same for all selected fluids. It is also correct for the irreversibility reduction trend and percentage.



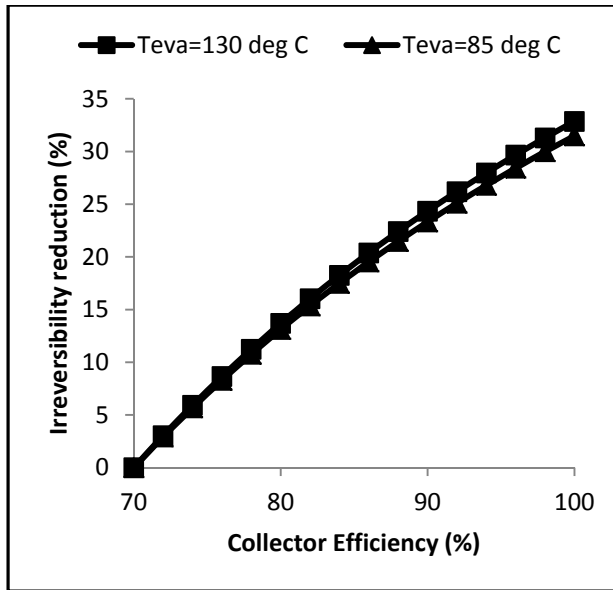
**Fig. 3.12** Net output power of the ORC for different working fluids at  $T_{eva}=85^\circ\text{C}$



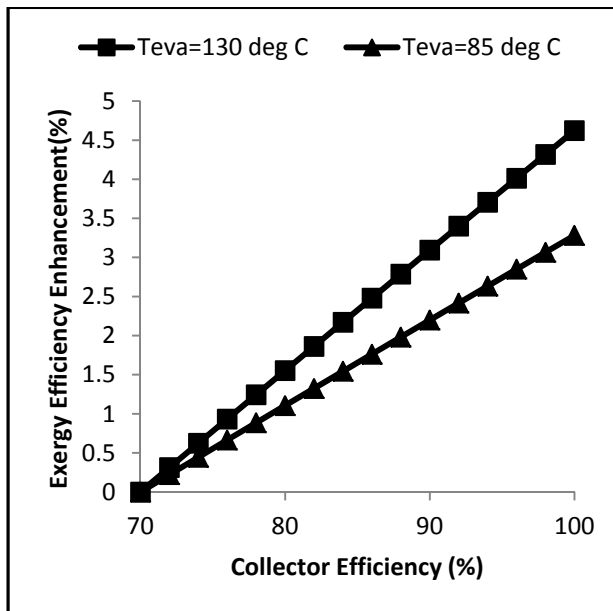
**Fig. 3.13** Vapor expansion ratio in the ORC for different working fluids at  $T_{eva}=85^{\circ}\text{C}$

Fig. (3.14) shows the variation of irreversibility reduction and exergy efficiency enhancement for Isopentane as a representative. As seen in Fig. (3.14), the theoretical limit for irreversibility reduction through collector efficiency improvement for two selected collector models, IND300 and LS-3, is 35%. It also shows this limit is 5% for the exergy efficiency enhancement.





(a)



(b)

**Fig. 3.14** (a) Irreversibility reduction, (b) Exergy efficiency enhancement by increasing collector efficiency from 70% to 100% for Isopentane.

The second method to reduce irreversibility of a cycle is using the regenerative cycle instead of the basic cycle. Regeneration reduces the absorption heat while keeping the net power output constant. In other words regeneration enhances thermal and exergy efficiency simultaneously. For the 11 selected fluids regenerative cycles with regeneration efficiency  $\epsilon_{reg} = 0.8$  have been investigated at low and medium temperature levels. As illustrated in Table 3.5, in contrast with collector efficiency improvement effect on the exergy efficiency of the cycle, regeneration's effect on the exergy efficiency of the ORC is fluid dependent.

**Table 3.5** Regeneration Effects on thermal efficiency, exergy efficiency, and irreversibility of a solar ORC employing IND300 and LS-3 solar collectors for different working fluids

Working fluid	$T_{eva} = 85^{\circ}\text{C}$					$T_{eva} = 130^{\circ}\text{C}$				
	$\Delta\eta_{th}$ (%)	$\Delta\eta_{ex}$ (%) for IND300	$\Delta L_{ex}$ (%) for IND300	$\Delta\eta_{ex}$ (%) for LS-3	$\Delta L_{ex}$ (%) for LS-3	$\Delta\eta_{th}$ (%)	$\Delta\eta_{ex}$ (%) for IND300	$\Delta L_{ex}$ (%) for IND300	$\Delta\eta_{ex}$ (%) for LS-3	$\Delta L_{ex}$ (%) for LS-3
Acetone	NA	NA	NA	NA	NA	0.02	0.02	0.14	0.02	0.15
Benzene	0.18	0.13	1.55	0.14	1.60	0.94	0.62	5.35	0.70	5.75
Butane	0.91	0.64	7.96	0.68	8.19	1.75	1.18	10.84	1.30	11.43
Cis-butene	0.40	0.29	3.58	0.30	3.70	0.73	0.54	5.10	0.60	5.41
Cyclohexane	0.76	0.53	6.28	0.57	6.48	2.27	1.48	12.23	1.66	13.02
E134	0.52	0.37	4.71	0.39	4.85	NA	NA	NA	NA	NA
Isobutene	0.62	0.44	5.52	0.46	5.69	NA	NA	NA	NA	NA
Isopentane	1.32	0.92	10.97	0.98	11.27	3.15	2.07	17.47	2.30	18.39
R245ca	1.05	0.74	8.95	0.78	9.19	2.35	1.57	13.75	1.74	14.49
R245fa	1.01	0.72	8.82	0.76	9.06	2.04	1.37	12.44	1.51	13.09
Trans-butene	0.56	0.40	5.01	0.43	5.16	1.02	0.69	6.45	0.76	6.83

Molecular complexity ( $\sigma$ ) is proposed as a criterion to find a trend of regeneration effect on the ORC performance. Molecular complexity is defined as:

$$\sigma = \left(\frac{T_{cr}}{R}\right) \left(\frac{\partial S}{\partial T}\right)_{SV, T_r=0.7} \quad (3.20)$$

where  $P_r$  and  $T_r$  are reduced pressure and temperature respectively,  $R$  is gas constant and  $SV$  stands for saturation vapor.

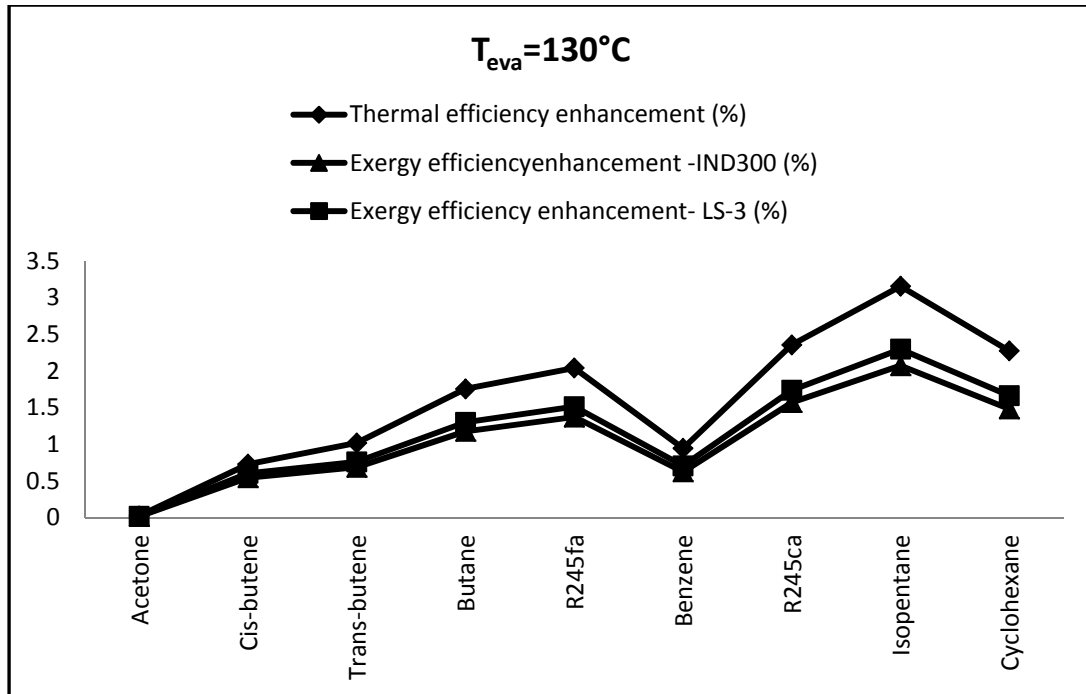
The higher slope of the entropy-temperature diagram results in higher molecular complexity. Table 3.6 shows the molecular complexity of selected fluids.

**Table 3.6** Molecular complexity of working fluids

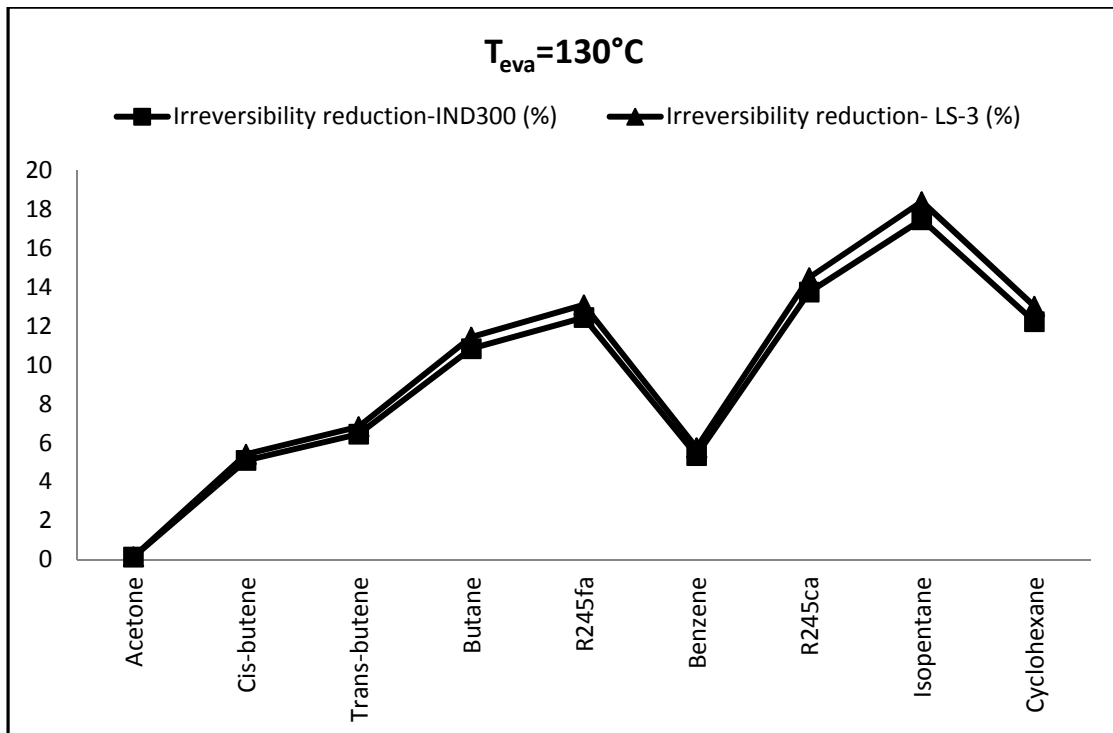
Working fluid	$\sigma$
Acetone	-2.13
Benzene	4.22
Butane	1.78
Cis-butene	-1.18
Cyclohexane	8.97
E134	-0.3
Isobutene	0.56
Isopentane	7.2
R245ca	4.33
R245fa	2.76
Trans-butene	0.14

Figures (3.15) and (3.16) show thermal and exergy efficiency enhancement and irreversibility reduction of the ORC by using the regenerative cycle for selected working fluids. In these figures fluids are arranged in the horizontal axis in ascending order of molecular complexity.

At both temperature levels and based on all performance factors discussed in this section higher molecular complexity results in a more effective regenerative cycle. The only exceptions to this rule are Benzene and Cyclohexane. This means that the regeneration will be more effective in ORCs employing high molecular complexity working fluids if they are not Cyclohydrocarbons.

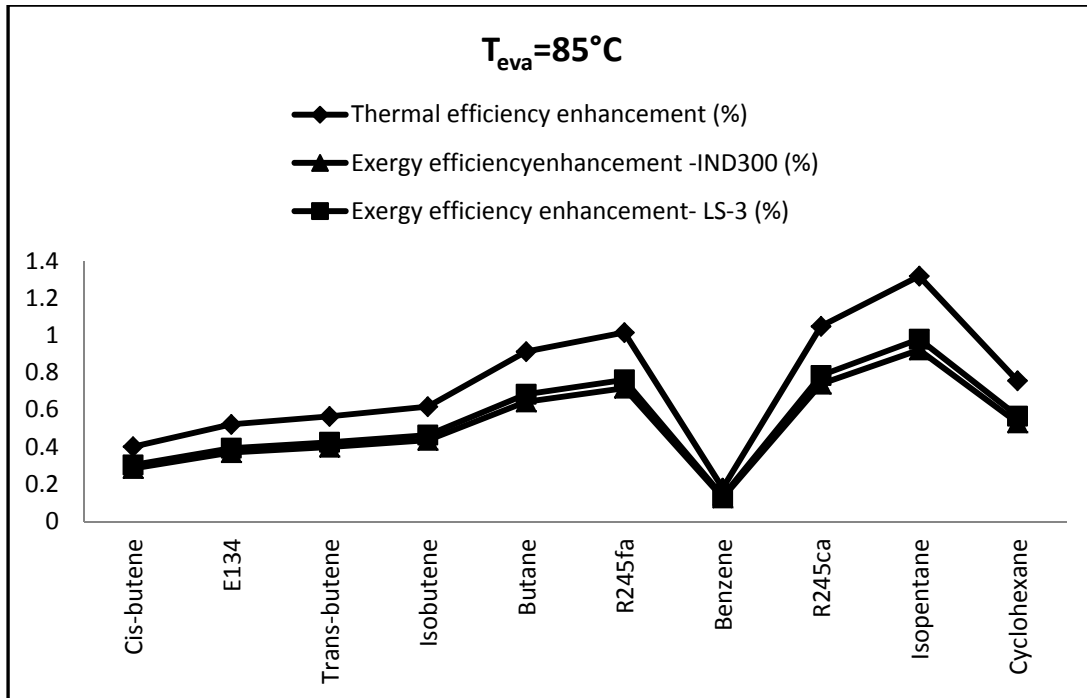


(a)

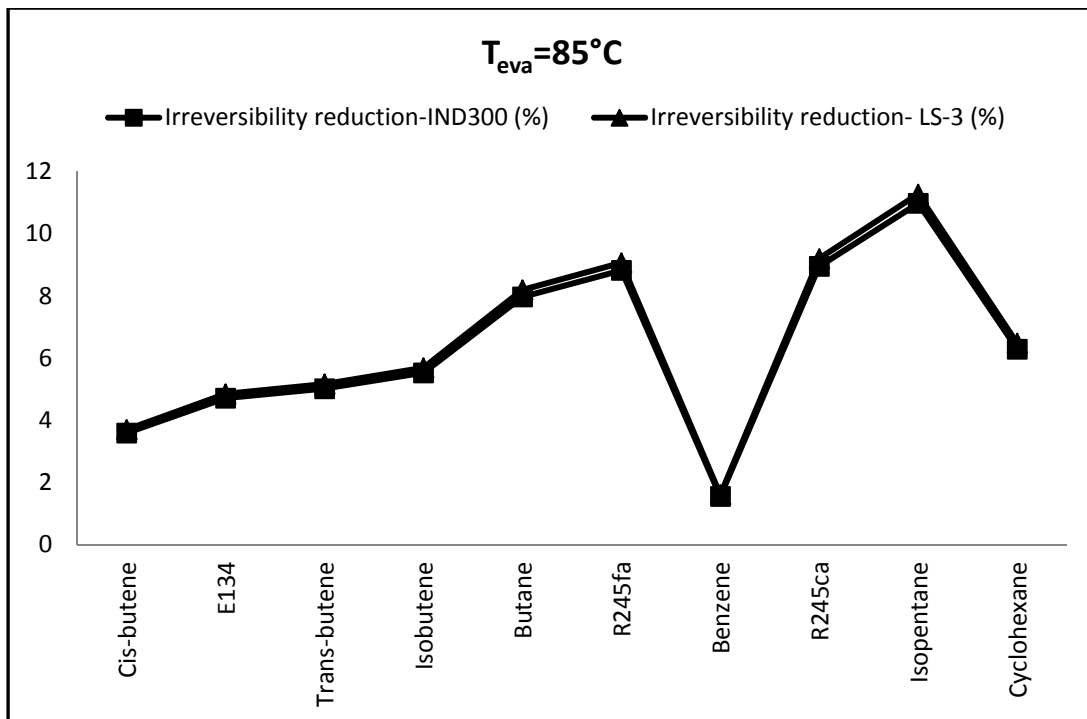


(b)

**Fig. 3.15** (a) Thermal and exergy efficiency enhancement, (b) Irreversibility reduction by using regenerative ORC based on molecular complexity of working fluids ( $T_{eva}=130^{\circ}\text{C}$ )



(a)



(b)

**Fig. 3.16** (a) Thermal and exergy efficiency enhancement, (b) Irreversibility reduction by using regenerative ORC based on molecular complexity of working fluids ( $T_{eva}=85^{\circ}\text{C}$ )

### 3.6. Conclusions

A comprehensive list of working fluids has been analyzed to find the most suitable fluids to operate a solar ORC. A procedure to compare working fluids capabilities when they are employed in the solar Rankine cycles with similar working conditions has been proposed. This procedure can be summarized and illustrated in Fig. (3.17).

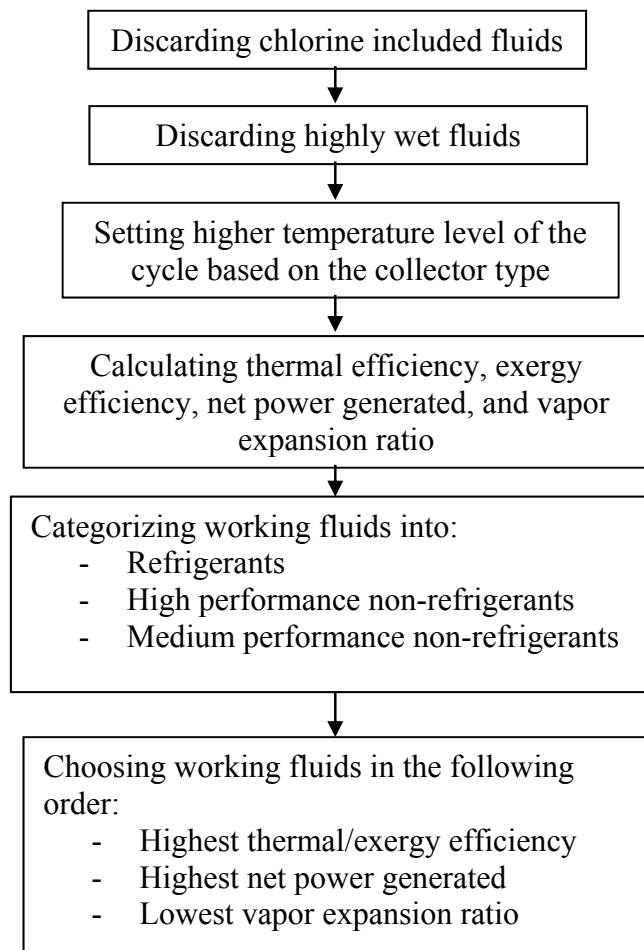


**Fig. 3.17** Proposed selection procedure of the working fluid in a solar ORC

At the first step of the procedure Chlorine included fluids and wet fluids have been discarded. The slope of the temperature-entropy curve for some wet fluids is very close to infinity. These fluids have been selected at this step.

The maximum practical thermal efficiency and corresponding performance factors for preselected working fluids confirm that fluids with higher critical temperature have better performance in the ORC. Calculation shows that the thermal efficiency higher than 25% and the exergy efficiency higher than 20% are achievable in ORCs.

In the next step a comparison between different ORC working fluids based on fluids effect on the thermal /exergy efficiency, net power generated, and vapor expansion ratio of the Rankine cycle has been accomplished. Thermal efficiency and exergy efficiency of the ORC have the same trend with respect to changing working fluids. Therefore thermal efficiency and exergy efficiency of the cycle play the same role in selecting a proper working fluid. In the investigation, two temperature levels for  $T_{eva}$  have been considered which are 85 °C and 130 °C as representatives of low temperature and medium temperature solar collectors.

The main criterion for selecting a working fluid in this study was the thermal/exergy efficiency. After that among fluids with the same order of thermal/exergy efficiency, net power output of the ORC is a determinant factor to select the working fluid. The third step will be eliminating fluids with a high vapor expansion ratio at the close level of cycle efficiencies and power outputs.

Fluids have been divided into two groups: refrigerants and non-refrigerants. Fluids with the best performance in the ORC have been recognized in each group. In the non-refrigerant's group, two different subdivisions have been considered: high

performance fluids and medium performance fluids. The reason for this subdivision is that most non-refrigerants are in the medium performance group. Then by considering all non-refrigerants as one group, a large group of fluids would be omitted from analysis.

At medium temperature level the final selected refrigerants through the introduced procedure are R245fa and R245ca. The final selected non-refrigerants at  $T_{eva}=130$  °C are Acetone and Benzene with the high performance and Butane, Isopentane, Transbutan, and Cis-butene with the medium performance.

At the low temperature level only a few numbers of fluids have been changed in comparison to fluids selected at the medium temperature level. At  $T_{eva}=85$  °C, E134 has been added to the selected refrigerants at  $T_{eva}=130$  °C. In the non-refrigerants group Acetone has been replaced by Cyclohexane and Isobutene has been added to the fluids with the medium performance capability.

Collector efficiency improvement and use of regenerative ORC instead of the basic cycle to reduce irreversibility of a solar ORC were investigated in the last section. Exergy efficiency enhancement and irreversibility reduction have been calculated for all 11 selected fluids when the collector efficiency increases from 70% to 100% at low and medium temperature levels. Calculation results show that the theoretical limit for irreversibility reduction through collector efficiency improvement for two selected collector models, IND300 and LS-3, is 35%. It also shows this limit is 5% for the exergy efficiency enhancement. For the 11 selected fluids a regenerative cycle with regeneration efficiency  $\varepsilon_{reg} = 0.8$  have been investigated at low and medium temperature levels. In contrast to collector efficiency improvement effect on the exergy efficiency of the cycle, regeneration's effect on the ORC is fluid dependent. Calculation results show, at the two



temperature level studied, the regeneration will be more effective in ORCs employing high molecular complexity working fluids except for Cyclohydrocarbons.

**CHAPTER 4**

**EXERGOECONOMIC ANALYSIS OF SOLAR ORGANIC RANKINE CYCLE**

**FOR A BUILDING IN HOT AND HUMID CLIMATE**

**4.1 Introduction**

In chapter 3 the optimal working fluids and cycle configuration have been determined by employing governing equations of basic and regenerative thermodynamic cycle with a consideration of exergetic measures. In this chapter, the optimization process of the solar ORC is finalized by identifying the best collector type and its corresponding temperature level, and exergoeconomic principles are applied on the optimal solar ORC. In the first section of chapter 4, the best collector-temperature combination for the solar ORC which maintains the electricity demand of a geothermal air-conditioned commercial building located in Pensacola of Florida is determined with exergetic and economic considerations. The 11 selected fluids in chapter 3 are employed in this analysis. The solar collector loop, building, and geothermal air conditioning system are modeled using TRNSYS. TRNSYS is a transient systems simulation FORTRAN program with a modular structure for simulating energy systems. TRNSYS is also notably powerful for steady problems. Available electricity bills of the building and the 3-week monitoring data on the performance of the geothermal system are employed to validate the simulation. The effect of the different solar radiations on the system requirements is also investigated. By the end of this section, the optimal working fluids, cycle configuration, solar collector type, and operation conditions of the solar ORC are determined.

Second section of chapter 4 discusses the exergoeconomic analysis of the optimal

solar ORC system. Among the methods have been used to evaluate the performance of a thermal energy system, there are techniques that combine thermodynamic and economic principles. Thermoconomics is a general term that describes any combination of a thermodynamic analysis with an economic one. Compared with energy, exergy is a more consistent measure of economic value. Exergoeconomics rests on the philosophy that exergy is the only rational basis for assigning monetary costs to the system interactions with its surroundings and to the sources of thermodynamic inefficiencies within it. The ratio  $R_{ex}$  of the exergy loss to the capital cost is the key parameter of exergoeconomic analysis of energy systems.

Geothermal systems and thermal power plants have been investigated through Exergoeconomic analysis while there are no studies to date on exergoeconomic evaluation of a solar ORC. For the first in this study, the exergoeconomic concept will be applied on a solar ORC in order to investigate the relation between the exergy loss and capital cost of the system.

## **4.2 TRNSYS Software**

TRNSYS is a transient systems simulation FORTRAN program with a modular structure for simulating energy systems. TRNSYS is also notably powerful for steady problems. A TRNSYS project is typically setup by connecting components graphically in an interface called Simulation Studio. TRNSYS components are often referred to as Types.

One of the key factors in TRNSYS' success over the last 35 years is its open, modular structure. The source code of the kernel as well as the component models is

delivered to the end users. This simplifies extending existing models to make them fit the user's specific needs. The DLL-based architecture allows users and third-party developers to easily add custom component models, using all common programming languages (C, C++, PASCAL, FORTRAN, etc.). In addition, TRNSYS can be easily connected to many other applications, for pre- or post-processing or through interactive calls during the simulation (e.g. Microsoft Excel, Matlab, COMIS, etc.).

The main visual interface of TRNSYS is the Simulation Studio. From there, you can create projects by drag-and-dropping components to the workspace, connecting them together and setting the global simulation parameters. The Simulation Studio saves the project information in a TRNSYS Project File. When a simulation is run; the Simulation Studio also creates a TRNSYS input file. The TRNSYS input file is a text file that contains all the information on the simulation but no graphical information.

The simulation Studio also includes an output manager from where the programmer can control which variables are integrated, printed and/or plotted, and a log/error manager that allows studying in detail what happened during a simulation. Many additional tasks can be performed from the Simulation Studio such as to generate projects using the "New Project Wizard", generate a skeleton for new components using the Fortran Wizard, view output files, and view and edit the components proformas. A proforma is the input/output/parameters description of a component.

### **4.3 Building and GSHP System Description**

Pensacola is a city in the state of Florida which has the hot and humid climate. Hot and humid climate has been selected for the study due to its high solar intensity and

long solar radiation time through the year. In addition in such a cooling dominant region, the GSHP system has a better annual performance and electricity demand profile of the building better follows the electricity generation profile by the solar ORC system.

The building is a one story commercial building with 395 m<sup>2</sup> floor area located in downtown Pensacola and is served by grid power. Its operation started on August 2010. The building consists of 8 offices, 1 conference room, 1 break room, 1 lay out room, 1 computer server room, two bathrooms, and a front office desk.

Table 4.1 shows key properties of constituent layers of the building envelope's main components.

The building has been equipped with two 6 ton geothermal heat pump units that condition the north zone and south zones of the building and a small 1 ton unit that compensates the heat load of the computer server's room. Each 6 ton unit is a WaterFurnace™, Envision ND072 and the 1 ton unit is a WaterFurnace™, Versatec V012. The GSHP system utilizes a closed loop vertical U-tube heat exchanger, which is composed of 14 boreholes reaching a depth of 300 feet. All buried pipes are made of Polyethylene. U-tube pipes are ¾" with 0.433 W/m.K thermal conductivity.

#### **4.4 Building and GSHP System Modeling Details**

The system consists of three main subsystems: the building, the GSHP system and the ORC system. In this section the building and the GSHP modeling details will be presented.

TRNSYS 17 has been employed for the modeling of the building and the GSHP system. The TRNSYS model of the building and the geothermal system has been

depicted in Fig. 4.1. The main TRNSYS modules used are the following:

- Weather data (Type 109): serves the main purpose of reading weather data at regular time intervals from a data file.

**Table 4.1** Key properties of constituent layers of the building envelope’s main components

Component	Constituent layer(s)	Key properties	U-value [W/m <sup>2</sup> K]
Exterior wall	Concrete	Thickness=15.2 cm Density=2400 kg/m <sup>3</sup>	0.251
	Gypsum board	Thickness=1.6 cm Density=900 kg/m <sup>3</sup>	
	Polystyrene	Thickness=13.0 cm Density=25 kg/m <sup>3</sup>	
	Face brick	Thickness=9.20 cm Density=1922 kg/m <sup>3</sup>	
Roof	Plaster board	Thickness=1.0 cm Density=950 kg/m <sup>3</sup>	0.156
	Horizontal air gap	NA	
	Polystyrene	Thickness=12.7 cm Density=25 kg/m <sup>3</sup>	
	Roof Deck	Thickness=35 cm Density=530 kg/m <sup>3</sup>	
Window	Glass	SHGC=0.397	1.26

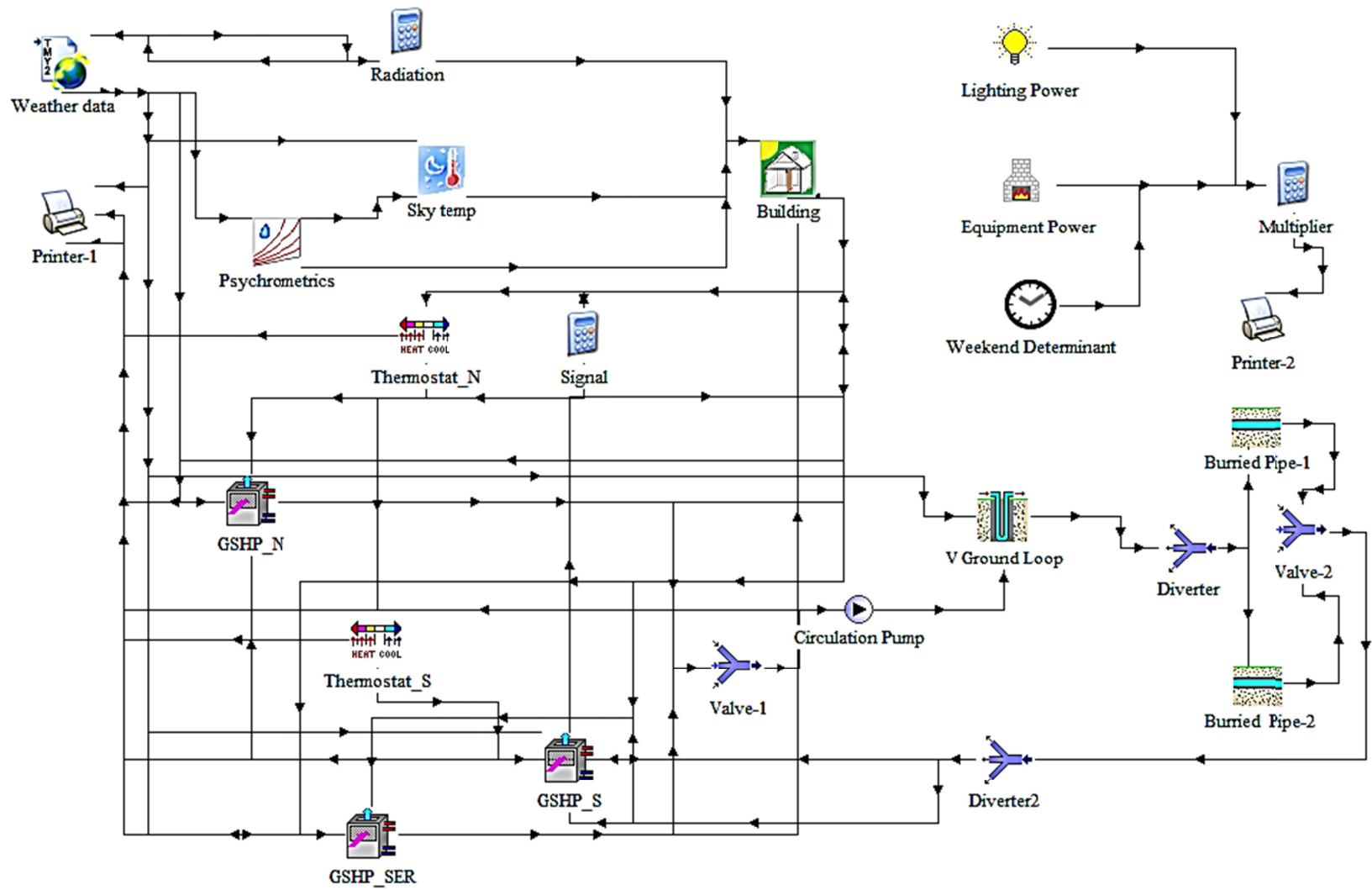


Fig 4.1 Building and GSHP system TRNSYS model

- Psychrometrics (Type 33): takes the dry bulb temperature and relative humidity of moist air as input and calculates the other thermodynamic properties of moist air.
- Sky temp (Type 69): determines an effective sky temperature, which is used to calculate the long-wave radiation exchange between an arbitrary external surface and the atmosphere.
- Building (Type 56): models the thermal behavior of a building having multiple thermal zones.
- Thermostat\_N/Thermostat\_S (Type 108): is modeled to output five on/off control functions that can be used to control a system having a two stage heat source, an auxiliary heater, and a two-stage cooling system. For this study only the first stages of heating and cooling have been applied to the model.
- GSHP\_N/GSHP\_S/GSHP\_SER (Type 504): models a single-stage liquid source heat pump.
- V Ground Loop (Type 557): models a vertical heat exchanger that interacts thermally with the ground.
- Buried Pipe (Type 31): models the fluid flow in a horizontal buried pipe.
- Circulation pump (Type 3): models the performance of a variable speed pump. In the created TRNSYS model, there is no continuous flow modulation. Consequently, the outlet flow rate and the power used are at their maximum value.
- Diverter (Type 647): models a diverting valve that splits a liquid inlet mass flow into fractional outlet mass flows.



- Valve (Type 649): models a mixing valve that combines individual liquid streams into a single outlet mass flow.
- Lighting/Equipment Power (Type 14): A time dependent forcing function which has a behavior characterized by a repeated pattern.
- Weekend Determinant (Type21): returns different time values at the current time step.

In addition to the above mentioned modules, some printers and equation blocks have been used in the TRNSYS model of the building and geothermal system. The printer component is used to print selected system variables at specified time intervals. The equation block recognizes some mathematical functions and acts like a calculator in the Simulation Studio environment.

Instead of entering the surfaces manually in TRNSYS, three dimensional data created by Trnsys3d for TRNSYS can be imported. Trnsys3d for TRNSYS is a plugin for Google SketchUp that allows you to create a building geometry from scratch: add zones, draw heat transfer surfaces, draw windows, draw shading surfaces, etc. Figure 4.2 shows the building geometry created in Google SketchUp.

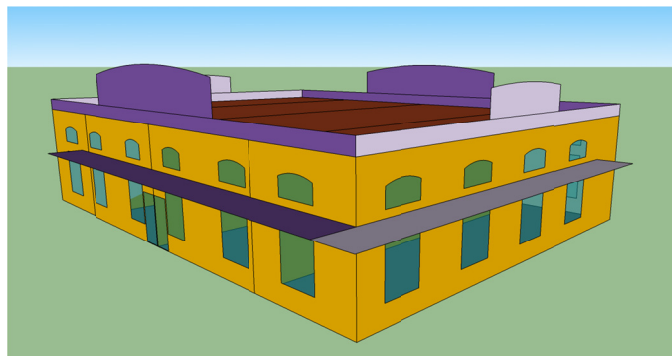


**Fig 4.2** The building geometry created in Google SketchUp

#### 4.5 Calibration Procedure

The performance of the GSHP system has been monitored for 20 days between Feb 18th and March 9th 2011. Monitoring data and available electricity bills of the building have been employed to calibrate the building and GSHP system simulation.

The TRNSYS model has been run for the monitoring period and 5 billing periods for calibration purposes. Table 4.2 shows the assumptions that have been made in the modeling. In this table the number of people and the type and number of equipment have been assumed based on collected information from the owner of the building. The building is a commercial building and the number of people as well as the equipment used during the first month the business ran was less than the following months. Some equipment such as the computer server work 24/7 but most of the equipment's power consumption coincides with the personal use of those present. Lighting power has been extracted from the lighting plan of the building. Heating and cooling set point temperatures have been derived from thermostats in the building. The occupants did not change thermostats set points upon exiting the building.

The following monitoring equipment was installed in the building:

- FLXIM™, Fluxus F601 ultrasonic energy meter, that was installed on the main ground loop to measure and log the water flow rate and supply and return temperatures of the main loop.
- Shenitech® STUF-R1B ultrasonic energy meter, which was installed on one of the 6 ton units that serves the north zone of the building to measure and log the water flow rate and supply and return temperatures of the unit.

**Table 4.2** Made assumptions in modeling building and GSHP.  
*Schedule A: Weekdays From 8:00 AM to 5:00 PM, Schedule B: 24/7*  
*Simulation period I: 1<sup>st</sup> billing period (7/30/2010-8/12/2010)*  
*Simulation period II: All other billing period, monitoring period, and annual period*

		Schedule	Simulation Period	
			I	II
Number of People		A	4	8
lighting [W/m <sup>2</sup> ]		A	13	13
Equipment [W]		A	920	920
Equipment [W]		B	920	4600
Heating set point [°F]	North Zone	B	72	72
	South Zone	B	70	70
Cooling set point [°F]	North Zone	B	75	75
	South Zone	B	73	73

- Wattnode® single phase AC power meter with CR-200 series Campbell Scientific data logger to measure and log the power consumption of the north zone heat pump unit.
- Hobo® data logger to measure and log the temperature and relative humidity of the inside and outside of the building.

Measured data by ultrasonic energy meters have been used to adjust the passing flow through main ground loop and each heat pump unit.

Figure 4.3 shows the power consumption of the north zone heat pump unit based on measured data and simulation results.

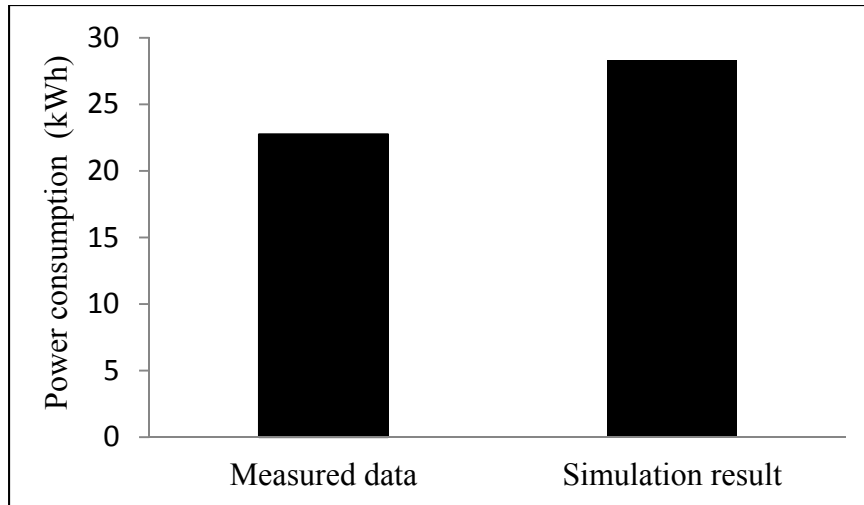


**Fig 4.3** The electrical power consumption of the north zone heat pump unit based on measured data and simulation results

The electrical power consumption of the north zone heat pump based on simulation results is 28.3 kWh while the measured power consumption is 22.8 kWh which is 20 percent lower than simulation results. The discrepancy is the result of the difference between real weather data and the TRNSYS weather data. TRNSYS weather data has been calculated based on the statistical weather data of previous years in the region.

Figures 4.4 and 4.5 illustrate the monthly average indoor and outdoor temperature for each hour in every day in February and March in Pensacola. As can be seen the difference between indoor measured temperature and simulation data is negligible for the most part of the day, while the TRNSYS outdoor temperature is lower than the measured data most of the time.

The temperature difference between the inside and outside of the building plays a key role in heat transfer rate from/to building. Table 4.3 shows the temperature difference between the inside and outside of the building for February and March in Pensacola

based on measured data and simulation results.  $\Delta T_{ME}$  and  $\Delta T_{TR}$  in Table 4.3 are defined using Equations (4.1) and (4.2).

$$\Delta T_{ME} = (T_{inside} - T_{outside})_{Measured} \quad (4.1)$$

$$\Delta T_{TR} = (T_{inside} - T_{outside})_{TRNSYS} \quad (4.2)$$

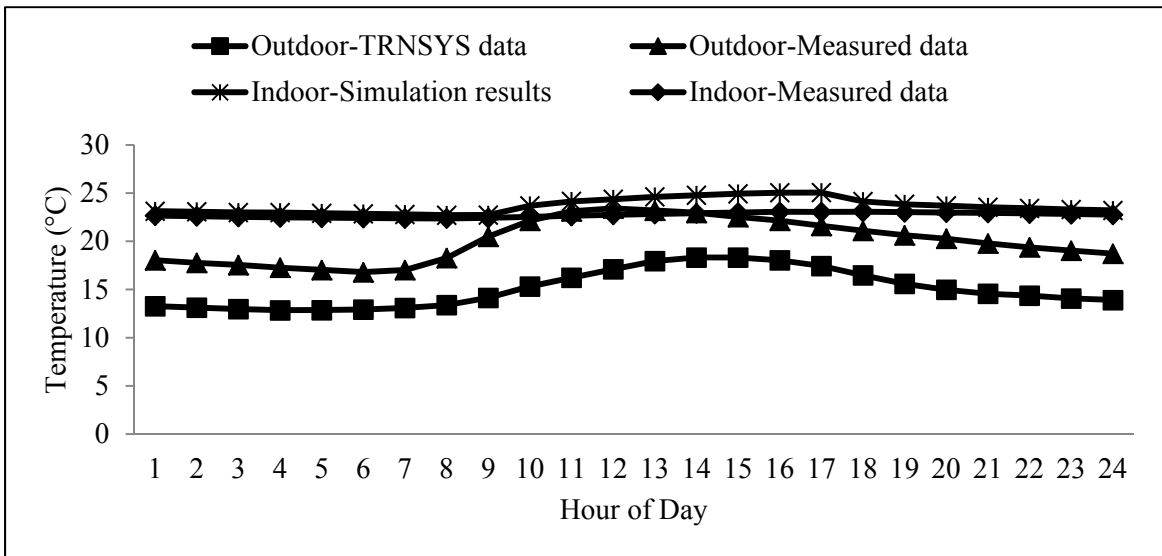


**Fig 4.4** Monthly average of indoor and outdoor temperatures for each hour of every day in February in Pensacola

The monitoring data show that the monitored heat pump unit had worked in heating mode during the whole monitoring period. It can be seen by viewing the simulation results and measured data that there are some hours of the day which units have been off. In February the system never turned on from 9 AM to Midnight every day. The average of  $\Delta T_{ME}$  for hours of the day which the system is on equals to 6.6. This average for  $\Delta T_{TR}$  is equal to 8.6. It means that the average of  $\Delta T_{ME}$  is 23 percent less than

the average of  $\Delta T_{TR}$  which can justify the 20 percent power consumption difference of simulation results and measured power consumption.

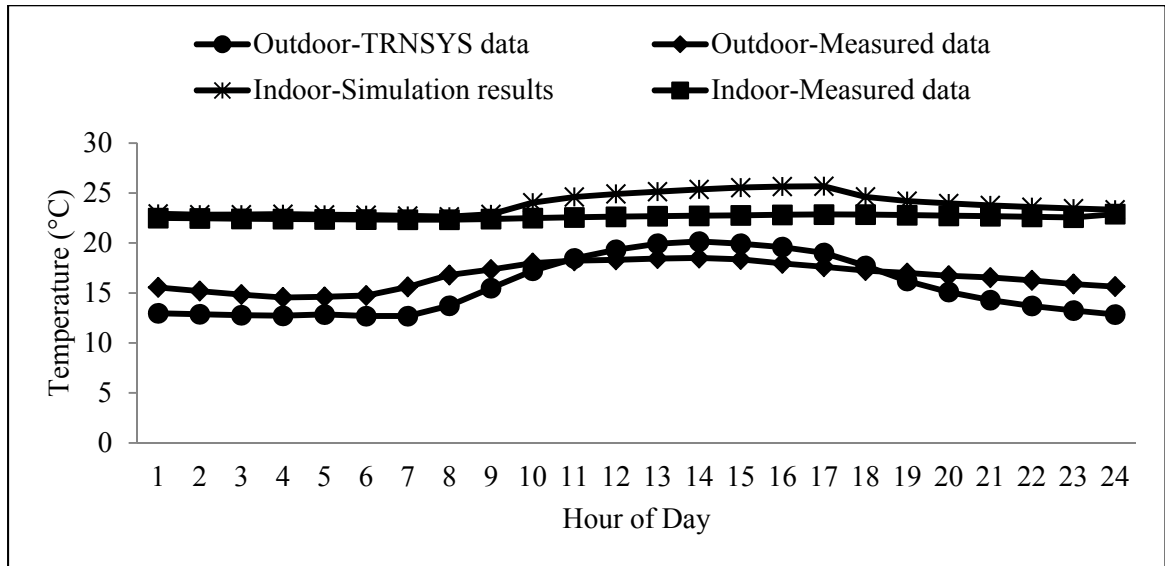


**Fig 4.5** Monthly average of indoor and outdoor temperature for each hour of every day in March in Pensacola

In the next step the TRNSYS model was run for the 5 billing periods. Table 4.4 shows the power consumption of the building based on simulation results and available billing information. As can be seen in Table 4.4 simulation results are in good conformity with the actual power consumption extracted from electricity bills of the building.

#### 4.6 ORC System Modeling Details

There are two steps in the ORC system analysis.

1. Modeling solar collector loop in order to calculate the annual heat gain of each collector unit at the specified working temperature.
2. Calculating the required number of collector units based on:
  - Calculated collector's annual heat gain in step one

- Thermal efficiency of ORC cycle for different working fluids (From chapter 3).
- Annual power demand of the building resulting from building and GSHP modeling.

**Table 4.3** Temperature difference between the inside and outside of the building for February and March in Pensacola based on measured data and simulation results.

Hour of the day	February		March	
	$\Delta T_{TR}$ [°C]	$\Delta T_{ME}$ [°C]	$\Delta T_{TR}$ [°C]	$\Delta T_{ME}$ [°C]
1	9.9	5.1	10.0	7.4
2	9.9	5.3	10.0	7.6
3	10.0	5.4	10.1	8.0
4	10.1	5.7	10.2	8.3
5	10.0	5.9	10.0	8.2
6	9.9	6.1	10.1	8.0
7	9.7	5.8	10.0	7.1
8	9.3	4.4	8.9	5.8
9	8.6	2.2	7.4	5.5
10	8.4	1.5	6.8	6.0
11	7.9	1.0	6.2	6.4
12	7.3	0.9	5.6	6.6
13	6.7	1.4	5.2	6.7
14	6.5	1.8	5.2	6.9
15	6.6	2.4	5.6	7.2
16	7.0	2.9	6.0	7.7
17	7.6	3.4	6.7	8.1
18	7.7	3.0	6.9	7.4
19	8.3	3.2	8.0	7.2
20	8.7	3.4	8.9	7.2
21	9.0	3.7	9.5	7.2
22	9.0	4.0	9.9	7.3
23	9.2	4.3	10.2	7.6
24	9.3	4.5	10.5	7.7

**Table 4.4** Power consumption of the building in Pensacola based on simulation results and available billing information

Billing Period	Simulation Results				Total Power Consumption [KWh]	Billed Total Power Consumption [kWh]	100x 1- (Simulation power/ Billed power ) [%]
	HVAC Power Consumption [kWh]	Non-HVAC Power Consumption [ kWh]					
		Equipment	Lighting	Total			
7/30/2010 - 8/12/2010	987.80	307.74	493.46	801.20	1789.00	1688.00	5.98
8/13/2010 - 9/16/2010	2608.87	1467.42	1028.04	2495.46	5104.33	5072.00	0.64
9/17/2010 - 10/13/2010	1639.49	1173.00	822.43	1995.43	3634.92	3668.00	-0.90
10/14/2010 - 11/11/2010	1229.99	1291.70	904.68	2196.38	3426.36	3379.00	1.40
11/12/2010 - 12/13/2010	1123.66	1348.72	945.80	2294.52	3418.18	3610.00	-5.31



In chapter 3, 11 fluids have been suggested to be employed in solar ORCs for two temperature levels of  $T_{\text{eva}}$  which are 85°C and 130°C.

For solar collector loop modeling, low temperature and medium temperature solar collectors should be selected first. Desired output temperature of the collector plays a key role in selecting the proper collector. The heat-carrying fluid temperature in the collector should be higher than the highest temperature in the ORC. As the working fluid in the evaporator of the ORC is in the phase change status with constant temperature, the temperature of the heat-carrying fluid in the collector should be high enough at the beginning of the heat transfer process with ORC in order to retain its heat capacity up to the end of the process. For this reason, the desired collector output temperature for low and medium ORC have been considered 120°C and 165°C respectively.

Table 4.5 shows the specifications of selected solar collectors for low and medium temperature ORCs. Being SRCC (Solar Rating and Certification Corporation) certified, and having relatively high efficiency have been considered in selecting the supplier and model of the collectors.

XCEL THERM® HT from Radco Industries has been selected as the heat-carrying fluid in the collectors. XCEL THERM® HT has an appropriate heat capacity and relatively low viscosity in comparison to similar commercial products.

The TRNSYS model of the solar collector loop has been depicted in Fig. 4.6. The main TRNSYS modules used are as follows:

- Weather (Type 109): serves the main purpose of reading weather data at regular time intervals from a data file.

- Collector (Type 1 for flat plate collector-Type 71 for evacuated tube collector): models the thermal performance of a flat plate/evacuated tube collector.
- Controller (Type 22): An iterative feedback controller that calculates the control signal required to maintain the controlled variable at a specified set point.
- Pump (Type 110): models a variable speed pump that is able to maintain any outlet mass flow rate between zero and a rated value. The mass flow rate of the pump varies linearly with control signal setting.

**Table 4.5** Selected solar collector specifications

Supplier		SunMaxx Solar	Apricus Inc.
Model		TitanPowerPlus-SU2	AP-20
Type		Flat plate	Evacuated tube
ORC temperature level		Low	Low - Medium
Gross area [m <sup>2</sup> ]		1.99	2.96
Efficiency coefficients	a <sub>0</sub>	0.754	0.456
	a <sub>1</sub> [w/m <sup>2</sup> K]	3.43	1.3509
	a <sub>2</sub> [w/m <sup>2</sup> K <sup>2</sup> ]	0.0106	0.00381
Unit price at May 2011 [USD]		786.85	1048.00

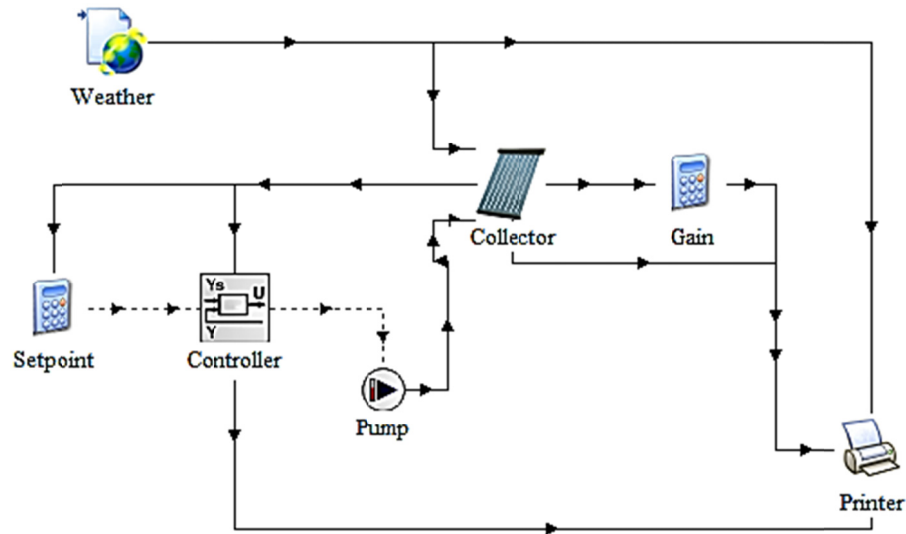


**Fig 4.6** Solar collector loop TRNSYS model

Printer and some equation blocks have been used in the TRNSYS model of the solar collector loop. In all solar collector loop simulations the slope of the collector surface is assumed  $45^\circ$ , facing the equator.

Solar collector is modeled in order to determine the annual heat gain of each collector unit at the specified working temperature. In this modeling the weather data, collector specifications such as efficiency coefficients, and collector outlet temperature set point are inputs of the model. Annual heat gain of the collector as the output of the solar collector loop modeling is used to calculate the required number of collector units needed to maintain the power demand of the building throughout the year.

#### **4.7 The Optimal Solar ORC Components and Working Condition**

In the first part of this section the required collector area and total collector price needed to maintain the power consumption of the building are compared for different ORC working fluids at two temperature levels. In chapter 3 it has been shown that the

regenerative ORC has the better performance in comparison to the basic ORC. It is for this reason that the regenerative ORC is considered in this chapter.

The collector heat-carrying fluid leaves the heat transfer process with the ORC at a relatively high temperature. This heat capacity can be used for water heating purposes. Water heating efficiency,  $\eta_{WH}$ , combined heat and power efficiency,  $\eta_{CHP}$ , the required collector area and the collector expense for the whole system has been compared for different ORC working fluids in Pensacola in Tables 4.6 to 4.8. Water heating efficiency, and combined heat and power efficiency are defined by equations (4.3) and (4.4) respectively.

$$\eta_{WH} = \frac{\textit{Water heating energy}}{\textit{Total energy gain by solar collector}} \quad (4.3)$$

$$\eta_{CHP} = \frac{\textit{Water heating energy} + \textit{ORC net output work}}{\textit{Total energy gain by solar collector}} \quad (4.4)$$

In the real case the circulation pump works continuously throughout the year regardless of heat pump units' working status. The total power consumption of the system will be decreased if the running time of the circulation pump is synchronized with the heat pump units' running time by using a proper controller.

**Table 4.6** Low temperature flat plate collector ORC system performance and collector requirements for different working fluids in Pensacola

Fluid	$\eta_{WH}$ [%]	$\eta_{CHP}$ [%]	Required area Synchronized pumping [m <sup>2</sup> ]	Required area continuous pumping [m <sup>2</sup> ]	Collector expense Synchronized pumping [ x 1000 USD]	Collector expense Continuous pumping [ x 1000 USD]	Required area (or collector expense) reduction by synchronized pumping [%]
Benzene	52.37	64.62	802.97	924.21	317.89	365.89	13.12
Butane	47.93	59.88	822.85	946.08	325.76	374.54	13.03
Cis-butene	48.64	60.42	834.77	959.99	330.48	380.05	13.04
Cyclohexane	52.28	64.86	783.10	898.38	310.02	355.66	12.83
E134	49.90	61.56	844.71	969.93	334.41	383.98	12.91
Isobutene	46.90	58.57	842.72	967.94	333.62	383.20	12.94
Isopentane	50.23	62.67	791.05	908.31	313.17	359.59	12.91
R245ca	49.12	61.33	806.95	926.20	319.46	366.67	12.88
R245fa	48.02	60.05	818.87	940.11	324.18	372.18	12.90
Trans-butene	48.24	60.06	832.79	956.02	329.69	378.47	12.89

**Table 4.7** Low temperature evacuated tube collector ORC system performance and collector requirements for different working fluids in Pensacola

Fluid	$\eta_{WH}$ [%]	$\eta_{CHP}$ [%]	Required area Synchronized pumping [m <sup>2</sup> ]	Required area continuous pumping [m <sup>2</sup> ]	Collector expense Synchronized pumping [ x 1000 USD]	Collector expense Continuous pumping [ x 1000 USD]	Required area (or collector expense) reduction by synchronized pumping [%]
Benzene	52.30	64.54	645.28	742.96	228.46	263.05	13.15
Butane	47.86	59.82	660.08	760.72	233.70	269.34	13.23
Cis-butene	48.57	60.35	671.92	769.60	237.90	272.48	12.69
Cyclohexane	52.21	64.79	627.52	722.24	222.18	255.71	13.11
E134	49.82	61.49	677.84	778.48	239.99	275.62	12.93
Isobutene	46.83	58.50	677.84	778.48	239.99	275.62	12.93
Isopentane	50.16	62.60	636.40	728.16	225.32	257.81	12.60
R245ca	49.05	61.26	648.24	742.96	229.51	263.05	12.75
R245fa	47.95	59.98	657.12	754.80	232.66	267.24	12.94
Trans-butene	48.17	59.99	668.96	766.64	236.85	271.43	12.74

**Table 4.8** Medium temperature evacuated tube collector ORC system performance and collector requirements for different working fluids in Pensacola

Fluid	$\eta_{WH}$ [%]	$\eta_{CHP}$ [%]	Required area Synchronized pumping [m <sup>2</sup> ]	Required area continuous pumping [m <sup>2</sup> ]	Collector expense Synchronized pumping [ x 1000 USD]	Collector expense Continuous pumping [ x 1000 USD]	Required area (or collector expense) reduction by synchronized pumping [%]
Acetone	54.00	71.41	837.68	962.00	296.58	340.60	12.92
Benzene	55.96	74.49	787.36	902.80	278.77	319.64	12.79
Butane	41.46	58.28	867.28	994.56	307.06	352.13	12.80
Cis-butene	45.69	62.29	879.12	1009.36	311.26	357.37	12.90
Cyclohexane	55.54	74.74	760.72	873.20	269.34	309.16	12.88
Isopentane	50.65	69.19	787.36	902.80	278.77	319.64	12.79
R245ca	47.68	65.48	819.92	941.28	290.30	333.26	12.89
R245fa	42.62	59.70	852.48	979.76	301.82	346.89	12.99
Trans-butene	43.32	59.83	882.08	1012.32	312.30	358.42	12.87

The presented results in Tables 4.6 to 4.8 show that the best collector-temperature combination for supplying the building power is the low temperature evacuated tube solar collector. In the real case, the minimum required collector area among all possible options is 722.54 m<sup>2</sup> which belongs to the low temperature ORC using the evacuated tube solar collector and Cyclohexane as its working fluid. This amount can be reduced to 627.52 m<sup>2</sup> by synchronizing circulation pump running time with the heat pump units' running time. It can be seen however that the power consumption rate of the circulation pump is low in comparison to units' power consumption; non-stop working of the pump can increase the required collector area and the corresponding expense up to 13 percent. After Cyclohexane, Isopentane with a 728.16 m<sup>2</sup> required collector area, and Benzene and R245ca each with a 742.96 m<sup>2</sup> required collector area to maintain the power demand of the building are the best working fluids to be employed in the ORC system.

Isopentane is a more optimal choice for working fluid in comparison to Cyclohexane, Benzene, and R245ca. Cyclohexane is a smog generating pollutant. Smog, which is ground-level Ozone, is formed when volatile organic compounds and oxides of nitrogen interact in the presence of sunlight. Exposure to elevated smog levels can cause serious respiratory problems, such as aggravate asthma and lead to increased respiratory infection rates. Benzene is also not a suitable choice due to its carcinogenic properties, while R245ca has a relatively high global warming potential, which makes it more undesirable as a working fluid.

While the thermal efficiency of the ORC for none of the fluids in this study can exceed 19.2 % at low or medium temperature levels, relatively high combined heat and power efficiencies up to 74% are achievable which makes the use of the ORC technology



more reasonable.

#### 4.8 Solar Radiation Intensity Effect on the Solar ORC Performance

In this section the effect of solar radiation intensity on the performance of the suggested technology is investigated. Pensacola, Miami and Houston have been selected as the representatives of hot and humid climate.

The required collector area for running the solar ORC which employs low temperature evacuated tube collector and Isopentane as the working fluid for the above mentioned cities have been depicted in Figure 4.7. As can be seen in Figure 4.7 the variation of required collector area versus working fluid has the same trend in all three cities. For all working fluids, the required collector area for Pensacola is less than that of Miami but more than that of Houston.

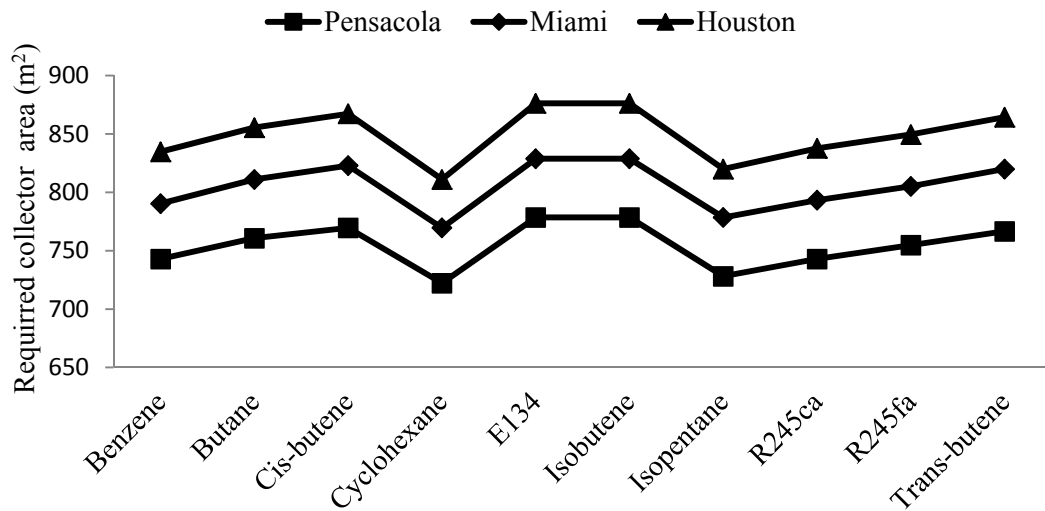


**Fig 4.7** Required collector area for running the solar ORC which employs low temperature evacuated tube collector and Isopentane as the working fluid for Pensacola, Miami and Houston

To find the reason for this trend, the monthly power generation of the aforementioned ORC system per collector unit and monthly average of solar radiation incident upon the collector surface for Miami, Pensacola and Houston have been presented in Figures 4.8 and 4.9.

Figures 4.8 and 4.9 show that the monthly variation of the power generation of the ORC per collector unit and the average solar radiation incident upon the surface follow the same pattern. This conformity is not just due to the order but the amount as well. For example, in months like January, February and December where the differences between the average solar radiations in the cities are significant, the differences between power generations of the system per collector unit in different cities are significant too. In months like August, September and October where the differences between average solar radiations in the cities are negligible, the power generations of the ORC per collector unit in three cities are very close to each other.

The power demand of the building is different in different cities due to their different weather conditions. Hence the annual power demand of the building should be considered in order to justify the differences between required collector areas needed to run the suggested ORC system in the cities presented in Fig. 4.7. Table 4.9 shows the annual power demand of the building and annual power generation per collector unit of the aforementioned ORC system in Pensacola, Miami and Houston.

Houston has the minimum power generation per collector unit using the suggested ORC while the power demand of the building in that city is higher than the demand in Pensacola. Hence in Houston, the maximum collector area needed to run the suggested

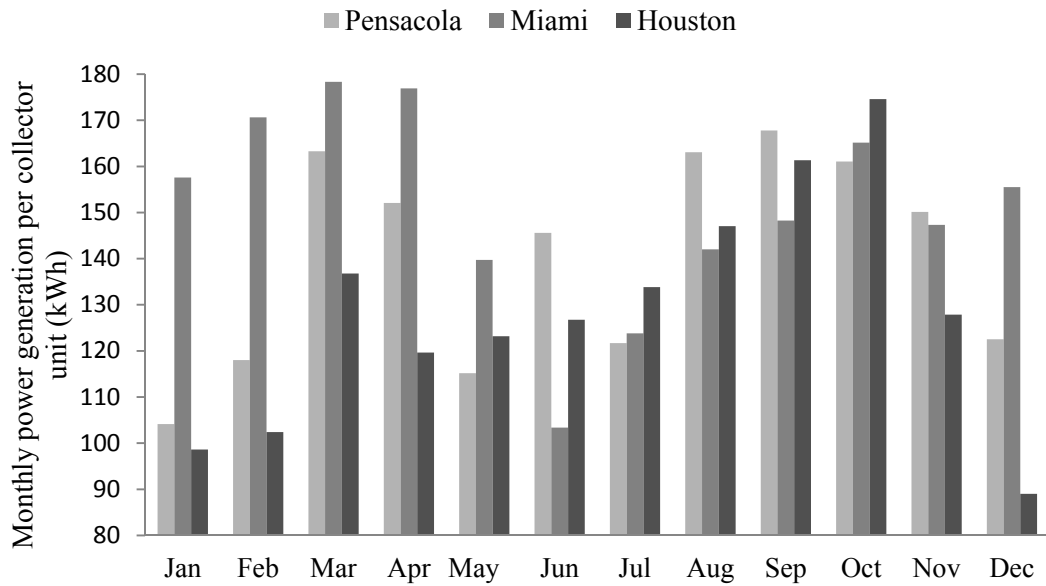


**Fig 4.8** Monthly power generation per collector unit for the solar ORC which employs low temperature evacuated tube collector and Isopentane as the working fluid for Pensacola, Miami and Houston

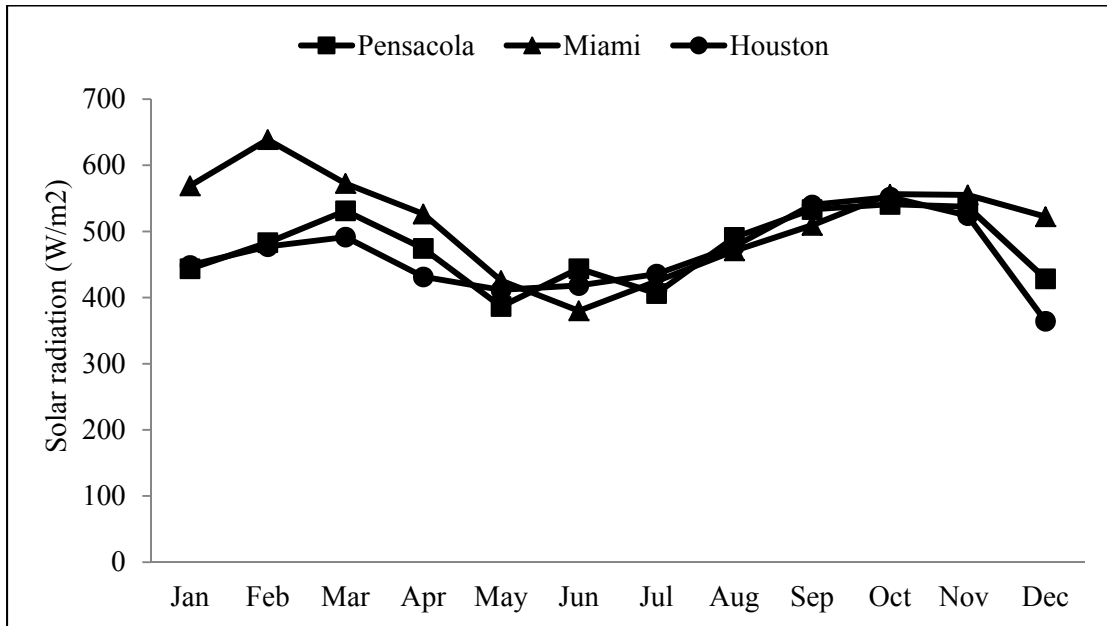


**Fig 4.9** Monthly average of solar radiation incident upon the collector surface for Miami, Pensacola and Houston

ORC system. In Miami the suggested ORC system can generate 7.4 percent more power per collector unit in comparison to the system in Pensacola while the power demand of the building in Miami is 14.5 percent more than the demand in Pensacola. Therefore the required collector area to run the system in Miami is higher than that in Pensacola.

**Table 4.9** Annual power demand of the building and the annual power generation per collector unit for the solar ORC which employs evacuated tube collector and Isopentane as the working fluid for Pensacola, Miami and Houston

	Pensacola	Miami	Houston
Annual power demand [kWh]	46408.0	53132.6	47784.1
Annual power generation per collector unit [kWh]	1684.6	1808.6	1541.1

#### 4.9 Economic Comparison between the Solar ORC and PV Panel System

Because of the low efficiency and high capital costs of PV panels and also the high energy consumption and CO<sub>2</sub> production rate of the manufacturing process of PV panels, this technology has not been widely commercialized for residential and commercial building application.

An economic comparison between the studied solar ORC system and a PV panel system that maintains the electricity demand of the building is presented in this section. PVWatts™ 2 is used to determine the required PV panel area and number of inverters to maintain the power demand of the building. PVWatts™ Grid Data calculator is an


internet-accessible simulation tool for providing quick estimates of the electrical energy produced by grid-connected crystalline silicon PV system for a location in United States from an interactive map. This tool has been provided by National Renewable Energy Library and it is available to public.

The Grid Data calculator employs a PV performance model and hourly typical meteorological year (TMY2) weather data to estimate annual energy production for a crystalline silicon PV system. It allows users to create estimated performance data of the PV system for any location in the United States or its territories by selecting a site on a 40-km gridded map. PVWatts™ 2 considers data from a climatologically similar typical meteorological year data station and site-specific solar resource and maximum temperature information to provide PV performance estimation. In version 2, performance is first calculated for the nearest TMY2 location and then translated to the desired 40-km grid cell location. Grid cell monthly values of solar radiation and meteorological parameters are used in the translation process.

The input factors of the PV system that should be determined by the user are as follows:

- Nameplate DC power rating
- DC-to-AC derate factor
- Array type (fixed, sun-tracking with one or two axes of rotation)
- Tilt angle
- Azimuth angle
- Electricity cost

Figure 4.10 shows a snapshot of the input page of the PVWatts 2. The DC-to-ACA derate factor is a multiplier that is applied by PVWatts to determine the AC power rating at Standard Test Conditions (STC). The overall DC-to-AC derate factor accounts for losses from the DC nameplate power rating and is the mathematical product of the derate factors for the components of the PV system. The default component derate factors used by the PVWatts calculator and their ranges are listed in the Table 4.10.



Click on **Calculate** if default values are acceptable, or after selecting your system specifications. Click on **Help** for information about system specifications. To use a DC to AC derate factor other than the default, click on **Derate Factor Help** for information.

---

**Site Location:**

Cell ID: 0239398  
 State: Florida  
 Latitude: 30.535  
 Longitude: -87.05

---

**PV System Specifications:**

DC Rating (kW):   
 DC to AC Derate Factor:  DERATE FACTOR HELP  
 Array Type:  ▾

Fixed Tilt or 1-Axis Tracking System:

Array Tilt (degrees):  (Default = Latitude)  
 Array Azimuth (degrees):  (Default = True South) [What's this?](#)

---

**Energy Data:**

Cost of Electricity (cents/kWh):

Fig 4.10 A snapshot of the input page of the PVWatts 2

**Table 4.10** Derate factors for AC power rating at Standard Testing Condition

Component derate factors	PVWatts default	Range
PV module nameplate DC rating	0.95	0.80–1.05
Inverter and transformer	0.92	0.88–0.98
Mismatch	0.98	0.97–0.995
Diodes and connections	1.00	0.99–0.997
DC wiring	0.98	0.97–0.99
AC wiring	0.99	0.98–0.993
Soiling	0.95	0.30–0.995
System availability	0.98	0.00–0.995
Shading	1.00	0.00–1.00
Sun-tracking	1.00	0.95–1.00
Age	1.00	0.70–1.00
Overall DC-to-AC derate factor	0.77	0.099–0.960

The component derate factors are described below.

- PV module nameplate DC rating derate factor accounts for the accuracy of the manufacturer's nameplate rating.
- Inverter and transformer derate factor reflects the inverter's and transformer's combined efficiency in converting DC power to AC power.
- The derate factor for PV module mismatch accounts for manufacturing tolerances that yield PV modules with slightly different current-voltage characteristics. Consequently, when connected together electrically, they do not operate at their

peak efficiencies.

- Diodes and connections derate factor accounts for losses from voltage drops across diodes used to block the reverse flow of current and from resistive losses in electrical connections.
- DC wiring derate factor for DC wiring accounts for resistive losses in the wiring between modules and the wiring connecting the PV array to the inverter.
- AC wiring derate factor for AC wiring accounts for resistive losses in the wiring between the inverter and the connection to the local utility service.
- The derate factor for soiling accounts for dirt, snow, and other foreign matter on the surface of the PV module that prevent solar radiation from reaching the solar cells.
- The derate factor for system availability accounts for times when the system is off because of maintenance or inverter or utility outages.
- The derate factor for shading accounts for situations in which PV modules are shaded by nearby buildings, objects, or other PV modules and arrays.
- The derate factor for sun-tracking accounts for losses for one- and two-axis tracking systems when the tracking mechanisms do not keep the PV arrays at the optimum orientation.
- The derate factor for age accounts for performance losses over time because of weathering of the PV modules.

Annual electricity production of each PV panel which is the output of the PVwatt™ 2 and the available annual power demand of the building are used to calculate the required number of PV panels and inverters to maintain the annual power demand.



Table 4.11 shows the specifications of selected PV panel and inverter.

**Table 4.11** Selected PV panel and inverter specifications

Supplier	Kyocera Solar	Fronius USA
Model	KD135GX-LPU	IG PLUS 5.0-1
Type	Multicrystal Sicilon module	Utility interactive
Maximum power at STC [w]	135	NA
Maximum power voltage at STC [V]	17.7	NA
Maximum power current at STC [A]	7.63	NA
Recommended PV power [w]	NA	4250-5750
Maximum input voltage [v]	NA	600
Nominal input current [A]	NA	13.8
Nominal output power [w]	NA	5000
Gross area [m <sup>2</sup> ]	1.00	NA
Unit price at May 2011 [USD]	365	3320

Table 4.12 shows the required area and total cost for the suggested solar ORC system (employing low-temperature evacuated tube and Isopentane as working fluid) and PV panel system to maintain the power demand of the building in Pensacola. It can be seen for the suggested ORC system the required collector area to maintain the power demand of the building is more than 60 percent less than required PV panel area to maintain the same amount of power. The total cost to establish the suggested solar ORC system is more than 50 percent less than total cost of running a PV panel system to

maintain the power demand of the building in Pensacola.

**Table 4.12** Required area and total cost for the suggested solar ORC system (employing low-temperature evacuated tube and Isopentane as working fluid) and PV panel system to maintain the power demand of the building

System	Required area [m <sup>2</sup> ]	Collector/ PV expense [ x 1000 USD]	ORC package/Inverter expense [ x 1000 USD]	Total cost [ x 1000 USD]
Solar ORC	728.16	257.81	75	332.81
PV	1839.00	671.24	33.2	704.44

#### 4.10 Exergoeconomic Analysis of the Optimal Solar ORC System

The main objective of this section is to examine the relation between the exergy loss and the capital cost of the optimal solar ORC system using the exergoeconomic key parameter  $R_{ex}$ .  $R_{ex}$  is defined by the Eq. (4.5).

$$R_{ex} = \frac{L_{ex}^a}{K_g} \quad (4.5)$$

where  $L_{ex}^a$  is the annual exergy loss in [kWh] and  $K_g$  is the capital cost in [USD].

$L_{ex}^a$  is calculated using Eq. (4.6).

$$L_{ex}^a = L_{ex} \frac{P_d^a}{W_{net}} \quad (4.6)$$

where  $L_{\text{ex}}$  is exergy loss of the cycle in [W],  $P_d^a$  is the annual power demand of the building in [kWh] and  $W_{\text{net}}$  is the net power output of the cycle in [W].

$P_d^a$  is one of the outputs of the building and the GSHP system modeling.  $L_{\text{ex}}$  and  $W_{\text{net}}$  are calculated by Equations (3.2) and (3.1) in chapter 3.

The main reason that the capital cost is the only considered economic item in this study is that the use of other economic details like maintenance cost, interest rate and equipment lifetimes increases significantly the complexity of the analysis. There are two main justifications for this simplification:

- Capital costs are often the most significant part of the total cost of the system. Hence, the consideration of only capital cost closely approximates the results when the total cost of the system is considered.
- The total cost components other than capital costs often are proportional to capital costs. Therefore, the identified trends in the present study will likely be in good conformity with those identified when the entire cost term is considered.

Ozgener et al. (2007) believe that for any technology there is an appropriate value for  $R_{\text{ex}}$  where the design of the device is more successful if the  $R_{\text{ex}}$  for that device approaches that appropriate value. Rosen et al. (2003a) speculate that mature technologies have achieved a balance of exergy loss and capital cost over the time that is appropriate to the circumstances.

Table 4.13 shows the exergy loss, capital cost, payback period and  $R_{\text{ex}}$  of the

ORC system which employs low temperature evacuated tube collector for different working fluids in Pensacola. Minor costs such as controllers' costs, in-line pumps' costs and piping costs have been neglected in comparison to collector and ORC system costs. The selected ORC system in this study is a 50 kW EletraTherm™ ORC package.

**Table 4.13** The exergy loss, capital cost, payback period and  $R_{ex}$  of the ORC system which employs low temperature evacuated tube collector for different working fluids in Pensacola

Fluid	$L_{ex}^a$ Annual exergy loss [kWh]	$K_g$ Capital cost [ USD]			Payback period [Year]	$R_{ex}$ [kWh/USD]
		Collector expense	ORC system expense	Total capital cost		
Benzene	443931.36	263048	75000	338048	48.92	1.313
Butane	455888.98	269336	75000	344336	49.83	1.324
Cis-butene	463228.06	272480	75000	347480	50.29	1.333
Cyclohexane	430868.52	255712	75000	330712	47.86	1.303
E134	468400.30	275624	75000	350624	50.74	1.336
Isobutene	468175.76	275624	75000	350624	50.74	1.335
Isopentane	435843.64	257808	75000	332808	48.16	1.310
R245ca	445392.91	263048	75000	338048	48.92	1.318
R245fa	452813.18	267240	75000	342240	49.53	1.323
Trans-butene	461579.86	271432	75000	346432	50.13	1.332

It can be seen that the payback period variation for different fluids follows the same pattern as  $R_{ex}$  variation. Fluids with lower payback period have a lower  $R_{ex}$ . This means that  $R_{ex}$  is an appropriate parameter for thermodynamic and economic evaluation of a solar ORC.

This analysis is done at different ambient temperatures  $T_0$  from 5 to 27 °C, for Cyclohexane, Isobutane, R245ca and Benzene. The results have been depicted in Fig.

4.11. Equations (4.7) to (4.9) present linear correlations for the  $R_{ex}$  of the system for each working fluid that has been depicted in Figure 4.11.

$$\text{Cyclohexane: } R_{ex}(T_0) = 0.0031 T_0 + 1.233 \quad (4.7)$$

$$\text{Isopentane: } R_{ex}(T_0) = 0.0031 T_0 + 1.2257 \quad (4.8)$$

$$\text{R245ca: } R_{ex}(T_0) = 0.0031 T_0 + 1.2194 \quad (4.9)$$

where  $T_0$  is the ambient temperature in [ $^{\circ}\text{C}$ ].

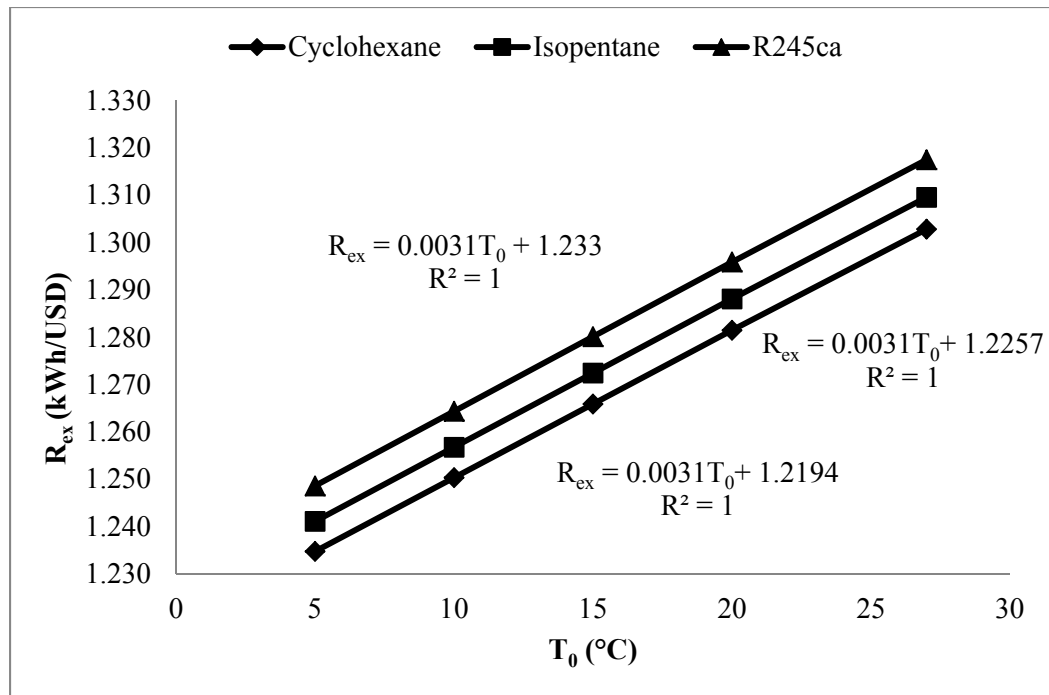


**Fig 4.11**  $R_{ex}$  variation versus ambient temperature for an ORC system which employs low temperature evacuated tube collector in Pensacola

Equations (4.7) to (4.9) confirm the exergoeconomic notion that states exergy is the commodity of value in the system. This means that there is a systematic correlation between the annual exergy loss and capital cost for the investigated solar ORC system.

#### 4.11 Conclusions

Exergoeconomic analysis of the optimal solar ORC system that maintains the electricity demand of a geothermal air conditioned commercial building has been accomplished in this chapter. The system requirements needed to run the solar ORC system has been considered as the criteria to select the optimal components and optimal working condition of the system such as collector type, working fluid and high temperature level of the ORC system.

TRNSYS 17 has been employed for the modeling of the building, GSHP system and solar collector loop. The building and GSHP modeling has been calibrated by measured data from a 20 day monitoring period and also available billing information.

The system requirements needed to maintain the electricity demand of the building with an ORC system has been compared for the 11 suggested fluids in chapter 3 for two temperature levels of 85°C and 130°C. The simulation results show that the best collector-temperature combination for supplying the building power is the low temperature evacuated tube solar collector. Cyclohexane and Isopentane with respectively 722.54 m<sup>2</sup> and 728.16 m<sup>2</sup> and Benzene and R245ca each with a 742.96 m<sup>2</sup> required collector area are the best working fluids to be employed in the ORC system to maintain the power demand of the building in Pensacola. Isopentane is a more optimal choice for working fluid in comparison to Cyclohexane, Benzene, and R245ca when considering environmental and health issues.

The effect of solar radiation intensity on the performance of the suggested technology was investigated. Pensacola, Miami and Houston were selected as the representatives of hot and humid climate cities. The results show that the monthly

variation of the power generation of the ORC per collector unit and the average solar radiation incident upon the surface follow the same pattern. This means that the solar radiation incident upon the collector surface is a determining factor of the required collector area to maintain a specific amount of electricity. The effect of weather condition on the building load and consequently on the power demand of the building should not be neglected.

An economic comparison between the solar ORC and PV panel system shows the suggested ORC system (employing low-temperature evacuated tube and Isopentane as working fluid) needs 60 percent less area and 50 percent less money than PV panel system to maintain the power demand of the commercial building in Pensacola.

Exergoeconomic analysis of the optimal ORC system shows that the ratio  $R_{ex}$  of the annual exergy loss to the capital cost can be considered as a key parameter in order to optimize a solar ORC system from the thermodynamic (exergy-based) and economic point of view. It also shows that there is a systematic correlation between the exergy loss and capital cost for the investigated solar ORC system.

## CHAPTER 5

### CONCLUSIONS AND FUTURE WORK

This research has been developed the applied guidelines for using a solar organic Rankine cycle for space air conditioning. By considering how the solar collector type, solar collector size, working fluid selection, temperature and pressure of each section of the cycle influence the exergy loss, as well as their effects on the capital costs of the solar ORC system, for a building with a specific power demand, a unique combination of all these parameters - the optimized condition – has been determined.

A procedure to compare working fluid capabilities when they are employed in the solar Rankine cycles with similar working conditions has been developed.

The exergoeconomic concept has been applied on the optimal solar ORC in order to investigate the relation between the exergy loss and capital cost of the system for the first time in this study. A systematic correlation between the annual exergy loss and capital cost for the optimal solar ORC system has been derived.

#### 5.1 Conclusions

A comprehensive list of working fluids has been analyzed to find the most suitable fluids to operate a solar ORC. A procedure to compare working fluid capabilities when they are employed in the solar Rankine cycles with similar working conditions has been proposed. This procedure has been summarized and illustrated in Fig. (5.1).

The maximum practical thermal efficiency and corresponding cycle performance factors confirm that fluids with a higher critical temperature have better performance in



the ORC. Calculation shows that a thermal efficiency higher than 25% and an exergy efficiency higher than 20% are achievable in ORCs.

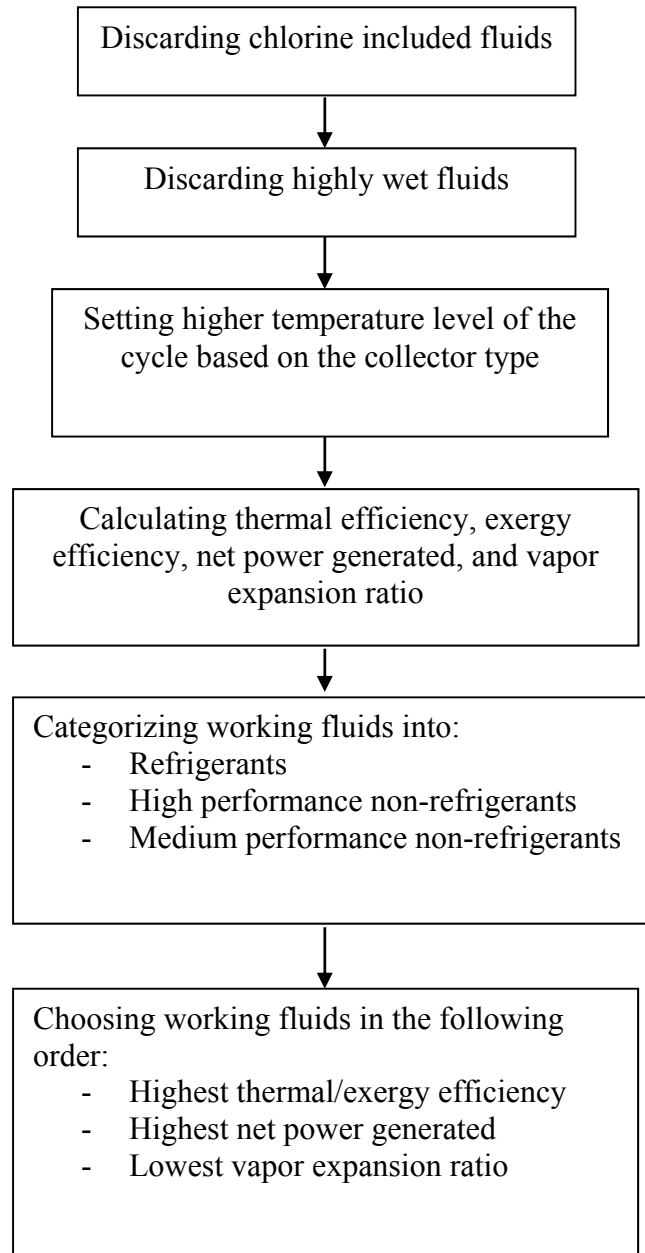


**Fig. 5.1** Proposed selection procedure of the working fluid in a solar ORC

In the investigation, two temperature levels for  $T_{eva}$  have been considered which are 85 °C and 130 °C as representatives of low temperature and medium temperature solar collectors.

Fluids have been divided into two groups: refrigerants and non-refrigerants. Fluids with the best performance in the ORC have been recognized in each group. In the non-refrigerant's group, two different subdivisions have been considered: high performance fluids and medium performance fluids. The reason for this subdivision is that most non-refrigerants are in the medium performance group. Then by considering all non-refrigerants as one group, a large group of fluids would be omitted from analysis.

At medium temperature level the final selected refrigerants through the introduced procedure are R245fa and R245ca. The final selected non-refrigerants at  $T_{eva}=130$  °C are Acetone and Benzene with high performance and Butane, Isopentane, Transbutan, and Cis-butene with medium performance.

At the low temperature level only a few numbers of fluids have been changed in comparison to fluids selected at the medium temperature level. At  $T_{eva}=85$  °C, E134 has been added to the selected refrigerants at  $T_{eva}=130$  °C. In the non-refrigerants group, Acetone has been replaced by Cyclohexane and Isobutene has been added to the fluids with the medium performance capability.

Exergy efficiency enhancement and irreversibility reduction have been calculated for all 11 selected fluids when the collector efficiency increases from 70% to 100% at low and medium temperature levels. Calculation results show that the theoretical limit for irreversibility reduction through collector efficiency improvement for two selected collector models, IND300 and LS-3, is 35%. It also shows this limit is 5% for the exergy

efficiency enhancement.

Different configurations of ORCs have different effects on the overall thermal efficiency of the cycle, the cycle total irreversibility, cycle second law efficiency, and the mass flow rate needed to generate a certain power output. Regenerative ORC is the most significant alternative configuration for basic ORC. The finite temperature difference during the heat transfer process is the main reason for irreversibility. The regenerative cycle reduces the irreversibility by using heat input from other parts of the system. In this study it has been investigated by what percentage the regenerative cycle outperforms the basic cycle with respect to the working fluid of the cycle. Calculation results show, at the two temperature levels studied, the regeneration will be more effective in ORCs employing high molecular complexity working fluids except for Cyclohydrocarbons.

The optimization process has been finalized by identifying the best collector type and its corresponding temperature level, and exergoeconomic principles were applied on the optimal solar ORC. The best collector-temperature combination for the solar ORC which maintains the electricity demand of a geothermal air-conditioned commercial building located in Pensacola of Florida is determined with exergetic and economic considerations.

The system requirements needed to maintain the electricity demand of the building with an ORC system has been compared for the 11 suggested fluids in the previous section for two temperature levels of 85°C and 130°C. The simulation results show that the best collector-temperature combination for supplying the building power is the low temperature evacuated tube solar collector. Cyclohexane and Isopentane with respectively 722.54 m<sup>2</sup> and 728.16 m<sup>2</sup> and Benzene and R245ca each with a 742.96 m<sup>2</sup>

required collector area are the best working fluids to be employed in the ORC system to maintain the power demand of the building in Pensacola. Isopentane is a more optimal choice for working fluid in comparison to Cyclohexane, Benzene, and R245ca when considering environmental and health issues.

The investigation of solar radiation intensity effect on the performance of the suggested technology shows that the monthly variation of the power generation of the ORC per collector unit and the average solar radiation incident upon the surface follow the same pattern. This means the solar radiation incident upon the collector surface is a determining factor of the required collector area needed to maintain a specific amount of electricity. The effect of weather condition on the building load and consequently on the power demand of the building should not be neglected.

An economic comparison between the solar ORC and PV panel system shows the suggested ORC system (employing low-temperature evacuated tube and Isopentane as working fluid) needs 60 percent less area and 50 percent less money than PV panel system to maintain the power demand of the commercial building in Pensacola.

Exergoeconomic analysis of the optimal ORC system shows that the ratio  $R_{ex}$  of the annual exergy loss to the capital cost can be considered a key parameter in order to optimize a solar ORC system from the thermodynamic (exergy-based) and economic point of view. It also shows that there is a systematic correlation between the annual exergy loss and capital cost for the investigated solar ORC system.

## 5.1 Future work

Possible future works include:

- Evaluation of different options to reach to net zero energy building such as:
  - Installing appropriate equipment to return the surplus electricity to the grid
  - Choosing an appropriate Thermal Energy Storage (TES) system
  - Using PV panels as a supplement to the power generation system and finding the best combination of ORC and PV panel system for this option
  
- All calculations of this study have been done in steady state mode and in an annual base. Performing a time dependent analysis will give a better understanding of the energy, exergy and cost flow in the system.
  
- A comprehensive comparison between the solar ORC and PV panel system which includes consumed energy and materials in manufacturing process of both technologies.
  
- Using Compound Parabolic Concentrating (CPC) collectors can be a solution to reduce the required collector area while there are no studies to date on using CPC collectors to generate power for a residential or commercial building. CPC collector products have not been commercialized for public use as of yet. For this reason the high price of CPC collectors is the main barrier of use in residential or commercial building application.

## LIST OF REFERENCES

- Angelino, G., and Di Paliano, P. C., 2000, "Organic Rankine cycles (ORCs) for energy recovery from molten carbonated fuel cell," *Proceedings of the Intersociety Energy Conversion Engineering Conference*, 2, pp. 1400-1409.
- Angelino, G., Gaia, M., and Macci, E., 1984, "A review of Italian activity in the field of organic Rankine cycles," *VDI Berichte*, pp. 465-482.
- Bejan, A., Entropy generation through heat and fluid flow, John Wiley and Sons Inc., 1982.
- Bruno, J.C., Lopez-Villada, J., Letelier, E., Romera, S., and Coronas, A., 2008, "Modeling and optimization of solar organic Rankine cycle engines for reverse osmosis desalination", *Applied Thermal Engineering*, 28:2212-2226.
- Cengel, Y.A., and Boles, M.A., Thermodynamics: An Engineering Approach, fifth ed., McGraw-Hill, 2006.
- Delgado-Torres, A. M., and Garcia-Rodriguez, L., 2007a, "Preliminary assessment of solar organic Rankine cycles for driving a desalination system," *Desalination*, 216, pp. 252-275.
- Delgado-Torres, A. M, and Garcia-Rodriguez, L., 2007b, "Double cascade organic Rankine cycle for solar driven reverse osmosis desalination," *Desalination*, 216, pp. 306-313.
- Drescher, U. and Bruggemann, D., 2007, "Fluid selection for the Organic Rankine Cycle (ORC) in biomass power and heat plants", *Applied Thermal Engineering*, 27:223-228.
- Eck, M., and Steinmann, W.D., 2002, Direct steam generation in parabolic troughs: First results of the DISS project, *ASME Journal of Solar Energy Engineering*, 124, pp. 134-139.
- Feng, M., 2008, "An exergy based engineering and economic analysis of sustainable building", *PhD Thesis*, Florida International University, Miami, Florida.
- Hermann, W. A., 2006, "Quantifying global exergy resources", *Energy*, 31(12):1349-1366.
- Hettiarachchi, H. D. M., Golubovic, M., Worek W. M., and Ikegami, Y., 2007, "Optimum design criteria for an Organic Rankine cycle using low-temperature geothermal heat sources," *Energy*, 32, pp. 1698-1706.
- Hung, T. C., 1995, "Waste heat recovery of organic Rankine cycle using dry fluids," *Energy Conversion and Management*, 42(5), pp. 539-553.

- Invernizzi, C., Iora, P., and Silva, P., 2007, "Bottoming micro-Rankine cycles for micro-gas turbines", *Applied Thermal Engineering*, 27:100-110.
- Karellas, S., and Schuster, A., 2008, "Supercritical fluid parameters in organic Rankine cycle applications," *International Journal of Thermodynamics*, 11(3), pp. 101-108.
- Larjola, J., 1995, "Electricity from industrial waste heat using high-speed organic Rankine cycle (ORC)," *International Journal of Production Economics*, 41(1-3), pp. 227-235.
- Lemmon, E.W., Huber, M.L., and McLinden, M.O., 2007, NIST Standard Reference Database 23: Reference Fluid Thermodynamic and Transport Properties-REFPROP, Version 8.0, National Institute of Standards and Technology, Standard Reference Data Program, Gaithersburg.
- Liu, B. T., Chien, K. H., and Wang, C. C., 2004, "Effect of working fluids on organic Rankine cycle for waste heat recovery," *Energy*, 29, pp. 1207-1217.
- Mago, P. J., Chamra, L. M., Srinivasan, K., and Somayaji, C., 2008, "An examination of regenerative organic Rankine cycles using dry fluids," *Applied Thermal Engineering*, 28, pp. 998-1007.
- Maizza, V., and Maizza, A., 1996, "Working fluids in non-steady flows for waste energy recovery systems," *Applied Thermal Engineering*, 16(7), pp. 579-590.
- Marion, B., Anderberg, M., George, R., Gary-Hann, P., and Heimiller D., "PVWATTS Version 2- Enhanced Spatial Resolution for Calculating Grid-Connected PV Performance," *National Renewable Energy Laboratory (NREL) publications*.
- Mills, D., 2004, "Advances in solar thermal electricity technology", *Solar Energy*, 76:19-31.
- National Renewable Energy Laboratory (NREL) renewable energy data center, Updated June 06 2011, Website: < <http://www.nrel.gov/rredc/pvwatts/grid.html> >.
- Ozgener, O., Hepbasli, A., and Ozgener, L., 2007, "A parametric study on the exergoeconomic assessment of a vertical ground-coupled (geothermal) heat pump system," *Building and Environment*, 42, pp. 1503-1509.
- Prabha, E., March 2006, "Solar Trough ORC Electricity System (STORES) Stage 1- Power plant optimization and economics," *National Renewable Energy Laboratory report*, NREL/SR-550-39433.
- Rabl, A., Active solar collectors and their applications, Oxford University Press, New York, 1985.
- Roodman, D.M. and Lenssen, N., 1995, "A building revolution: How ecology and health concerns are transforming construction", *Worldwatch Paper*, Worldwatch Institute, Washington, DC.

Rayegan, R., and Tao, Y.X., 2009, "A critical review on single component working fluids for Organic Rankine Cycles (ORCs)," *ASME Early Career Technical Journal*, 8(1), pp. 20.1-20.8.

Rayegan, R., and Tao, Y. X., 2011, "A procedure to select working fluids for solar Organic Rankine Cycles (ORCs)," *Renewable Energy*, Vol. 36 (2), pp. 659-670.

Rosen, M.A., and Dincer, I., 2003a, "Exergoeconomic analysis of power plants operating on various fuels," *Applied Thermal Engineering*, Vol. 23, pp. 643-658.

Rosen, M.A., and Dincer, I., 2003b, "Thermoeconomic analysis of power plants: an application to a coal fired electrical generating station," *Energy Conversion and Management*, Vol. 44, pp. 2743-2761.

Torcellini, P., Pless, S., and Deru, M., 2006, "Zero energy buildings: A critical look at the definition", *National Renewable Energy Laboratory report*, NREL/CP-550-39833.

TRNSYS 17 Main Reference Manual.

Tsatsaronis, G., 2007, "Definitions and nomenclature in exergy analysis and exergoeconomics", *Energy*, 32(4):249-253.

Tsatsaronis, G., and Winhold, M., 1985, "Exergoeconomic analysis and evaluation of energy conversion plants: I.A new General methodology", *Energy*, 10(1):69-80.

United Nations Environmental Programme, September 2006, "Montreal protocol on substances that deplete the ozone layer," Website: <[http://ozone.unep.org/teap/Reports/TEAP\\_Reports/Teap-CUN-final-report-Sept-2006.pdf](http://ozone.unep.org/teap/Reports/TEAP_Reports/Teap-CUN-final-report-Sept-2006.pdf)>.

Zhang, X. R., Yamaguchi, H., Unedo, D., Fujima, K., Enomoto, M., and Sawada, N., 2006, "Analysis of a novel solar energy-powered Rankine cycle for combined power and heat generation using supercritical carbon dioxide," *Renewable Energy*, 31, pp. 1839-1854.



## VITA

### RAMBOD RAYEGAN

#### EDUCATION

- |      |   |
|------|---|
| 1996 | B.Sc., Mechanical Engineering<br>University of Tehran<br>Tehran, Iran                                   |
| 1998 | M.Sc., Mechanical Engineering<br>University of Tehran<br>Tehran, Iran                                   |
| 2009 | Doctoral Candidate in Mechanical Engineering<br>Florida International University<br>Miami, Florida, USA |

#### AWARDS

Florida International University, University Graduate School, Doctoral Evidence Acquisition Fellowship, Summer and Fall 2009.

Florida International University, Student Government Association, Graduate Student Leadership Scholarship, 2008.

#### PUBLICATIONS

##### Book Chapter

Tao, Y. X., Rayegan, R., "Solar energy applications and comparisons," in *Energy and Power Generation Handbook*, Editor: K. R. Rao, Publisher: ASME Press (In Press)

## Papers

Rayegan, R., Tao, Y.X., 2011, "Analysis of solar Organic Rankine Cycle for a building in hot and humid climate," *ASME 2011 International Mechanical Engineering Congress and Exposition*, Denver, Colorado, USA. (Accepted)

Rayegan, R., Tao, Y. X., 2011 "A procedure to select working fluids for solar Organic Rankine Cycles (ORCs)," *Renewable Energy*, 36 (2), pp. 659-670.

Rayegan, R., Tao, Y. X., 2009, "A critical review on single component working fluids for Organic Rankine Cycles (ORCs)," *ASME Early Career Technical Journal*, 8(1), pp. 20.1-20.8.

Mun, J., **Rayegan, R.**, Phadtare, S., Zhu, Y., and Tao, Y.X., "Feasibility Study of Horizontal Ground Loop Modules of EnergyPlus on Geothermal Heat Pump System Simulation," *ASME International Mechanical Engineering Congress & Exposition*, Denver, Colorado, November 2011 (Accepted).

Jones, W.K., Zheng, F., Siddiqui, M., Rayegan, R., Tao, Y.X., 2008, "Development of 3-D channels in LTCC for capillary cooling structures for thermal management," *IMAPS/ACerS 4<sup>th</sup> International Conference and Exhibition on CICMT*, Munich, Germany.

Rayegan, R., Tao, Y. X., 2007, "A critical review of hot gas and reverse cycle defrost methods," *ASME Early Career Technical Journal*, 6(1), pp. 9.1-9.8.

Rayegan, R., Ziari A., 2006, "Analysis of energy and cost reduction in a typical residential building due to using appropriate thermal insulation materials," The 5th Conference of Iranian Fuel Consumption Optimization (I.F.C.O.), Tehran, Iran.

Rayegan, R., Jahani, N., 2004, "Ocean Thermal Energy Conversion (OTEC) power plants," Proceedings of the 1st International Conference on Eco-energy, Uruma, Iran.

Nourbakhsh, A., Rayegan, R., 2001, "Cavitation erosion testing techniques," *Journal of Faculty of Engineering*, University of Tehran, 34(1), pp. 96-107.